

A Comprehensive Effective Field Theory Framework for Coherent Elastic Neutrino-Nucleus Scattering

Gang Li,^a Chuan-Qiang Song,^{b,c,d} Feng-Jie Tang,^a Jiang-Hao Yu^{b,c,d,e}

^a*School of Physics and Astronomy, Sun Yat-sen University, Zhuhai 519082, P. R. China*

^b*School of Fundamental Physics and Mathematical Sciences, Hangzhou Institute for Advanced Study, UCAS, Hangzhou 310024, China*

^c*School of Physical Sciences, University of Chinese Academy of Sciences, Beijing 100049, P.R. China*

^d*Institute of Theoretical Physics, Chinese Academy of Sciences, Beijing 100190, P. R. China*

^e*International Centre for Theoretical Physics Asia-Pacific, Beijing/Hangzhou, China*

E-mail: ligang65@mail.sysu.edu.cn, songchuanqiang21@mails.ucas.ac.cn,
tangfj7@mail2.sysu.edu.cn, jhyu@itp.ac.cn

ABSTRACT: Coherent elastic neutrino-nucleus scattering (CE ν NS) stands out as a pivotal process for precision tests of the Standard Model electroweak sector, investigations of neutrino properties, and searches for new physics (NP). Recent experimental measurements by COHERENT, CONUS+, and ton-scale xenon detectors—including PandaX-4T and XENONnT—underscore the need for a systematic theoretical framework to bridge high-energy physics scenarios with low-energy observational data. In this work, we develop a comprehensive end-to-end effective field theory (EFT) framework for CE ν NS, encompassing the complete energy scale hierarchy spanning the ultraviolet (UV) regime down to the nuclear sector. We consider the low-energy EFT (LEFT) operators up to dimension 8, incorporating their QCD renormalization group running effects, and employ the systematic spurion method to achieve the matching between these operators and the chiral Lagrangian. A full power counting analysis is performed, extending to nuclear response functions, which evaluates contributions from LEFT operators up to dimension 8 while accounting for the nucleon number enhancement effect intrinsic to CE ν NS. Moreover, we match the relevant LEFT operators for CE ν NS onto operators up to dimension 8 within the Standard Model EFT. By also providing their complete tree-level ultraviolet completions, this procedure establishes a consistent top-down theoretical workflow. Leveraging a broad suite of CE ν NS experimental data, this framework enables a combined analysis to extract constraints on the scales of EFT operators and neutrino non-standard interaction parameters.

Contents

1	Introduction	2
2	LEFT Operators	4
3	Chiral Lagrangian	5
3.1	Mesonic Sector	7
3.2	Nucleon Sector	9
4	Power Counting in LEFT and χPT	14
5	Neutrino-Nucleus Scattering Cross Section	17
5.1	Interactions of Neutrinos with Non-relativistic Nucleons	17
5.2	Nuclear Response	19
5.3	Cross Section for Neutrino-Nucleus Scattering	23
6	Experimental Constraints	26
6.1	Experiments	26
6.2	Constraints on NP scales and NSI parameters	28
7	SMEFT Operators and UV Completions	31
7.1	SMEFT Operators	31
7.2	UV Completions	33
8	Conclusion	39
A	Expansion of Chiral Operators in Pion Fields	40
B	Naive Dimension Analysis	42
C	Values of Low Energy Constants	43
D	Nuclear Response	45
E	Operator Matching: From SMEFT to LEFT	46

1 Introduction

Coherent elastic neutrino-nucleus scattering (CE ν NS) is a process in which the neutrino elastically scatters from an entire nucleus [1]. It provides a powerful tool for precision tests of the Standard Model (SM) electroweak sector, studies of neutrino properties, nuclear form factors, and astrophysical phenomena [2–27] (see also Ref. [28]). Since the experimental discovery of this process [29], CE ν NS measurements are performed across accelerator-, solar-, and reactor-based neutrino sources and multiple target nuclei [30–43]. In parallel, ton-scale xenon detectors have reported the first indications of solar 8 B neutrinos via CE ν NS [44, 45]. The reactor experiment CONUS has set stringent constraints [31, 46], while recently CONUS+ achieved a direct observation of CE ν NS [47].

In the SM, CE ν NS is mediated by the exchange of Z boson, and thus provides a sensitive probe of neutral-current neutrino interactions. This process can also be induced by new physics (NP) beyond the SM, such as Z' boson [3, 48] or leptoquark [49, 50]. While these model-dependent scenarios have been explored, effective field theory (EFT) offers a systematic way to study CE ν NS [12]. In the EFT approach, NP effects are encoded in a series of effective operators, for which the Wilson coefficients and NP scales are given in specific ultraviolet (UV) models. Besides, in comparison with the studies using the weak charge supplemented by empirical nuclear form factors [51, 52], the EFT approach allows for power countings and controlled theoretical uncertainties, which enables *ab initio* calculations of the nuclear structures [53–58].

The neutrino-matter interactions in CE ν NS considered are shown in Fig. 1. After integrating out possible new particles, which are assumed to be heavier than ~ 100 GeV, the interactions are given by dimension-5, 6, 7 and 8 operators in the standard model EFT (SMEFT) [59–65], respecting the SM gauge symmetries. At lower energy scale, CE ν NS is characterized by effective interactions between neutrinos and quarks, such as $\nu + u \rightarrow \nu + u$, in the low-energy EFT (LEFT) [66–68] systematically, including neutrino non-standard interactions (NSIs), electromagnetic dipole operators and gluonic operators.

At energy scale down to ~ 1 GeV, CE ν NS is described as the scattering between neutrinos and the constituent hadrons, namely pions and nucleons. Within the framework of chiral perturbation theory (χ PT), the relevant weak and potential NP interactions involving the neutrino current are incorporated using the external source method [69–71] or, more generally, the systematic spurion method [72, 73]. The low-energy constants (LECs) that arise from non-perturbative QCD effects are determined either from experiments/lattice QCD calculations or estimated using naive dimensional analysis (NDA) [74–76]. At the scale below ~ 100 MeV, neutrino interacts coherently with the entire nucleus. Analogous to dark matter-nucleus scattering [77–79], the nuclear response in CE ν NS is described by a limited number of nuclear response functions [12, 18].

In this work, we establish a comprehensive EFT framework for the studies of CE ν NS with the following key features:

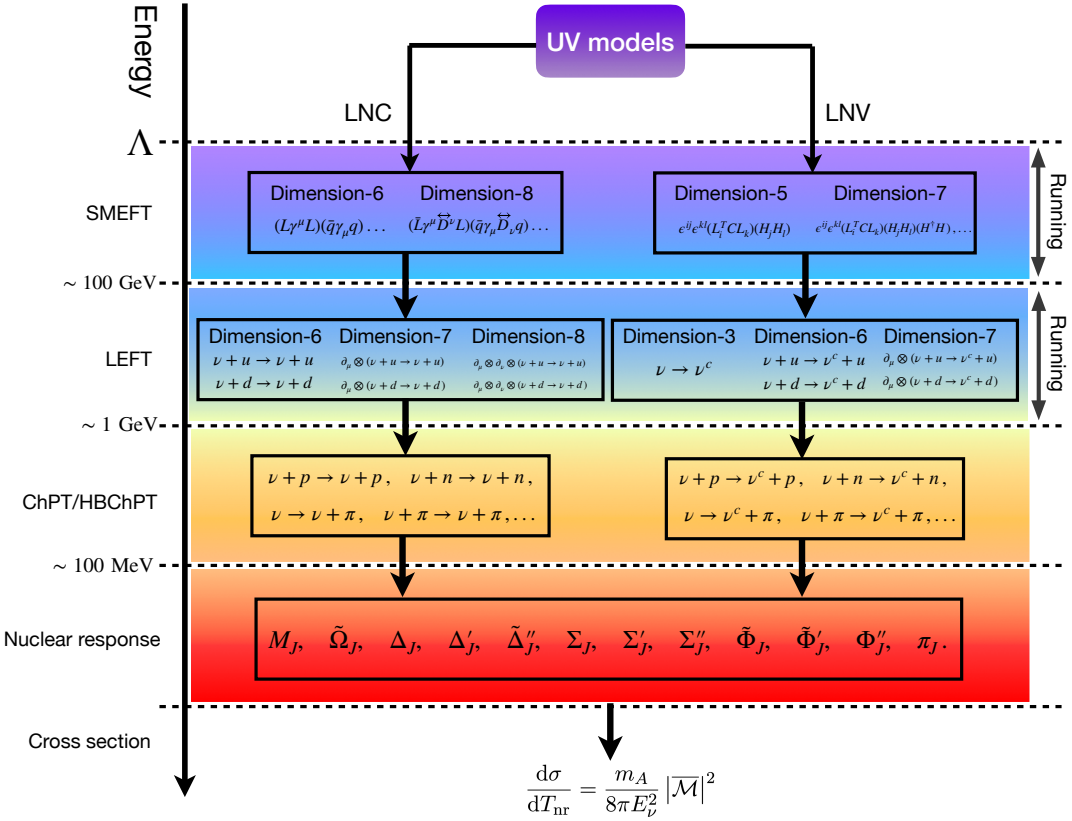


Figure 1: Effective field theory approach to evaluate the cross section of CE ν NS.

- A complete matching of the EFTs for CE ν NS across the relevant energy scales is accomplished, and the QCD renormalization-group (RG) running effects are included.
- A systematic power counting at different levels is developed. At hadronic level, it enables a clear comparison between contributions from one-body and two-body currents. At nuclear level, the CE ν NS cross section is enhanced by the nucleon number, which is incorporated via the nuclear response functions.
- Full tree-level UV completions for relevant SMEFT operators are provided, relating CE ν NS signals to the parameters of UV models.
- New constraints are derived from the latest CE ν NS observation by the CONUS+ experiment.

The remainder of this paper is organized as follows. In Sec. 2, we provide the LEFT operators for CE ν NS up to dimension 8, and the QCD RG running is considered. In Sec. 3, we perform the matching of the relevant LEFT operators onto the chiral effective Lagrangian using a systematic spurion method. The power counting from the electroweak scale down to

the hadronic scale is then discussed using a unified NDA master formula in Sec. 4. In Sec. 5, neutrino-nucleus scattering cross section is calculated in the approach of nuclear response function. In Sec. 6, the constraints on the NP scales as well as the NSI parameters are derived using the experimental measurements. In Sec. 7, we match the LEFT operators onto the SMEFT operators, and obtain various kinds of tree-level UV completions. We conclude in Sec. 8, and provide more details of the matching, NDA, LECs and chiral expansion in the appendices.

2 LEFT Operators

Starting from the scale below ~ 100 GeV, the effective Lagrangian in the LEFT can be written as

$$\mathcal{L}_{\text{LEFT}} = \sum_{d,a} \hat{\mathcal{C}}_a^d \mathcal{O}_a^d, \quad (2.1)$$

where \mathcal{O}_a^d denote the a -th independent LEFT operator of mass dimension d , and $\hat{\mathcal{C}}_a^d$ is the corresponding Wilson coefficient with mass dimension $4 - d$.

The lepton-number-conserving (LNC) operators up to dimension 8 are given by [66–68]

$$\mathcal{O}_1^{6u/d} = (\bar{\nu}_{L\alpha} \gamma^\mu \nu_{L\beta})(\bar{q} \gamma_\mu \tau^{u/d} q), \quad \mathcal{O}_2^{6u/d} = (\bar{\nu}_{L\alpha} \gamma^\mu \nu_{L\beta})(\bar{q} \gamma^5 \gamma_\mu \tau^{u/d} q), \quad (2.2)$$

$$\mathcal{O}_1^{7u/d} = (\bar{\nu}_{L\alpha} \gamma^\mu \nu_{L\beta})(\bar{q} \overset{\leftrightarrow}{D}_\mu \tau^{u/d} q), \quad \mathcal{O}_2^{7u/d} = (\bar{\nu}_{L\alpha} \gamma^\mu \nu_{L\beta})(\bar{q} \gamma^5 \overset{\leftrightarrow}{D}_\mu \tau^{u/d} q), \quad (2.3)$$

$$\mathcal{O}_1^{8u/d} = (\bar{\nu}_{L\alpha} \gamma^\mu \overset{\leftrightarrow}{D}^\nu \nu_{L\beta})(\bar{q} \gamma_\mu \overset{\leftrightarrow}{D}_\nu \tau^{u/d} q), \quad \mathcal{O}_2^{8u/d} = (\bar{\nu}_{L\alpha} \gamma^\mu \overset{\leftrightarrow}{D}^\nu \nu_{L\beta})(\bar{q} \gamma^5 \gamma_\mu \overset{\leftrightarrow}{D}_\nu \tau^{u/d} q), \quad (2.4)$$

$$\mathcal{O}_3^{8u/d} = (\bar{\nu}_{L\alpha} \gamma^\mu \nu_{L\beta})(\bar{q} \gamma^\nu T^A \tau^{u/d} q) G_{\mu\nu}^A, \quad \mathcal{O}_4^{8u/d} = (\bar{\nu}_{L\alpha} \gamma^\mu \nu_{L\beta})(\bar{q} \gamma^5 \gamma^\nu T^A \tau^{u/d} q) G_{\mu\nu}^A, \quad (2.5)$$

$$\mathcal{O}_5^{8u/d} = (\bar{\nu}_{L\alpha} \gamma^\mu \nu_{L\beta}) D^2 (\bar{q} \gamma_\mu \tau^{u/d} q), \quad \mathcal{O}_6^{8u/d} = (\bar{\nu}_{L\alpha} \gamma^\mu \nu_{L\beta}) D^2 (\bar{q} \gamma^5 \gamma_\mu \tau^{u/d} q), \quad (2.6)$$

$$\mathcal{O}_7^{8u/d} = (\bar{\nu}_{L\alpha} \gamma^\mu \nu_{L\beta})(\bar{q} \gamma^\nu T^A \tau^{u/d} q) \tilde{G}_{\mu\nu}^A, \quad \mathcal{O}_8^{8u/d} = (\bar{\nu}_{L\alpha} \gamma^\mu \nu_{L\beta})(\bar{q} \gamma^5 \gamma^\nu T^A \tau^{u/d} q) \tilde{G}_{\mu\nu}^A, \quad (2.7)$$

$$\mathcal{O}_9^8 = (\bar{\nu}_{L\alpha} \gamma^\mu \overset{\leftrightarrow}{D}^\nu \nu_{L\beta}) G_\mu^A G_\nu^{A\rho}. \quad (2.8)$$

In the above, the isospin doublet quark field $q = (u, d)^T$, and ν_L denotes the left-handed neutrino field, with Greek indices α and β labeling the neutrino flavors. The isospin projectors are defined as $\tau^{u/d} \equiv (1 \pm \tau^3)/2$, where τ^3 is the third Pauli matrix. The Hermitian derivative acting on a fermion bilinear is $\bar{\psi} \overset{\leftrightarrow}{D}^\mu \psi \equiv \bar{\psi} (D^\mu \psi) - (D^\mu \bar{\psi}) \psi$. The covariant derivative is

$$D_\mu = \partial_\mu + ig_3 T^A G_\mu^A + ieQ A_\mu, \quad (2.9)$$

where A_μ and G_μ^A represent the photon and gluon fields, respectively. eQ is the electromagnetic charge operator, g_3 is the strong coupling constant, and T^A ($A = 1, \dots, 8$) are the generators of the $SU(3)$ color group. The dual of the QCD field-strength tensor is defined as $\tilde{G}_{\mu\nu}^A = \frac{1}{2} \varepsilon_{\mu\nu}^{\rho\lambda} G_{\rho\lambda}^A$, with the Levi-Civita tensor $\varepsilon_{0123} = -1$.

The lepton-number-violating (LNV) operators up to dimension 7 are [67, 68]

$$\mathcal{O}_1^5 = \frac{e}{8\pi^2} (\nu_{L\alpha}^T C \sigma^{\mu\nu} \nu_{L\beta}) F_{\mu\nu}, \quad \mathcal{O}_3^{7u/d} = m_q (\nu_{L\alpha}^T C \sigma^{\mu\nu} \nu_{L\beta}) (\bar{q} \sigma_{\mu\nu} \tau^{u/d} q), \quad (2.10)$$

$$\mathcal{O}_4^{7u/d} = m_q (\nu_{L\alpha}^T C \nu_{L\beta}) (\bar{q} \tau^{u/d} q), \quad \mathcal{O}_5^{7u/d} = m_q (\nu_{L\alpha}^T C \nu_{L\beta}) (\bar{q} \gamma^5 \tau^{u/d} q), \quad (2.11)$$

$$\mathcal{O}_6^7 = \frac{\alpha_s}{\pi} (\nu_{L\alpha}^T C \nu_{L\beta}) G_{\mu\nu}^A G^{A\mu\nu}, \quad \mathcal{O}_7^7 = \frac{\alpha_s}{\pi} (\nu_{L\alpha}^T C \nu_{L\beta}) \tilde{G}_{\mu\nu}^A G^{A\mu\nu}, \quad (2.12)$$

Here, $F_{\mu\nu}$ denotes the electromagnetic field-strength tensor, α_s is the QCD coupling constant, and $C = i\gamma^0\gamma^2$ denotes the usual charge-conjugation matrix. The quark mass m_q corresponds to the flavor $q = u, d$. All these LNV operators vanish for the same neutrino flavor, $\alpha = \beta$.

The QCD RG running of the Wilson coefficients in Eq. (2.1) from the electroweak scale ~ 100 GeV to the hadronic scale ~ 1 GeV are given by [80, 81]

$$\frac{d}{d \ln \mu} \hat{\mathcal{C}}_3^{7u/d} = 2C_F \frac{\alpha_s}{4\pi} \hat{\mathcal{C}}_3^{7u/d}, \quad (2.13)$$

$$\frac{d}{d \ln \mu} \hat{\mathcal{C}}_{4,5}^{7u/d} = -6C_F \frac{\alpha_s}{4\pi} \hat{\mathcal{C}}_{4,5}^{7u/d}, \quad (2.14)$$

$$\frac{d}{d \ln \mu} \hat{\mathcal{C}}_{1,2}^{7u/d} = 2C_F \frac{\alpha_s}{4\pi} \hat{\mathcal{C}}_{1,2}^{7u/d}, \quad (2.15)$$

$$\frac{d}{d \ln \mu} \begin{pmatrix} \hat{\mathcal{C}}_{1,2}^{8u/d} \\ \hat{\mathcal{C}}_{5,6}^{8u/d} \end{pmatrix} = \frac{\alpha_s}{4\pi} \begin{pmatrix} -\frac{8}{3}C_F & 0 \\ \frac{4}{3}C_F & 0 \end{pmatrix} \begin{pmatrix} \hat{\mathcal{C}}_{1,2}^{8u/d} \\ \hat{\mathcal{C}}_{5,6}^{8u/d} \end{pmatrix}, \quad (2.16)$$

where $C_F \equiv (N_c^2 - 1)/(2N_c)$ with N_c being the color number. Note that the neutrino dipole operator and operators involving vector or axial-vector currents do not run in QCD. The RG running for the dimension-8 operators involving explicit gluon field-strength tensors are not available in the literature and are therefore not considered in this work.

3 Chiral Lagrangian

Having obtained the LEFT operators and considered the QCD RG running, the next step is to match the quark-level interactions onto a low-energy hadronic description at the scale $\Lambda_\chi \sim 1$ GeV in chiral perturbation theory (χ PT).

The spontaneous breaking of the chiral symmetry $SU(2)_L \times SU(2)_R$ down to its vector subgroup $SU(2)_V$ gives rise to three pseudo-Nambu-Goldstone bosons (pions). Within the Coleman-Callan-Wess-Zumino (CCWZ) coset construction [82, 83], these bosons are nonlinearly realized and are collectively parameterized by a unitary matrix field

$$u(x) = \exp \left(\frac{i\Pi(x)}{2f} \right), \quad (3.1)$$

where the Hermitian matrix $\Pi(x)$ contains the three pion fields

$$\Pi(x) = \sum_{a=1}^3 \phi^a(x) \tau^a = \begin{pmatrix} \pi^0 & \sqrt{2}\pi^+ \\ \sqrt{2}\pi^- & -\pi^0 \end{pmatrix}. \quad (3.2)$$

Here τ^a are the Pauli matrices and ϕ^a represent the three NGB degrees of freedom. Under chiral transformations, $u(x)$ transforms as $u(x) \rightarrow Ru(x)V^{-1} = Vu(x)L^{-1}$, with $L \in SU(2)_L$, $R \in SU(2)_R$, and $V \in SU(2)_V$ being the compensating transformation that preserves the vector subgroup. The constant $f \simeq 92$ MeV is the pion decay constant at leading order (LO) in the chiral expansion.

The matching between LEFT and χ PT has been systematically performed in Ref. [72]. Following that work, we define the following building blocks

$$\begin{aligned} u_\mu &= i(u^\dagger \partial_\mu u - u \partial_\mu u^\dagger), \\ \chi_\pm &= u^\dagger \chi u^\dagger \pm u \chi^\dagger u, \\ \Sigma_\pm &= u^\dagger \tau u^\dagger \pm u \tau u, \\ Q_\pm &= u^\dagger \tau u \pm u \tau u^\dagger, \\ \nabla_\mu &= \partial_\mu + \frac{1}{2}(u^\dagger \partial_\mu u + u \partial_\mu u^\dagger), \end{aligned} \quad (3.3)$$

where τ is the spurion corresponding to the matrix $\tau^{u/d}$ appearing in the LEFT operators. Notice that the covariant derivative ∇_μ and chiral vielbein u_μ do not contain the vector and axial-vector external sources. We have defined

$$\chi = 2B_0 \mathcal{M}_q, \quad \mathcal{M}_q \equiv \begin{pmatrix} m_u & 0 \\ 0 & m_d \end{pmatrix}, \quad (3.4)$$

where $B_0 \simeq 2.8$ GeV parameterizes the quark condensate and is evaluated at the scale $\mu = 2$ GeV. The C and P transformation properties of the building blocks are summarized in Tab. 1.

	Σ_+	Σ_-	Q_+	Q_-	χ_+	χ_-	u_μ
P	+	-	+	-	+	-	-
C	+	+	+	-	+	+	+

Table 1: The P and C transformation properties of the chiral building blocks.

In addition, the nucleon is included in χ PT and form a doublet N in the fundamental representation of $SU(2)_V$,

$$N = \begin{pmatrix} p \\ n \end{pmatrix}, \quad (3.5)$$

which transforms as $N \rightarrow VN$ under the chiral symmetry.

The chiral Lagrangian relies on an expansion in p/Λ_χ . However, each operator in the chiral Lagrangian comes with a LEC. Fortunately, several standard LECs—including those

associated with vector, axial-vector, scalar, and pseudo-scalar interactions—have been determined in hadronic physics. The unknown LECs for interactions involving higher-dimensional LEFT operators can be estimated using NDA.

3.1 Mesonic Sector

In the mesonic sector, we construct the chiral Lagrangian from the building blocks $(u_\mu, \Sigma_\pm, Q_\pm, \chi_\pm)$, together with covariant derivatives and neutrino fields. Moreover, LEFT operators involving gluons need to be matched onto the chiral Lagrangian. The matching of gluonic operators can be derived analogously using a systematic spurion method.

As a concrete illustration, we consider the dimension-8 operator $\mathcal{O}_3^{8u/d}$ in Eq. (2.2). The gluon field-strength tensor transforms trivially under the chiral symmetry, and is $C - P+$ under CP transformations. Thus, the chiral properties of $\mathcal{O}_3^{8u/d}$ are entirely determined by the quark-bilinear factor $(\bar{q}\gamma^\nu T^A \tau^{u/d} q)$. The relevant chiral building blocks are $(Q_\pm, u_\mu, \chi_\pm, \nu_L)$, which transform as $(VQ_\pm V^\dagger, Vu_\mu V^\dagger, V\chi_\pm V^\dagger, \nu_L)$ under chiral symmetry. Furthermore, the quark-gluon component of $\mathcal{O}_3^{8u/d}$ is $C + P+$, and the corresponding chiral operator must likewise possess identical CP transformation properties.

Chiral operators are constructed order-by-order in the chiral expansion, i.e., in powers of p/Λ_χ . At LO, the operator of type $\nu_L^2 Q_\pm u_\mu$ is constructed by the building blocks (u_μ, Q_\pm, ν_L) . Using Young tensor technique [64, 84, 85], the we obtain two chiral operators

$$\text{LO} : \quad (\bar{\nu}_{L\alpha} \gamma^\mu \nu_{L\beta}) \langle u_\mu Q_+ \rangle, \quad (\bar{\nu}_{L\alpha} \gamma^\mu \nu_{L\beta}) \langle u_\mu Q_- \rangle. \quad (3.6)$$

However, the hadronic parts of these two operators are $C + P-$ and $C - P+$, respectively, and are therefore incompatible with $\mathcal{O}_3^{8u/d}$. Therefore, next-to-leading order (NLO) chiral operators are required. We then construct the complete set of independent chiral operators of the types $\nu_L^2 Qu\chi$, $\nu_L^2 Qu^3$, and $\nu_L^2 Qu^2\nabla$ as

$$\begin{aligned} \text{NLO} : \quad & (\bar{\nu}_{L\alpha} \gamma^\mu \nu_{L\beta}) \langle u_\mu [Q_+, \chi_+] \rangle, \quad (\bar{\nu}_{L\alpha} \gamma^\mu \nu_{L\beta}) \langle u_\mu [Q_+, \chi_-] \rangle, \quad (\bar{\nu}_{L\alpha} \gamma^\mu \nu_{L\beta}) \langle u_\mu [Q_-, \chi_+] \rangle, \\ & (\bar{\nu}_{L\alpha} \gamma^\mu \nu_{L\beta}) \langle u_\mu [Q_-, \chi_-] \rangle, \quad (\bar{\nu}_{L\alpha} \gamma^\mu \nu_{L\beta}) \langle u_\mu Q_+ \rangle \langle u_\nu u^\nu \rangle, \quad (\bar{\nu}_{L\alpha} \gamma^\mu \nu_{L\beta}) \langle u_\mu Q_- \rangle \langle u_\nu u^\nu \rangle, \\ & (\bar{\nu}_{L\alpha} \gamma^\mu \nu_{L\beta}) \langle u_\nu Q_+ \rangle \langle u_\mu u^\nu \rangle, \quad (\bar{\nu}_{L\alpha} \gamma^\mu \nu_{L\beta}) \langle u_\nu Q_- \rangle \langle u_\mu u^\nu \rangle, \\ & (\bar{\nu}_{L\alpha} \gamma^\mu \nu_{L\beta}) \langle Q_+ [\nabla_\nu u_\mu, u^\nu] \rangle, \quad (\bar{\nu}_{L\alpha} \gamma^\mu \nu_{L\beta}) \langle Q_- [\nabla_\nu u_\mu, u^\nu] \rangle. \end{aligned} \quad (3.7)$$

Using the CP properties listed in Tab. 1, we identify a single chiral operator with $C + P+$ transformation properties:

$$(\bar{\nu}_{L\alpha} \gamma^\mu \nu_{L\beta}) \langle u_\mu [Q_-, \chi_+] \rangle. \quad (3.8)$$

Analogously, the corresponding chiral operators for $\mathcal{O}_{3,4,5,6,7,8}^{8u/d}$ can be derived. It is noted that $\mathcal{O}_{5,8}^{8u/d}$ and $\mathcal{O}_{6,7}^{8u/d}$ share identical CP properties and spurion structure with $\mathcal{O}_{1,2}^{6u/d}$. Consequently, these higher-dimensional operators yield the same chiral operators and therefore contribute to the same physical processes as the dimension-6 operators. However, the dimension-8

operators are always suppressed by a factor of order q^2/Λ^2 relative to their dimension-6 counterparts. For this reason, the matching between LEFT and χ PT for operators $\mathcal{O}_{5,6,7,8}^{8u/d}$ is omitted in the present analysis.

In particular, \mathcal{O}_6^7 , \mathcal{O}_7^7 and \mathcal{O}_8^8 contain no quark bilinear and therefore transform in the trivial representation of $SU(2)_L \times SU(2)_R$. Accordingly, the corresponding chiral building blocks are u_μ , χ_\pm , and ν_L , without additional spurions. The operator \mathcal{O}_7^7 is absorbed into the QCD θ term, which is removed by an anomalous chiral rotation, and this mesonic sector is neglected in this work, as it does not contribute to $\text{CE}\nu\text{NS}$ via the leading-order pion exchange. In addition, the covariant derivative D_μ in Eq. (2.9) reduces to ∂_μ in the matching procedure, owing to the intrinsic properties of neutrinos.

Different chiral operators come up with different LECs. In Ref. [72], the spurion method has been compared to the external source method, which allows us to extract LECs for the corresponding chiral operators. In addition, LEFT operators of dimension 7 and 8 are not included in the external source method; we therefore use NDA to estimate the corresponding LECs. Consequently, the matching results for the full set of LEFT operators in the mesonic sector can be written as

$$\begin{aligned}
\mathcal{L}_\pi = & \frac{f^2}{2} \hat{\mathcal{C}}_{1,2}^{6u/d} (\bar{\nu}_{L\alpha} \gamma^\mu \nu_{L\beta}) \langle Q_\mp u_\mu \rangle + \frac{f^2 B_0 m_q}{2} \hat{\mathcal{C}}_{4,5}^{7u/d} (\nu_{L\alpha}^T C \nu_{L\beta}) \langle \Sigma_\pm \rangle \\
& + \hat{\mathcal{C}}_3^{7u/d} \Lambda_2 (\nu_{L\alpha}^T C \sigma^{\mu\nu} \nu_{L\beta}) \langle \Sigma_+ [u_\mu, u_\nu] \rangle \\
& + \hat{\mathcal{C}}_{1,2}^{7u/d} (\bar{\nu}_{L\alpha} \gamma^\mu \nu_{L\beta}) \left\{ g_1^\pi \langle \Sigma_\pm [\nabla^\nu u_\mu, u_\nu] \rangle + g_2^\pi \langle \nabla^\nu \Sigma_\pm [u_\mu, u_\nu] \rangle \right. \\
& \quad \left. + g_3^\pi \langle \Sigma_\pm [u_\mu, \chi_-] \rangle + g_4^\pi \langle \Sigma_\mp [u_\mu, \chi_+] \rangle + g_5^\pi \varepsilon_{\mu\nu\rho\lambda} \langle u^\nu u^\rho \nabla^\lambda \Sigma_\mp \rangle \right\} \\
& + \hat{\mathcal{C}}_6^7 (\nu_{L\alpha}^T C \nu_{L\beta}) \left\{ a_1 \frac{f^2}{4} \langle u_\mu u^\mu \rangle + a_2 \frac{f^2}{4} \langle \chi_+ \rangle \right\} \\
& + \hat{\mathcal{C}}_{1,2}^{8u/d} g_6^\pi (\bar{\nu}_{L\alpha} \gamma^\mu \overset{\leftrightarrow}{\partial}^\nu \nu_{L\beta}) \langle Q_\pm \chi_+ \rangle \langle u_\mu u_\nu \rangle \\
& + \hat{\mathcal{C}}_{3,4}^{8u/d} g_7^\pi (\bar{\nu}_{L\alpha} \gamma^\mu \nu_{L\beta}) \langle u_\mu [Q_\mp, \chi_+] \rangle \\
& + \hat{\mathcal{C}}_9^{8u/d} g_8^\pi (\bar{\nu}_{L\alpha} \gamma^\mu \overset{\leftrightarrow}{\partial}^\nu \nu_{L\beta}) \langle u_\mu u_\nu \rangle + \dots, \tag{3.9}
\end{aligned}$$

where the tensor LEC is determined to be $\Lambda_2 = 8.99_{-0.23}^{+0.17}$ [86], the LECs $a_1 = 4/27$, $a_2 = 2/9$ [87], $(\nu_{L\alpha} \gamma^\mu \overset{\leftrightarrow}{\partial}^\nu \nu_{L\beta}) = (\partial^\nu \nu_{L\alpha} \gamma^\mu \nu_{L\beta}) - (\nu_{L\alpha} \gamma^\mu \partial^\nu \nu_{L\beta})$. The dots denote terms that are of higher orders in the chiral expansion and are omitted.

The u/d designation of the LEFT Wilson coefficients is tied to the spurion structure defined in Eq. (2.2) via $\tau^{u/d}$. Furthermore, the subscript index of each Wilson coefficient corresponds to the \pm designation of the associated spurion. For instance, $\hat{\mathcal{C}}_1^{6u/d}$ corresponds to the chiral operator $(\bar{\nu}_{L\alpha} \gamma^\mu \nu_{L\beta}) \langle Q_- u_\mu \rangle$ and $\hat{\mathcal{C}}_2^{6u/d}$ corresponds to $(\bar{\nu}_{L\alpha} \gamma^\mu \nu_{L\beta}) \langle Q_+ u_\mu \rangle$. The unknown LECs g_1^π , g_2^π , g_3^π , g_4^π , g_5^π , g_6^π , g_7^π , g_8^π are estimated through NDA as detailed in App. B and the full results are summarized in Tab. 2.

3.2 Nucleon Sector

In the nucleon sector, the nucleon field N is included as a degree of freedom in the fundamental representation of $SU(2)_V$ which is similar with Ref. [73]. All building blocks transform as

$$\begin{pmatrix} \chi_{\pm} \\ \Sigma_{\pm} \\ Q_{\pm} \\ N \\ \bar{N} \\ \nu_L \\ \bar{\nu}_L \end{pmatrix} \rightarrow \begin{pmatrix} V\chi_{\pm}V^{\dagger} \\ V\Sigma_{\pm}V^{\dagger} \\ VQ_{\pm}V^{\dagger} \\ VN \\ \bar{N}V^{\dagger} \\ \nu_L \\ \bar{\nu}_L \end{pmatrix}, \quad V \in SU(2)_V, \quad (3.10)$$

under the chiral symmetry. With the above framework established, the interactions within the nucleon sector are systematically constructed through Young tensor technique. As a representative example, we consider the type $N^2\nu^2Q$. The complete set of chiral operators at LO is given by

$$\begin{aligned} (\bar{\nu}_{L\alpha}\gamma^{\mu}\nu_{L\beta})(\bar{N}\gamma_{\mu}Q_{\pm}N), & \quad (\bar{\nu}_{L\alpha}\gamma^{\mu}\nu_{L\beta})(\bar{N}\gamma_{\mu}N)\langle Q_{\pm} \rangle, \\ (\bar{\nu}_{L\alpha}\gamma^{\mu}\nu_{L\beta})(\bar{N}\gamma^5\gamma_{\mu}Q_{\pm}N), & \quad (\bar{\nu}_{L\alpha}\gamma^{\mu}\nu_{L\beta})(\bar{N}\gamma^5\gamma_{\mu}N)\langle Q_{\pm} \rangle, \\ (\nu_{L\alpha}^T C \nu_{L\beta})(\bar{N}Q_{\pm}N), & \quad (\nu_{L\alpha}^T C \nu_{L\beta})(\bar{N}N)\langle Q_{\pm} \rangle, \\ (\nu_{L\alpha}^T C \nu_{L\beta})(\bar{N}\gamma^5Q_{\pm}N), & \quad (\nu_{L\alpha}^T C \nu_{L\beta})(\bar{N}\gamma^5N)\langle Q_{\pm} \rangle, \\ (\nu_{L\alpha}^T C \sigma^{\mu\nu}\nu_{L\beta})(\bar{N}\sigma_{\mu\nu}Q_{\pm}N), & \quad (\nu_{L\alpha}^T C \sigma^{\mu\nu}\nu_{L\beta})(\bar{N}\sigma_{\mu\nu}N)\langle Q_{\pm} \rangle, \end{aligned} \quad (3.11)$$

which correspond to some dimension-6 LEFT operators. For operator $\mathcal{O}_1^{6u/d}$, we construct the following LO hadronic operators with $C - P+$ symmetry that contain the neutrino current $(\bar{\nu}_{L\alpha}\gamma^{\mu}\nu_{L\beta})$:

$$\begin{aligned} (\bar{\nu}_{L\alpha}\gamma^{\mu}\nu_{L\beta})(\bar{N}\gamma_{\mu}Q_{+}N), & \quad (\bar{\nu}_{L\alpha}\gamma^{\mu}\nu_{L\beta})(\bar{N}\gamma_{\mu}N)\langle Q_{+} \rangle, \\ (\bar{\nu}_{L\alpha}\gamma^{\mu}\nu_{L\beta})(\bar{N}\gamma^5\gamma_{\mu}Q_{-}N), & \quad (\bar{\nu}_{L\alpha}\gamma^{\mu}\nu_{L\beta})(\bar{N}\gamma^5\gamma_{\mu}N)\langle Q_{-} \rangle, \end{aligned} \quad (3.12)$$

where only the first two terms are considered in this work after performing the power counting for the whole process. Thus, only the interactions without pions that contribute directly to neutrino-nucleon interactions are calculated in the framework of this analysis.

In this work, we also include iso-singlet currents in the chiral operators; therefore the building blocks $\langle Q_{\pm} \rangle$ are retained. We can then obtain the chiral operators for LEFT operators without explicit pions; the corresponding Wilson coefficients and LECs are included as

follows

$$\begin{aligned}
\mathcal{L}_{\pi N} = & \hat{\mathcal{C}}_1^{6u/d} (\bar{\nu}_{L\alpha} \gamma^\mu \nu_{L\beta}) \left\{ (\bar{N} \gamma_\mu Q_+ N) + (\bar{N} \gamma_\mu N) \langle Q_+ \rangle + \frac{L_1}{m_N} \partial^\nu (\bar{N} \sigma_{\mu\nu} Q_+ N) \right. \\
& + \frac{L_2}{m_N} \partial^\nu (\bar{N} \sigma_{\mu\nu} N) \langle Q_+ \rangle \left. \right\} + \hat{\mathcal{C}}_2^{6u/d} (\bar{\nu}_{L\alpha} \gamma^\mu \nu_{L\beta}) \left\{ L_3 (\bar{N} \gamma^5 \gamma_\mu Q_+ N) + L_4 (\bar{N} \gamma^5 \gamma_\mu N) \langle Q_+ \rangle \right\} \\
& + \hat{\mathcal{C}}_3^{7u/d} (\nu_{L\alpha}^T C \sigma^{\mu\nu} \nu_{L\beta}) \left\{ L_5 (\bar{N} \sigma_{\mu\nu} \Sigma_+ N) + L_6 (\bar{N} \sigma_{\mu\nu} N) \langle \Sigma_+ \rangle + \frac{L_7}{m_N} \partial_\nu (\bar{N} \gamma_\mu \Sigma_+ N) \right. \\
& + \frac{L_8}{m_N} \partial_\nu (\bar{N} \gamma_\mu N) \langle \Sigma_+ \rangle \left. \right\} + \hat{\mathcal{C}}_4^{7u/d} (\nu_{L\alpha}^T C \nu_{L\beta}) \left\{ L_9 (\bar{N} \Sigma_+ N) + L_{10} (\bar{N} N) \langle \Sigma_+ \rangle \right\} \\
& + \hat{\mathcal{C}}_5^{7u/d} (\nu_{L\alpha}^T C \nu_{L\beta}) \left\{ L_{11} (\bar{N} \gamma^5 \Sigma_+ N) + L_{12} (\bar{N} \gamma^5 N) \langle \Sigma_+ \rangle \right\} \\
& + \hat{\mathcal{C}}_6^{7u/d} (\bar{\nu}_{L\alpha} \gamma^\mu \nu_{L\beta}) (\bar{N} N) + \hat{\mathcal{C}}_7^{7u/d} (\nu_{L\alpha}^T C \nu_{L\beta}) (\bar{N} \gamma^5 N) \\
& + \hat{\mathcal{C}}_1^{7u/d} (\bar{\nu}_{L\alpha} \gamma^\mu \nu_{L\beta}) \left\{ g_1 (\bar{N} \gamma_\mu \Sigma_+ N) + g_2 (\bar{N} \gamma_\mu N) \langle \Sigma_+ \rangle \right\} \\
& + \hat{\mathcal{C}}_2^{7u/d} (\bar{\nu}_{L\alpha} \gamma^\mu \nu_{L\beta}) \left\{ \frac{g_3}{m_N} \partial^\nu (\bar{N} i \gamma^5 \sigma_{\mu\nu} \Sigma_+ N) + \frac{g_4}{m_N} \partial^\nu (\bar{N} i \gamma^5 \sigma_{\mu\nu} N) \langle \Sigma_+ \rangle \right\} \\
& + \hat{\mathcal{C}}_1^{8u/d} (\bar{\nu}_{L\alpha} \gamma^\mu \overset{\leftrightarrow}{\partial} \nu_{L\beta}) \left\{ g_5 (\bar{N} \gamma_\mu \overset{\leftrightarrow}{\partial}_\nu Q_+ N) + g_6 (\bar{N} \gamma^\mu \overset{\leftrightarrow}{\partial}_\nu N) \langle Q_+ \rangle \right\} \\
& + \hat{\mathcal{C}}_2^{8u/d} (\bar{\nu}_{L\alpha} \gamma^\mu \overset{\leftrightarrow}{\partial} \nu_{L\beta}) \left\{ g_7 (\bar{N} \gamma^5 \gamma_\mu \overset{\leftrightarrow}{\partial}_\nu Q_+ N) + g_8 (\bar{N} \gamma^5 \gamma_\mu \overset{\leftrightarrow}{\partial}_\nu N) \langle Q_+ \rangle \right\} \\
& + \hat{\mathcal{C}}_9^{8u/d} (\bar{\nu}_{L\alpha} \gamma^\mu \overset{\leftrightarrow}{\partial} \nu_{L\beta}) (\bar{N} \gamma_\mu \overset{\leftrightarrow}{\partial}_\nu N) + \dots, \tag{3.13}
\end{aligned}$$

where the LECs $L_{1\sim 14}$ can be calculated from experiment and lattice QCD results, and the details of these LECs have been discussed in App. C. The other LECs $g_{1\sim 9}$, which involve derivative dimension-7 and dimension-8 LEFT operators, can be estimated by NDA. The complete LECs are listed in Tab. 2. Moreover, the chiral operators of $\mathcal{O}_{3,4}^{8u/d}$ are not presented in Eq. (3.13), because the chiral operators of $\mathcal{O}_{3,4}^{8u/d}$ can not contribute to the neutrino-nucleon interactions directly and are highly suppressed.

Moreover, the chiral expansion p/Λ_χ is invalid due to heavy nucleon mass $m_N \sim \Lambda_\chi$ of the nucleon field. The heavy baryon form [88, 89] is needed for the nucleon field. According to the discussion above, the baryon is so heavy that it is non-relativistic when interacting with other degrees of freedom. It is therefore natural to expand the operators containing baryons in terms of the inverse of their mass $1/m_N$. For any time-like vector v^μ satisfying $v^2 = 1$, we can define the projection operators as $P_v^\pm = (1 + \not{v})/2$, and the Dirac spinors are expressed as

$$\Psi(x) = e^{-imv \cdot x} \left[\underbrace{e^{imv \cdot x} P_v^+ \Psi(x)}_{\equiv N_v(x)} + \underbrace{e^{imv \cdot x} P_v^- \Psi(x)}_{\equiv \mathcal{H}_v(x)} \right]. \tag{3.14}$$

Then a general pion-nucleon interaction is expanded as

$$\mathcal{L}_{\pi N} = \bar{N}_v A N_v + \bar{\mathcal{H}}_v B N_v + \bar{N}_v \gamma^0 B^\dagger \gamma^0 \mathcal{H}_v - \bar{\mathcal{H}}_v C \mathcal{H}_v, \tag{3.15}$$

LEC	value	LEC	value
$B_0 m_u$	$(6200 \pm 400) \text{ MeV}^2$	$B_0 m_d$	$(13300 \pm 400) \text{ MeV}^2$
L_1	$1.355(14)$	L_2	$-1.535(10)$
L_3	$0.6377(7)$	L_4	$-0.220(10)$
L_5	$0.41(17) \text{ MeV}$	L_6	$0.49(80) \text{ MeV}$
L_7	$-1.68(25) \text{ MeV}$	L_8	$0.88(20) \text{ MeV}$
L_9	$11.52(25) \text{ MeV}$	L_{10}	$24.05(48) \text{ MeV}$
L_{11}	$-42.96(24) \text{ MeV}$	L_{12}	$-36.75(36) \text{ MeV}$
L_{13}	$-50.4(6) \text{ MeV}$	L_{14}	$-0.306(28) \text{ GeV}$
g_1^π	$\mathcal{O}(\Lambda_\chi)$	g_2^π	$\mathcal{O}(\Lambda_\chi)$
g_3^π	$\mathcal{O}(\Lambda_\chi)$	g_4^π	$\mathcal{O}(\Lambda_\chi)$
g_5^π	$\mathcal{O}(\Lambda_\chi)$	g_6^π	$\mathcal{O}(1)$
g_7^π	$\mathcal{O}(\Lambda_\chi^2)$	g_8^π	$\mathcal{O}(\Lambda_\chi^2)$
g_1	$\mathcal{O}(\Lambda_\chi)$	g_2	$\mathcal{O}(\Lambda_\chi)$
g_3	$\mathcal{O}(\Lambda_\chi)$	g_4	$\mathcal{O}(\Lambda_\chi)$
g_5	$\mathcal{O}(1)$	g_6	$\mathcal{O}(1)$
g_7	$\mathcal{O}(1)$	g_8	$\mathcal{O}(1)$
g_9	$\mathcal{O}(1)$		

Table 2: Values of the LECs required for CE ν NS. More details are given in App. C. The unknown LECs are estimated using NDA.

where A , B , C are composed of the mesonic fields. Integrating out the heavy component \mathcal{H}_v , and expanding C^{-1} in inverse power of the nucleon mass, the Lagrangian is expanded in terms of N_v [90, 91],

$$\begin{aligned} \mathcal{L}_{\pi N} \rightarrow & \bar{N}_v (A + \gamma^0 B^\dagger \gamma^0 C^{-1}) N_v \\ &= \bar{N}_v (A^{(1)} + A^{(2)} + \frac{1}{2m_N} \gamma^0 B^{\dagger(1)} \gamma^0 B^{(1)} + \dots) N_v. \end{aligned} \quad (3.16)$$

Then the power counting for the pion-nucleon interaction is consistent with the chiral La-

grangian. In the heavy baryon framework, the nucleon bilinear can be expanded as

$$\begin{aligned}
\bar{N}1N &= \bar{N}_v 1 N_v + \dots, \\
\bar{N}\gamma^5 N &= \frac{1}{m_N} \partial_\mu (\bar{N}_v S^\mu N_v) + \dots, \\
\bar{N}\gamma^\mu N &= \bar{N}_v v^\mu N_v + \frac{1}{2m_N} \bar{N}_v (i \overleftrightarrow{\partial}^\mu - v^\mu \not{v}) N_v - \frac{1}{m_N} \varepsilon^{\mu\nu\rho\lambda} \partial_\nu (\bar{N}_v v_\rho S_\lambda N_v) + \dots, \\
\bar{N}\gamma^5 \gamma^\mu N &= 2\bar{N}_v S^\mu N_v - \frac{i}{m_N} v^\mu \bar{N}_v S^\nu \overleftrightarrow{\partial}_\nu N_v \dots, \\
\bar{N}\sigma^{\mu\nu} N &= -2\varepsilon^{\mu\nu\rho\lambda} \bar{N}_v v_\rho S_\lambda N_v - \frac{1}{2m_N} (2i\varepsilon^{\mu\rho\lambda\sigma} \bar{N}_v v_\sigma [S_\lambda, v^\nu] \overleftrightarrow{\partial}_\rho u N_v + [v^\mu, \partial^\nu] (\bar{N}_v N_v)) \dots, \\
\bar{N}i \overleftrightarrow{D}^\mu N &= \bar{N}_v v^\mu N_v + \frac{1}{2m_N} \bar{N}_v i \overleftrightarrow{\partial}^\mu N_v - \frac{1}{m_N} \varepsilon^{\mu\nu\rho\lambda} \partial_\nu (\bar{N}_v v_\rho S_\lambda N_v) + \dots,
\end{aligned} \tag{3.17}$$

where v_μ is the four-velocity of the nucleon N_v , S_μ is the spin-operator of the nucleon, and the dots denote terms that are of higher order in the chiral expansion. The four-velocity v_μ and spin-operator satisfy the relations

$$S^\mu = \frac{i}{2} \gamma^5 \sigma^{\mu\nu} v^\nu, \quad S \cdot v = 0, \quad \{S^\mu, S^\nu\} = \frac{1}{2} (v^\mu v^\nu - g^{\mu\nu}), \quad [S^\mu, S^\nu] = i \varepsilon^{\mu\nu\rho\lambda} v_\rho S_\lambda. \tag{3.18}$$

Thus, we consider the non-relativistic pion-nucleon interactions in the chiral expansion framework. Here, we expand the pion-nucleon interactions to $1/m_N$ order in the heavy baryon

approach. Thus, the involved chiral operators can be selected as

$$\begin{aligned}
\mathcal{L}_{\pi N}^{\text{HB}} = & \hat{\mathcal{C}}_1^{6u/d}(\bar{\nu}_{L\alpha}\gamma^\mu\nu_{L\beta}) \left\{ (\bar{N}_v v_\mu Q_+ N_v) + \frac{1}{2m_N} (\bar{N}_v i \overset{\leftrightarrow}{\partial}^\mu Q_+ N_v) - \frac{1+2L_1}{m_N} \varepsilon^{\mu\nu\rho\lambda} \partial_\nu (\bar{N}_v v_\rho S_\lambda Q_+ N_v) \right\} \\
& + \hat{\mathcal{C}}_1^{6u/d}(\bar{\nu}_{L\alpha}\gamma^\mu\nu_{L\beta}) \left\{ (\bar{N}_v v_\mu N_v) \langle Q_+ \rangle + \frac{1}{2m_N} (\bar{N}_v i \overset{\leftrightarrow}{\partial}^\mu N_v) \langle Q_+ \rangle - \frac{1+2L_2}{m_N} \varepsilon^{\mu\nu\rho\lambda} \partial_\nu (\bar{N}_v v_\rho S_\lambda N_v) \langle Q_+ \rangle \right\} \\
& + \hat{\mathcal{C}}_2^{6u/d}(\bar{\nu}_{L\alpha}\gamma^\mu\nu_{L\beta}) \left\{ 2L_3 (\bar{N}_v S_\mu Q_+ N_v) - \frac{L_3}{m_N} (\bar{N}_v v^\mu S^\nu i \overset{\leftrightarrow}{\partial}_\nu Q_+ N_v) \right\} \\
& + \hat{\mathcal{C}}_2^{6u/d}(\bar{\nu}_{L\alpha}\gamma^\mu\nu_{L\beta}) \left\{ 2L_4 (\bar{N}_v S_\mu N_v) \langle Q_+ \rangle - \frac{L_4}{m_N} (\bar{N}_v v^\mu S^\nu i \overset{\leftrightarrow}{\partial}_\nu N_v) \langle Q_+ \rangle \right\} \\
& - \hat{\mathcal{C}}_3^{7u/d}(\nu_{L\alpha}^T C \sigma^{\mu\nu} \nu_{L\beta}) \left\{ 2L_5 (\bar{N}_v v_\mu S_\nu \Sigma_+ N_v) + \frac{L_5}{m_N} \varepsilon^{\mu\rho\lambda\sigma} \bar{N}_v v_\sigma S_\lambda v^\nu i \overset{\leftrightarrow}{\partial}_\rho \Sigma_+ N_v \right. \\
& \quad \left. + \frac{L_5 + L_7}{m_N} \partial_\mu (\bar{N}_v v_\nu \Sigma_+ N_v) \right\} - \hat{\mathcal{C}}_3^{7u/d} g_1^{\pi N} (\nu_{L\alpha}^T C \sigma^{\mu\nu} \nu_{L\beta}) \left\{ 2L_6 (\bar{N}_v v_\mu S_\nu N_v) \langle \Sigma_+ \rangle \right. \\
& \quad \left. + \frac{L_6}{m_N} \varepsilon^{\mu\rho\lambda\sigma} (\bar{N}_v v_\sigma S_\lambda v^\nu i \overset{\leftrightarrow}{\partial}_\rho N_v) \langle \Sigma_+ \rangle + \frac{L_6 + L_8}{m_N} \partial_\mu (\bar{N}_v v_\nu N_v) \langle \Sigma_+ \rangle \right\} \\
& + \hat{\mathcal{C}}_4^{7u/d}(\nu_{L\alpha}^T C \nu_{L\beta}) \left\{ L_9 (\bar{N}_v \Sigma_+ N_v) + L_{10} (\bar{N}_v N_v) \langle \Sigma_+ \rangle \right\} \\
& + \hat{\mathcal{C}}_5^{7u/d}(\nu_{L\alpha}^T C \nu_{L\beta}) \left\{ \frac{L_{11}}{m_N} \partial^\mu (\bar{N}_v S_\mu \Sigma_+ N_v) + \frac{L_{12}}{m_N} \partial^\mu (\bar{N}_v S_\mu N_v) \langle \Sigma_+ \rangle \right\} \\
& + \hat{\mathcal{C}}_6^{7u/d}(\nu_{L\alpha}^T C \nu_{L\beta}) (\bar{N}_v N_v) + \hat{\mathcal{C}}_7^{7u/d} \frac{L_{14}}{m_N} (\nu_{L\alpha}^T C \nu_{L\beta}) \partial^\mu (\bar{N}_v S_\mu N_v) \\
& + \hat{\mathcal{C}}_1^{7u/d}(\bar{\nu}_{L\alpha}\gamma^\mu\nu_{L\beta}) \left\{ g_1 (\bar{N}_v v_\mu \Sigma_+ N_v) + g_2 (\bar{N}_v v_\mu N_v) \langle \Sigma_+ \rangle \right\} \\
& + \hat{\mathcal{C}}_2^{7u/d}(\bar{\nu}_{L\alpha}\gamma^\mu\nu_{L\beta}) \left\{ \frac{2g_3}{m_N} \partial^\nu (\bar{N}_v S_{[\nu} v_{\mu]} \Sigma_+ N_v) + \frac{2g_4}{m_N} \partial^\nu (\bar{N}_v S_{[\nu} v_{\mu]} N_v) \langle \Sigma_+ \rangle \right\} \\
& + \hat{\mathcal{C}}_1^{8u/d}(\bar{\nu}_{L\alpha}\gamma^\mu \overset{\leftrightarrow}{\partial}^\nu \nu_{L\beta}) \left\{ g_5 (\bar{N}_v v_\mu v_\nu Q_+ N_v) + g_6 (\bar{N}_v v_\mu v_\nu N_v) \langle Q_+ \rangle \right\} \\
& + \hat{\mathcal{C}}_2^{8u/d}(\bar{\nu}_{L\alpha}\gamma^\mu \overset{\leftrightarrow}{\partial}^\nu \nu_{L\beta}) \left\{ 2g_7 (\bar{N}_v S_\mu v_\nu Q_+ N_v) + 2g_8 (\bar{N}_v S_\mu v_\nu N_v) \langle Q_+ \rangle \right\} \\
& + \hat{\mathcal{C}}_9^{8u/d}(\bar{\nu}_{L\alpha}\gamma^\mu \overset{\leftrightarrow}{\partial}^\nu \nu_{L\beta}) (\bar{N}_v v_\mu v_\nu N_v) + \dots, \tag{3.19}
\end{aligned}$$

where the dots denote terms that are of higher order in the chiral expansion and are omitted.

In addition, the standard pion-nucleon Lagrangian has been constructed and we consider the LO for the pion-nucleon interaction

$$\mathcal{L}_{\pi N} = (\bar{N}_v i v_\mu \nabla^\mu + g_A S_\mu u^\mu N_v). \tag{3.20}$$

There is also the photon-hadron interaction generated from the QED covariant derivative. These interactions are given by

$$\begin{aligned}
\mathcal{L}_{\pi N}^{\text{QED}} = & A^\mu (\bar{N}_v v_\mu Q_+^A N_v) + \frac{\varepsilon_{\mu\nu\rho\lambda}}{m_N} \partial^\nu A^\mu \left[g_\mu (\bar{N}_v v^\rho S^\lambda Q_+^A N_v) + g'_\mu (\bar{N}_v v^\rho S^\lambda N_v) \langle Q_+^A \rangle \right] + \dots, \tag{3.21}
\end{aligned}$$

where A_μ is the photon field, and Q_+^A is the spurion. The dots denote terms that are of higher orders in the chiral expansion and are omitted. Here, the two spurions interactions will not be considered which contribute to the higher-order. Moreover, the last two terms can contribute to the proton and neutron magnetic moments ($\mu^p/m_N, \mu^n/m_N$). Thus, the values of the coefficients g_μ and g'_μ should be fixed to $g_\mu = \mu^p - \mu^n$ and $g'_\mu = \mu^p + 2\mu^n$.

4 Power Counting in LEFT and χ PT

At low energies, neutrino-nucleus scattering is described within χ PT. We adopt Weinberg power counting [92–97], in which amplitudes are organized as an expansion in a soft momentum scale q relative to the chiral scale Λ_χ , and use this counting to estimate the size of different contributions to CE ν NS. The procedure consists of two steps. First, we determine the chiral order of each vertex by expanding the chiral building blocks that appear in the operators. Second, we combine the vertex orders with the topology of a given diagram to obtain the overall scaling of the corresponding contribution.

For each LEFT operator in Eqs. (2.2), (2.10), and (3.13), the momentum dependence of the associated vertices follows from the χ PT expansion of the building blocks appearing in the corresponding chiral operators. The standard blocks ($u_\mu, \Sigma_\pm, Q_\pm, \chi_\pm, \nabla_\mu$) have been introduced above, and their explicit expansions are summarized in App. A. At leading chiral order, $u_\mu, \Sigma_-, Q_-,$ and χ_- start at $\mathcal{O}(\pi)$ and therefore contain an odd number of pion fields, whereas $\nabla_\mu, \Sigma_+, Q_+,$ and χ_+ contain an even number of pion fields and include a nonvanishing pion-independent term. Each pion field attached to a vertex contributes a factor $1/(2f)$, so that a term with n_π pion fields carries an additional factor $[1/(2f)]^{n_\pi}$. The overall normalization of the induced chiral operators is fixed using the NDA matching rules [73, 75, 76] given in App. B; representative estimates are given in Tab. 2. In addition, insertions proportional to the light-quark mass m_q count as $\mathcal{O}(q^2)$.

As an explicit example of vertex counting, consider the chiral operator

$$\hat{\mathcal{C}}_1^{6u/d} (\bar{\nu}_{L\alpha} \gamma^\mu \nu_{L\beta}) \langle Q_- u_\mu \rangle. \quad (4.1)$$

According to the NDA matching rule in Eq. (B.6), its overall normalization scales as $(\Lambda_\chi/\Lambda_{\text{EW}})^2$ where Λ_{EW} denotes the scale corresponding to LEFT operators. The leading nonvanishing contribution arises from the two-pion term with $n_\pi = 2$, which supplies a factor $[1/(2f)]^2$. Moreover, u_μ contains one derivative and therefore contributes a factor $\mathcal{O}(q)$. The leading two-pion vertex thus scales as

$$\left(\frac{\Lambda_\chi}{\Lambda_{\text{EW}}}\right)^2 \left(\frac{q}{\Lambda_\chi}\right) \left(\frac{1}{2f}\right)^2. \quad (4.2)$$

For the full scattering process, power counting requires not only vertex scaling but also the scaling associated with propagators, loops, and diagram topology. In multi-nucleon systems, intermediate states can include purely nucleonic configurations in which nucleons interact through pion exchange and short-range contact interactions. In Weinberg power counting,

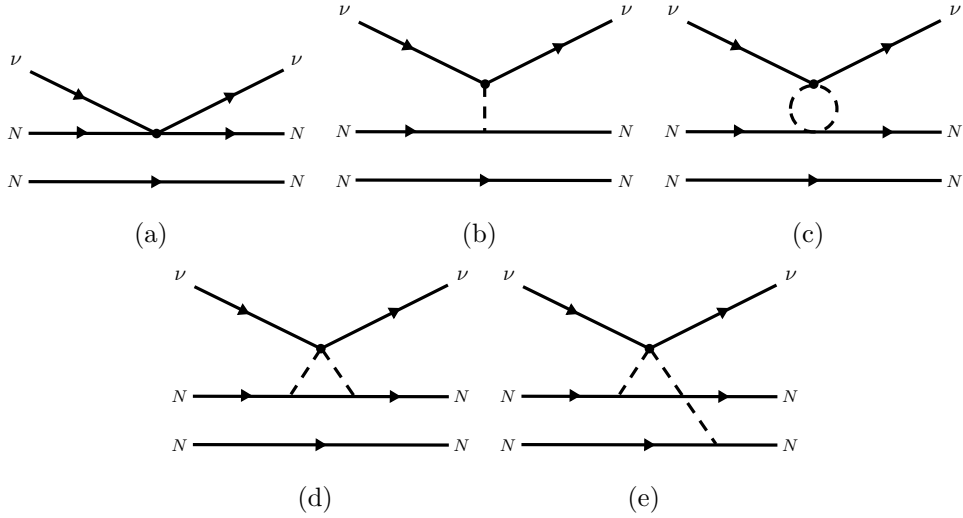


Figure 2: Diagrams (a) and (b) show the leading-order one-body current contributions. Diagrams (c) and (d) show loop corrections to the one-body current. Diagram (e) shows the two-body current contribution.

the pion mass is counted as soft, $m_\pi \sim \mathcal{O}(q)$ [92–94, 97]. For irreducible diagrams, i.e. diagrams that do not contain purely nucleonic intermediate states that can go on shell, pion and nucleon propagators scale as $1/q^2$ and $1/q$, respectively, and each loop contributes a factor $q^4/(16\pi^2)$. For reducible diagrams, which do contain purely nucleonic intermediate states, the non-relativistic nucleon propagator scales as m_N/q^2 , each loop contributes $q^5/(16\pi^2 m_N)$, and pion propagators still scale as $1/q^2$ [95].

Different chiral operators contribute to different topologies in Fig. 2 because the expansions of the operators contain different numbers of pion fields. Operators whose leading term involves no pion fields generate one-body νN contact currents in diagram (a), whereas operators whose leading term contains a single pion field induce long-range contributions mediated by single-pion exchange in diagram (b). In the following, we work at leading order with the mesonic Lagrangian in Eq. (3.9) and the pion-nucleon Lagrangian in Eq. (3.19). NP effects enter only through semileptonic LEFT operators acting on the leptonic current, while all πN vertices are from the SM.

Separating the operator normalization from the chiral order generated by vertices, propagators, and loops, we write the parametric scaling as

$$\left(\frac{\Lambda_\chi}{\Lambda_{\text{EW}}}\right)^{d-4} \left(\frac{q}{\Lambda_\chi}\right)^n \left(\frac{q}{m_N}\right)^m \sim \mathcal{O}(\Lambda_{\text{EW}}^{4-d}) \cdot \mathcal{O}(\Lambda_\chi^{-n}) \cdot \mathcal{O}(m_N^{-m}), \quad (4.3)$$

for an amplitude induced by a dimension- d LEFT operator, where the overall factor $(\Lambda_\chi/\Lambda_{\text{EW}})^{d-4}$ is fixed by the operator dimension and follows from the NDA matching rules. The integer n collects the chiral suppression in powers of q/Λ_χ arising from derivatives, insertions of m_π , and the counting of propagators and loops. For bookkeeping, the integer m

tracks explicit $1/m_N$ effects from the heavy baryon χ PT Lagrangian, written as a separate factor $(q/m_N)^m$.

Applying this counting to the diagrams in Fig. 2, we focus on the leading contributions induced by dimension-6 LEFT operators, which carry the electroweak suppression $\mathcal{O}(\Lambda_{\text{EW}}^{-2})$. We further retain only the leading term in the $1/m_N$ expansion, i.e. $\mathcal{O}(m_N^0)$. Under these assumptions, the one-current tree-level contributions in Fig. 2 (a) and (b) scale as

$$\mathcal{O}(\Lambda_{\text{EW}}^{-2}) \cdot \mathcal{O}(\Lambda_\chi^0) \cdot \mathcal{O}(m_N^0). \quad (4.4)$$

The one-current one-loop diagrams in Fig. 2 (c) and (d) scale as

$$\mathcal{O}(\Lambda_{\text{EW}}^{-2}) \cdot \mathcal{O}(\Lambda_\chi^{-2}) \cdot \mathcal{O}(m_N^0). \quad (4.5)$$

The two-body current diagram in Fig. 2 (e) is irreducible and has the same scaling,

$$\mathcal{O}(\Lambda_{\text{EW}}^{-2}) \cdot \mathcal{O}(\Lambda_\chi^{-2}) \cdot \mathcal{O}(m_N^0). \quad (4.6)$$

Thus, diagrams (a) and (b) contribute at the same chiral order, while the one-current one-loop diagrams (c) and (d) and the two-body tree-level diagram (e) are suppressed by two additional powers of q/Λ_χ with respect to the leading one-current tree-level diagrams. Diagrams with three currents or with two loops are further suppressed in our power counting and will not be considered. The corresponding chiral orders for one- and two-body neutrino-nucleus currents induced by different LEFT operators can be expressed in terms of $\varepsilon_\chi \equiv q/\Lambda_\chi$ and $\varepsilon_N \equiv q/m_N$ and are summarized in Tab. 3.

In summary, Tab. 3 shows that all dimension-6 operators that contribute to one-body tree-level currents enter at the same chiral order as diagrams (a) and (b), while loop-induced one-body corrections and two-body currents are suppressed by at least two additional powers of q/Λ_χ . Dimension-7 and dimension-8 operators can generate chiral structures analogous to those from dimension-6 operators; despite the additional $(\Lambda_\chi/\Lambda_{\text{EW}})$ suppression, their ultraviolet origin may differ, so their contributions are not necessarily negligible in well-motivated scenarios.

With this in mind, in the following analysis we retain the leading one-body currents in Fig. 2 (a) and (b), and defer a systematic treatment of subleading chiral corrections to the discussion after nuclear correlations are introduced in the next section.

LEFT operators	One-body (a)	One-body (b)	Two-body (c, d)	Two-body (e)
$\mathcal{O}_1^{6u/d}$	1	—	ε_χ^2	ε_χ^2
$\mathcal{O}_2^{6u/d}$	1	1	—	—
$\mathcal{O}_1^{7u/d}$	1	—	ε_χ^2	ε_χ^2
$\mathcal{O}_2^{7u/d}$	ε_m	—	ε_χ^2	ε_χ^2
$\mathcal{O}_3^{7u/d}$	ε_χ^2	—	ε_χ^4	ε_χ^4
$\mathcal{O}_4^{7u/d}$	ε_χ^2	—	ε_χ^4	ε_χ^4
$\mathcal{O}_5^{7u/d}$	$\varepsilon_\chi^2 \varepsilon_m$	ε_χ^4	—	—
$\mathcal{O}_6^{7u/d}$	ε_χ^2	—	ε_χ^4	ε_χ^4
$\mathcal{O}_7^{7u/d}$	$\varepsilon_\chi^2 \varepsilon_m$	ε_χ^4	—	—
$\mathcal{O}_1^{8u/d}$	1	—	ε_χ^2	ε_χ^2
$\mathcal{O}_2^{8u/d}$	1	—	—	—
$\mathcal{O}_9^{8u/d}$	1	—	ε_χ^2	ε_χ^2

Table 3: Chiral power counting for one- and two-body neutrino-nucleus currents induced by LEFT operators. Entries indicate the leading suppression in powers of q/Λ_χ and q/m_N in the amplitude, as in Eq. (4.3); we define $\varepsilon_\chi \equiv q/\Lambda_\chi$ and $\varepsilon_N \equiv q/m_N$. The one-body tree-level currents define the leading chiral order, while one-body one-loop corrections and two-body currents appear at higher orders as indicated.

5 Neutrino-Nucleus Scattering Cross Section

Having established the power counting for CE ν NS, we derive the leading one-body non-relativistic neutrino-nucleon interactions from the chiral Lagrangian and express the scattering amplitude in terms of nuclear response functions using a multipole expansion [98, 99] to obtain the differential cross section.

5.1 Interactions of Neutrinos with Non-relativistic Nucleons

The power counting for neutrino-nucleus scattering implies that one-body contributions dominate. We therefore restrict our analysis to one-body currents, leaving the inclusion of two-body currents to future work. From diagrams (a) and (b) in Fig. 2, the neutrino interaction with non-relativistic nucleons is described by the effective Lagrangian

$$\mathcal{L}_{\text{NR}} = c_{i,N} \mathcal{O}_{i,N}, \quad (5.1)$$

where $N = p, n$ labels the nucleon species. The momenta of the incoming and outgoing neutrinos (nucleons) are denoted by p_1 and p_2 (k_1 and k_2), and we define

$$q = p_1 - p_2, \quad P = p_1 + p_2, \quad K = k_1 + k_2. \quad (5.2)$$

The nuclear recoil energy is defined as $T_{\text{nr}} = |q^0|$, where q^0 is the zero component of the momentum transfer q . The incoming neutrino energy is $E_\nu = p_1^0$.

The non-relativistic neutrino-nucleon interactions are obtained by evaluating the Feynman diagrams (a) and (b) in Fig. 2 using the chiral Lagrangian introduced in Sec. 3. The neutrino-nucleon interaction terms in Eq. (3.19) contribute directly to diagram (a). In addition, diagram (b) receives contributions from the neutrino-pion interactions in Eq. (3.9) together with the pion-nucleon interactions in Eq. (3.20). Moreover, the dipole operator \mathcal{O}_1^5 induces neutrino-nucleon interactions via the photon-nucleon couplings in Eq. (3.21). Consequently, the corresponding NR operators are given by

$$\mathcal{O}_{1,p} = (\nu_{L\alpha} \gamma^\mu \nu_{L\beta}) v_\mu (\bar{p}_v p_v), \quad \mathcal{O}_{2,p} = (\nu_{L\alpha} \gamma^\mu \nu_{L\beta}) (\bar{p}_v S_\mu p_v), \quad (5.3)$$

$$\mathcal{O}_{3,p} = (\nu_{L\alpha}^T C \nu_{L\beta}) (\bar{p}_v p_v), \quad \mathcal{O}_{4,p} = (\nu_{L\alpha}^T C \sigma^{\mu\nu} \nu_{L\beta}) v_\nu (\bar{p}_v S_\mu p_v), \quad (5.4)$$

$$\mathcal{O}_{5,p} = (\nu_{L\alpha} \gamma^\mu \nu_{L\beta}) (\bar{p}_v \frac{K^\mu}{2m_N} p_v), \quad \mathcal{O}_{6,p} = \varepsilon_{\mu\nu\rho\lambda} (\nu_{L\alpha} \gamma^\mu \nu_{L\beta}) v^\rho (\bar{p}_v \frac{q^\nu S^\lambda}{m_N} p_v), \quad (5.5)$$

$$\mathcal{O}_{7,p} = (\nu_{L\alpha} \gamma^\mu \nu_{L\beta}) v_\mu (\bar{p}_v \frac{K_\nu S^\nu}{2m_N} p_v), \quad \mathcal{O}_{8,p} = \varepsilon_{\mu\rho\lambda\sigma} (\nu_{L\alpha}^T C \sigma^{\mu\nu} \nu_{L\beta}) v_\nu v_\sigma (\bar{p}_v \frac{K^\rho S^\lambda}{m_N} p_v), \quad (5.6)$$

$$\mathcal{O}_{9,p} = (\nu_{L\alpha}^T C \sigma^{\mu\nu} \nu_{L\beta}) v_\nu (\bar{p}_v \frac{q_\mu}{m_N} p_v), \quad \mathcal{O}_{10,p} = (\nu_{L\alpha}^T C \nu_{L\beta}) (\bar{p}_v \frac{S^\mu q_\mu}{m_N} p_v), \quad (5.7)$$

$$\mathcal{O}_{11,p} = (\nu_{L\alpha} \gamma^\mu \nu_{L\beta}) v_\mu (\bar{p}_v \frac{q^\nu S_\nu}{m_N} p_v), \quad \mathcal{O}_{12,p} = \varepsilon_{\mu\nu\rho\lambda} (\nu_{L\alpha}^T C \nu_{L\beta}) \frac{P^\mu q^\nu}{m_N^2} v^\rho (\bar{p}_v S^\lambda p_v), \quad (5.8)$$

$$\mathcal{O}_{13,p} = (\nu_{L\alpha} \gamma^\mu \nu_{L\beta}) P^\nu v_\mu v_\nu (\bar{p}_v p_v), \quad \mathcal{O}_{14,p} = (\nu_{L\alpha} \gamma^\mu \nu_{L\beta}) P^\nu v_\nu (\bar{p}_v S_\mu p_v). \quad (5.9)$$

According to the chiral operators in Sec. 3, the corresponding coefficients are

$$c_{1,p} = 2\hat{\mathcal{C}}_1^{6u} + \hat{\mathcal{C}}_1^{6d} + (g_1 + g_2)\hat{\mathcal{C}}_1^{7u} + g_2\hat{\mathcal{C}}_1^{7d}, \quad (5.10)$$

$$c_{2,p} = 2(L_3 + L_4)\hat{\mathcal{C}}_2^{6u} + 2L_4\hat{\mathcal{C}}_2^{6d}, \quad (5.11)$$

$$c_{3,p} = \sigma_u^p\hat{\mathcal{C}}_4^{7u} + \sigma_d^p\hat{\mathcal{C}}_4^{7d} + L_{13}\hat{\mathcal{C}}_6^7 - \frac{2\alpha\bar{E}_\nu}{\pi q^2}\hat{\mathcal{C}}_1^5, \quad (5.12)$$

$$c_{4,p} = 2(L_5 + L_6)\hat{\mathcal{C}}_3^{7u} + 2L_6\hat{\mathcal{C}}_3^{7d}, \quad (5.13)$$

$$c_{5,p} = 2\hat{\mathcal{C}}_1^{6u} + \hat{\mathcal{C}}_1^{6d}, \quad (5.14)$$

$$c_{6,p} = (2 + 2L_1 + 2L_2)\hat{\mathcal{C}}_1^{6u} + (1 + 2L_2)\hat{\mathcal{C}}_1^{6d}, \quad (5.15)$$

$$c_{7,p} = 2(L_3 + L_4)\hat{\mathcal{C}}_2^{6u} + 2L_4\hat{\mathcal{C}}_2^{6d}, \quad (5.16)$$

$$c_{8,p} = (L_5 + L_6)\hat{\mathcal{C}}_3^{7u} + L_6\hat{\mathcal{C}}_3^{7d}, \quad (5.17)$$

$$c_{9,p} = (L_5 + L_6 + L_7 + L_8)\hat{\mathcal{C}}_3^{7u} + (L_6 + L_8)\hat{\mathcal{C}}_3^{7d}, \quad (5.18)$$

$$c_{10,p} = \frac{B_0 g_A}{m_\pi^2 - q^2} (m_u\hat{\mathcal{C}}_5^{7u} - m_u\hat{\mathcal{C}}_5^{7d}) + (L_{11} + L_{12})\hat{\mathcal{C}}_5^{7u} + L_{12}\hat{\mathcal{C}}_5^{7d} + L_{14}\hat{\mathcal{C}}_7^7, \quad (5.19)$$

$$c_{11,p} = 4(g_3 + g_4)\hat{\mathcal{C}}_2^{7u} + 4g_4\hat{\mathcal{C}}_2^{7d}, \quad (5.20)$$

$$c_{12,p} = \frac{\alpha m_N}{3\pi q^2} (1 + 2L_1)\hat{\mathcal{C}}_1^5, \quad (5.21)$$

$$c_{13,p} = (g_5 + g_6)\hat{\mathcal{C}}_1^{8u} + g_6\hat{\mathcal{C}}_1^{8d} + g_9\hat{\mathcal{C}}_9^8, \quad (5.22)$$

$$c_{14,p} = 2(g_7 + g_8)\hat{\mathcal{C}}_1^{8u} + 2g_8\hat{\mathcal{C}}_1^{8d}, \quad (5.23)$$

where \bar{E}_ν is the average energy of the neutrino before and after scattering. It should be emphasized that there exists explicit isospin breaking in the scalar current, and the chiral Lagrangian is insufficient to describe the quark-nucleon matching process comprehensively. The matching relation between the scalar quark current and the nucleon current has been derived as follows [100–103]

$$\begin{aligned} \sigma_u^p &= 16.3(2.5) \text{ MeV}, \sigma_d^p = 30.6(4.2) \text{ MeV}, \\ \sigma_u^n &= 14.5(2.2) \text{ MeV}, \sigma_d^n = 34.5(4.0) \text{ MeV}. \end{aligned} \quad (5.24)$$

The operators $\mathcal{O}_{3,p}$ and $\mathcal{O}_{12,p}$ can be generated via photon exchange induced by the QED dipole operator \mathcal{O}_1^5 . The SM photon-nucleon interactions are given in Eq. (3.21). Notably, for neutron scattering, the contribution mediated by \mathcal{O}_1^5 does not generate $\mathcal{O}_{3,n}$ because the neutron carries zero electric charge. In addition, the pseudo-scalar current can contribute to the neutrino-nucleon interactions via the pion exchange, while its direct contact contributions are at the NLO relative to the pion-exchange channel. Both types of contributions are included in our analysis. However, the axial-vector current contributions arising from pion exchange are proportional to the neutrino masses and are therefore neglected.

5.2 Nuclear Response

With the one-body neutrino-nucleon interaction specified, we now incorporate nuclear-structure effects by performing a multipole expansion of the nuclear current. The effective

operators can be written as matrix elements between external neutrino and nuclear states. Since the neutrino is ultra-relativistic while nucleons inside the nucleus are well described in the non-relativistic limit, we factorize the matrix element into leptonic and hadronic pieces,

$$\langle f | \mathcal{O} | i \rangle \sim \langle \nu'_{L\alpha} | \mathcal{O}_\nu | \nu_{L\beta} \rangle \langle N' | \mathcal{O}_N | N \rangle, \quad (5.25)$$

where $\langle f |$ and $|i\rangle$ denote the final and initial states, respectively, and $|N\rangle = |p\rangle, |n\rangle$ denotes a proton or neutron state.

We formulate the nuclear dynamics in terms of non-relativistic three-vector components. In the laboratory frame, the nucleon four-velocity is $v^\mu = (1, 0, 0, 0)$, which contracts with the neutrino Dirac structures. The spin four-vector S_μ then reduces to the three-component nucleon spin vector \mathbf{S}_N . The momentum transfer q_μ can be identified with its spatial component \mathbf{q} , while K_μ corresponds to the nucleon three-momentum \mathbf{K}_N . The NR operators are classified into the charge (ℓ_0), axial charge (ℓ_0^A), axial vector (ℓ_5), vector magnetic (ℓ_M) and vector electric (ℓ_E) [77, 78], where the ℓ presents the neutrino bilinear concluding the coefficients:

$$\ell_0 \cdot 1_N + \ell_5 \cdot (2\mathbf{S}_N) + \ell_{0,A} \cdot \left(\frac{\mathbf{K} \cdot \mathbf{S}_N}{m_N} \right) + \ell_M \cdot \left(\frac{\mathbf{K}_N}{2m_N} \right) + \ell_E \cdot \left(-i \frac{\mathbf{K} \times \mathbf{S}_N}{m_N} \right), \quad (5.26)$$

where $1_N = \bar{N}N$, $\mathbf{S}_N = \bar{N}\mathbf{S}N$, $\mathbf{K}_N = \bar{N}\mathbf{K}N$. The operators containing nucleus information (\mathbf{K} , \mathbf{S}) can be separated as follows:

$$\left\{ 1_N, 2\mathbf{S}_N, \frac{\mathbf{K} \cdot \mathbf{S}_N}{m_N}, \frac{\mathbf{K}}{2m_N}, -i \frac{\mathbf{K}_N \times \mathbf{S}_N}{m_N} \right\}. \quad (5.27)$$

The remaining coefficients and the neutrino bilinears do not carry any information about the nuclear structure and are therefore grouped into the leptonic structure introduced above. In our framework, the operators 1_N and $2\mathbf{S}_N$ arise already at leading order in the chiral expansion, while the operators with the momentum-dependent structures $\mathbf{K} \cdot \mathbf{S}_N/m_N$, $\mathbf{K}/(2m_N)$ and $-i\mathbf{K}_N \times \mathbf{S}_N/m_N$ are suppressed by one power of $1/m_N$.

The nuclear operators are local density operators in coordinate space and the matrix element can be written as a Fourier transform,

$$\langle f | \mathcal{O} | i \rangle \rightarrow \langle \nu'_{L\alpha} | \mathcal{O}_\nu | \nu_{L\beta} \rangle \int d\mathbf{x} e^{-i\mathbf{q} \cdot \mathbf{x}} \langle N' | \mathcal{O}_N(\mathbf{x}) | N \rangle. \quad (5.28)$$

In neutrino-nucleus scattering, assuming that the nucleus remains unexcited and in an eigenstate of total angular momentum $|j_N\rangle$, the nuclear matrix element $e^{-i\mathbf{q} \cdot \mathbf{x}} \langle j_{N'} | \mathcal{O}_N(\mathbf{x}) | j_N \rangle$ can be expanded in multipoles. The multipole operators can be expressed in terms of eleven single-particle operators [77, 78, 98, 104, 105]

$$M_J, \tilde{\Omega}_J, \Delta_J, \Delta'_J, \tilde{\Delta}''_J, \Sigma_J, \Sigma'_J, \Sigma''_J, \tilde{\Phi}_J, \tilde{\Phi}'_J, \Phi''_J. \quad (5.29)$$

If we restrict the nuclear ground state to have good parity and CP symmetry, the matrix elements $\langle j_{N'} | O | j_N \rangle$ vanish for $O = \tilde{\Omega}_J, \Sigma_J, \Delta'_J, \tilde{\Delta}''_J, \tilde{\Phi}_J$. These operators therefore do not contribute to the scattering amplitude. The non-vanishing single-particle operators are

$$M_J, \Delta_J, \Sigma'_J, \Sigma''_J, \tilde{\Phi}'_J, \Phi''_J. \quad (5.30)$$

The operator M_J is related to the total number (or charge) of nucleons in the nucleus, while the operators Σ'_J and Σ''_J are associated with the nuclear spin. These three responses receive contributions from leading-order chiral operators and are not suppressed in the chiral expansion. In contrast, the operators Δ_J , $\tilde{\Phi}'_J$ and Φ''_J arise from NLO chiral interactions and are suppressed by $\mathcal{O}(1/m_N)$.

The many-body nuclear matrix elements can be expressed in terms of one-body density matrices¹. They are parametrized through nuclear response functions,

$$W_{OO'} = \sum_J \langle j_{N'} | O_J | j_N \rangle \langle j_{N'} | O'_J | j_N \rangle. \quad (5.31)$$

In terms of these response functions, the spin-averaged squared amplitude can be written as

$$\begin{aligned} |\overline{\mathcal{M}}|^2 = & \frac{4\pi}{2J_A + 1} \sum_{\tau, \tau'} \left\{ \left[R_{MM}^{\tau\tau'} W_{MM}^{\tau\tau'}(y) + R_{\Sigma''\Sigma''}^{\tau\tau'} W_{\Sigma''\Sigma''}^{\tau\tau'}(y) + R_{\Sigma'\Sigma'}^{\tau\tau'} W_{\Sigma'\Sigma'}^{\tau\tau'}(y) \right] \right. \\ & + \frac{|\mathbf{q}|^2}{m_N^2} \left[R_{\Phi''\Phi''}^{\tau\tau'} W_{\Phi''\Phi''}^{\tau\tau'}(y) + R_{\tilde{\Phi}'\tilde{\Phi}'}^{\tau\tau'} W_{\tilde{\Phi}'\tilde{\Phi}'}^{\tau\tau'}(y) + R_{\Delta\Delta}^{\tau\tau'} W_{\Delta\Delta}^{\tau\tau'}(y) \right] \\ & \left. - \frac{2|\mathbf{q}|}{m_N} \left[R_{\Phi''M}^{\tau\tau'} W_{\Phi''M}^{\tau\tau'}(y) + R_{\Delta\Sigma'}^{\tau\tau'} W_{\Delta\Sigma'}^{\tau\tau'}(y) \right] \right\}, \end{aligned} \quad (5.32)$$

where $y = (|\mathbf{q}|b/2)^2$ with b the harmonic-oscillator parameter, and $\hat{q} = \mathbf{q}/|\mathbf{q}|$. The indices $\tau, \tau' = 0, 1$ label isoscalar and isovector components, and J_A denotes the spin of the target nucleus.

In this context, the amplitude squared can be separated into the kinematic terms ($R^{\tau\tau'}$) and the nuclear response functions ($W^{\tau\tau'}$). The expressions of R are

$$\begin{aligned} R_{MM}^{\tau\tau'} &= l_0^\tau l_0^{\tau'\dagger}, \\ R_{\Sigma''\Sigma''}^{\tau\tau'} &= (\hat{q} \cdot \mathbf{l}_5^\tau) (\hat{q} \cdot \mathbf{l}_5^{\tau'\dagger}), \\ R_{\Sigma'\Sigma'}^{\tau\tau'} &= \frac{1}{2} (\mathbf{l}_5^\tau \cdot \mathbf{l}_5^{\tau'\dagger} - \hat{q} \cdot \mathbf{l}_5^\tau \hat{q} \cdot \mathbf{l}_5^{\tau'\dagger}), \\ R_{\Phi''\Phi''}^{\tau\tau'} &= (\hat{q} \cdot \mathbf{l}_E^\tau) (\hat{q} \cdot \mathbf{l}_E^{\tau'\dagger}), \\ R_{\tilde{\Phi}'\tilde{\Phi}'}^{\tau\tau'} &= \frac{1}{2} (\mathbf{l}_E^\tau \cdot \mathbf{l}_E^{\tau'\dagger} - \hat{q} \cdot \mathbf{l}_E^\tau \hat{q} \cdot \mathbf{l}_E^{\tau'\dagger}), \\ R_{\Delta\Delta}^{\tau\tau'} &= \frac{1}{2} (\mathbf{l}_M^\tau \cdot \mathbf{l}_M^{\tau'\dagger} - \hat{q} \cdot \mathbf{l}_M^\tau \hat{q} \cdot \mathbf{l}_M^{\tau'\dagger}), \\ R_{\Phi''M}^{\tau\tau'} &= \hat{q} \cdot \text{Re} [\mathbf{l}_E^\tau l_0^{\tau'\dagger}], \\ R_{\Delta\Sigma'}^{\tau\tau'} &= 2\hat{q} \cdot \text{Re} [i\mathbf{l}_M^\tau \times \mathbf{l}_5^{\tau'\dagger}], \end{aligned} \quad (5.33)$$

¹Details of the one-body density matrices are given in App. D.

where l_0^τ , l_5^τ , l_M^τ and l_E^τ denote the neutrino matrix elements (including the corresponding Wilson coefficients) of the leptonic structures introduced in Eq. (5.26).

In the long-wavelength limit, the nuclear response functions W_{MM} , $W_{\Phi''\Phi''}$ and $W_{\Phi''M}$ receive coherent enhancement proportional to the nucleon number (nuclear number enhancement). In contrast, the responses $W_{\Sigma''\Sigma''}$, $W_{\Sigma'\Sigma'}$, $W_{\tilde{\Phi}'\tilde{\Phi}'}$, $W_{\Delta\Delta}$ and $W_{\Delta\Sigma'}$ do not exhibit such enhancement and become phenomenologically important in regimes where the spin-independent contribution is suppressed.

LEFT operators		Response function	Nuclear effect
$\mathcal{O}_1^{6u/d}$	$(\bar{\nu}_{L\alpha}\gamma^\mu\nu_{L\beta})(\bar{q}\gamma_\mu\tau^{u/d}q)$	W_{MM}	A
		$W_{\Sigma'\Sigma'}, W_{\Sigma''\Sigma''}$	1
		$W_{\Delta\Delta}$	$\mathcal{O}(m_N^{-1}) \cdot 1$
		$W_{\Delta\Sigma'}$	$\mathcal{O}(m_N^{-1}) \cdot 1$
$\mathcal{O}_2^{6u/d}$	$(\bar{\nu}_{L\alpha}\gamma^\mu\nu_{L\beta})(\bar{q}\gamma^5\gamma_\mu\tau^{u/d}q)$	$W_{\Sigma'\Sigma'}, W_{\Sigma''\Sigma''}$	1
$\mathcal{O}_1^{7u/d}$	$(\bar{\nu}_{L\alpha}\gamma^\mu\nu_{L\beta})(\bar{q}\overset{\leftrightarrow}{\partial}_\mu\tau^{u/d}q)$	W_{MM}	A
$\mathcal{O}_2^{7u/d}$	$(\bar{\nu}_{L\alpha}\gamma^\mu\nu_{L\beta})(\bar{q}\gamma^5\overset{\leftrightarrow}{\partial}_\mu\tau^{u/d}q)$	$W_{\Sigma'\Sigma'}, W_{\Sigma''\Sigma''}$	1
$\mathcal{O}_3^{7u/d}$	$m_q(\nu_{L\alpha}^T C \sigma^{\mu\nu} \nu_{L\beta})(\bar{q}\sigma_{\mu\nu}\tau^{u/d}q)$	W_{MM}	$\mathcal{O}(m_N^{-1}) \cdot A$
		$W_{\Sigma'\Sigma'}, W_{\Sigma''\Sigma''}$	1
		$W_{\Phi''\Phi''}$	$\mathcal{O}(m_N^{-2}) \cdot A$
		$W_{\tilde{\Phi}'\tilde{\Phi}'}$	$\mathcal{O}(m_N^{-2}) \cdot 1$
$\mathcal{O}_4^{7u/d}$	$m_q(\nu_{L\alpha}^T C \nu_{L\beta})(\bar{q}\tau^{u/d}q)$	$W_{\Phi''M}$	$\mathcal{O}(m_N^{-2}) \cdot A$
		W_{MM}	A
		$W_{\Sigma'\Sigma'}, W_{\Sigma''\Sigma''}$	1
		W_{MM}	A
$\mathcal{O}_6^{7u/d}$	$(\nu_{L\alpha}^T C \nu_{L\beta})G_{\mu\nu}^A G^{A\mu\nu}$	$W_{\Sigma'\Sigma'}, W_{\Sigma''\Sigma''}$	1
$\mathcal{O}_7^{7u/d}$	$(\nu_{L\alpha}^T C \nu_{L\beta})\tilde{G}_{\mu\nu}^A G^{A\mu\nu}$	W_{MM}	A
$\mathcal{O}_1^{8u/d}$	$(\bar{\nu}_{L\alpha}\gamma^\mu\overset{\leftrightarrow}{\partial}^\nu\nu_{L\beta})(\bar{q}\gamma_\mu\overset{\leftrightarrow}{\partial}_\nu\tau^{u/d}q)$	$W_{\Sigma'\Sigma'}, W_{\Sigma''\Sigma''}$	1
		W_{MM}	A
		$W_{\Phi''M}$	$\mathcal{O}(m_N^{-1}) \cdot A^2$
		W_{MM}	A
$\mathcal{O}_3^{8u/d}$	$(\bar{\nu}_{L\alpha}\gamma^\mu\overset{\leftrightarrow}{\partial}^\nu\nu_{L\beta})G_{\mu\rho}^A G_\nu^{A\rho}$	W_{MM}	A

Table 4: Power counting for the LEFT operators, including the relevant response functions and coherent nuclear enhancement effects, for contributions of overall order $\mathcal{O}(\Lambda_\chi^0)$. Here only the leading coherent enhancement is considered, and $\mathcal{O}(m_N^0)$ is abbreviated as $\mathcal{O}(1)$.

Collecting the above results, we can summarize the relative sizes of the nuclear responses as follows. The response W_{MM} receives a fully coherent enhancement and scales as $W_{MM} \sim A^2$, where A represent the number of nucleons. The interference term $(q/m_N) W_{\Phi''M}$ is also coherently enhanced, but carries an additional factor of $1/m_N$, so that it scales as $(q/m_N) W_{\Phi''M} \sim \mathcal{O}(m_N^{-1}) \cdot A^2$. The response $(q^2/m_N^2) W_{\Phi''\Phi''}$ is likewise coherently enhanced, but suppressed by $\mathcal{O}(m_N^{-2}) \cdot A^2$ in the chiral expansion. In contrast, the responses $W_{\Sigma'\Sigma'}$ and

$W_{\Sigma''\Sigma''}$ do not receive coherent enhancement and are of order $\mathcal{O}(1)$. When the leading-order operators do not generate a coherently enhanced contribution, subleading chiral operators that do so can become phenomenologically important. For this reason we retain the contribution $(q^2/m_N^2) W_{\Phi''\Phi''} \sim \mathcal{O}(m_N^{-2}) \cdot A^2$. The remaining response functions are even more suppressed.

Restricting ourselves to the long-wavelength limit and keeping only the chiral order and coherent enhancement, we treat $\mathcal{O}(m_N^{-2}) \cdot A^2$ and $\mathcal{O}(1)$ as parametrically comparable. The hierarchy of responses can then be written schematically as

$$\begin{aligned} W_{MM} &\gg \frac{q}{m_N} W_{\Phi''M} \gg \left\{ W_{\Sigma'\Sigma'}, W_{\Sigma''\Sigma''}, \frac{q^2}{m_N^2} W_{MM}, \frac{q^2}{m_N^2} W_{\Phi''\Phi''} \right\} \\ &\gg \left\{ \frac{q}{m_N} W_{\Delta\Sigma'}, \frac{q^2}{m_N^2} W_{\Delta\Delta}, \frac{q^2}{m_N^2} W_{\tilde{\Phi}'\tilde{\Phi}'} \right\}. \end{aligned} \quad (5.34)$$

More specifically, for large nuclei and sufficiently high momentum transfer the scaling $\mathcal{O}(m_N^{-2}) \cdot A^2$ can become larger than $\mathcal{O}(1)$. In this regime the explicit factors of $|\mathbf{q}|/m_N$ and $|\mathbf{q}|^2/m_N^2$ provide an additional momentum enhancement, so that the terms $(q/m_N) W_{\Phi''M}$ and $(q^2/m_N^2) W_{\Phi''\Phi''}$ yield momentum-dependent corrections to the leading coherent contribution W_{MM} .

Including these response-function enhancements allows us to perform a rough dimensional analysis of the tree-level diagram (a), summarized in Tab. 4. There we see that the vector LEFT operators $\mathcal{O}_1^{6u/d}$ induce coherently enhanced contributions already at leading chiral order. Although the dimension-7 and dimension-8 operators are suppressed by powers of the electroweak scale, it is possible that new physics contributes only to these higher-dimensional LEFT operators. The scalar operators $\mathcal{O}_4^{7u/d}$ are also coherently enhanced at leading chiral order. In particular, the tensor operators $\mathcal{O}_3^{7u/d}$ do not receive coherent enhancement at leading chiral order for $W_{\Sigma'\Sigma'}, W_{\Sigma''\Sigma''}$. However, NLO chiral operators generate coherently enhanced contributions $\mathcal{O}(m_N^{-1}) \cdot A$ that can even dominate over the leading chiral order terms which are consistent with the tensor-current enhancement reported in Ref. [27]. From the other leading-order chiral power counting, we find that the operators $\mathcal{O}_1^{7u/d}$, $\mathcal{O}_6^{7u/d}$, $\mathcal{O}_1^{8u/d}$, and $\mathcal{O}_9^{8u/d}$ are coherently enhanced.

For diagram (b), the nucleon current is proportional to $\bar{N}S^\mu N$ and therefore does not give rise to coherent enhancement. Its contribution is purely subleading and mainly provides a controlled correction to the leading-order diagram (a).

5.3 Cross Section for Neutrino-Nucleus Scattering

In a typical neutrino detection experiment the target nuclei are at rest in the laboratory frame. The differential scattering cross section with respect to the nuclear recoil energy T_{nr} is then given by

$$\frac{d\sigma}{dT_{\text{nr}}} = \frac{m_A}{8\pi E_\nu^2} |\bar{\mathcal{M}}|^2, \quad (5.35)$$

where m_A is the mass of the target nucleus. Here $|\bar{\mathcal{M}}|^2$ stands for the squared scattering amplitude, summed over final spins and averaged over the initial nuclear spin projections.

According to Eq. (5.26) the neutrino-nucleon interaction can be organized in terms of the five leptonic Dirac structures l ($l_0, l_5, l_0^A, l_M, l_E$) each accompanied by appropriate Wilson coefficients for the specific process under consideration. The leading one-body contribution to the scattering amplitude diagram (a) and (b) in Fig. 2 can be written as

$$\mathcal{M} = \ell_0 \cdot \bar{N} N + \ell_5 \cdot (\bar{N} 2\mathbf{S} N) + \ell_M \cdot \left(\frac{1}{2m_N} \bar{N} \mathbf{K} N \right) + \ell_E \cdot \left(-\frac{i}{m_N} \bar{N} (\mathbf{K} \times \mathbf{S}_N) N \right), \quad (5.36)$$

where $N = p, n$.

These different leptonic structures project onto different kinematic response functions $R_X^{\tau\tau'}$ introduced in Eq. (5.33). In particular, ℓ_0 contributes to $R_{MM}^{\tau\tau'}$ and $R_{\Phi''M}^{\tau\tau'}$, The ℓ_5 contributes to $R_{\Sigma'\Sigma'}^{\tau\tau'}$, $R_{\Sigma''\Sigma''}^{\tau\tau'}$ and $R_{\Delta\Sigma'}^{\tau\tau'}$, while ℓ_0^A does not contribute at this order. The magnetic structure ℓ_M only enters the subleading responses $R_{\Delta\Delta}^{\tau\tau'}$ and $R_{\Delta\Sigma'}^{\tau\tau'}$, and the electric structure ℓ_E contributes to $R_{\Phi'\Phi'}^{\tau\tau'}$, $R_{\Phi''\Phi''}^{\tau\tau'}$ and $R_{\Phi''M}^{\tau\tau'}$.

The leptonic structure $\ell_0, \ell_5, \ell_0^A, \ell_M$ and ℓ_E can be expressed in terms of the underlying LEFT Wilson coefficients as

$$\begin{aligned} \ell_{0,p} &= c_{1,p} (\bar{\nu}_{L\alpha} \gamma^\mu \nu_{L\beta}) v_\mu + c_{13,p} (\bar{\nu}_{L\alpha} \gamma^\mu \nu_{L\beta}) v_\mu v_\nu P^\nu \\ &\quad + c_{3,p} (\nu_{L\alpha}^T C \nu_{L\beta}) + c_{9,p} \frac{q_\mu}{m_N} (\nu_{L\alpha}^T C \sigma^{\mu\nu} \nu_{L\beta}) v_\nu, \\ \ell_{5,p}^\mu &= \frac{1}{2} c_{2,p} (\bar{\nu}_{L\alpha} \gamma^\mu \nu_{L\beta}) + c_{6,p} \frac{q_\rho}{2m_N} (\bar{\nu}_{L\alpha} \gamma_\nu \nu_{L\beta}) \varepsilon^{\mu\nu\rho\lambda} v_\lambda \\ &\quad + c_{11,p} \frac{q^\mu}{2m_N} (\bar{\nu}_{L\alpha} \gamma^\nu \nu_{L\beta}) v_\nu + \frac{1}{2} c_{14,p} (\bar{\nu}_{L\alpha} \gamma^\mu \nu_{L\beta}) P^\nu v_\nu \\ &\quad + \frac{1}{2} c_{4,p} (\nu_{L\alpha}^T C \sigma^{\mu\nu} \nu_{L\beta}) v_\nu + c_{10,p} \frac{q^\mu}{2m_N} (\nu_{L\alpha}^T C \nu_{L\beta}) \\ &\quad + c_{12,p} (\nu_{L\alpha}^T C \nu_{L\beta}) P^\mu q^\nu v_\nu, \\ \ell_{M,p}^\mu &= c_{5,p} (\bar{\nu}_{L\alpha} \gamma^\mu \nu_{L\beta}), \\ \ell_{E,p}^\mu &= i c_{8,p} (\nu_{L\alpha}^T C \sigma^{\mu\nu} \nu_{L\beta}) v_\nu, \end{aligned} \quad (5.37)$$

where the subscript $N = p, n$. Eq. (5.37) contains both diagram (a) and (b).

There are two classes of neutrino bilinears in our framework, corresponding to lepton-number-conserving (LNC) and lepton-number-violating (LNV) structures,

$$\begin{aligned} \text{LNC: } & \bar{\nu}_{L\alpha} \gamma^\mu \nu_{L\beta}, \\ \text{LNV: } & \nu_{L\alpha}^T C \nu_{L\beta}, \nu_{L\alpha}^T C \sigma^{\mu\nu} \nu_{L\beta}, \end{aligned} \quad (5.38)$$

where ν_L denotes the left-handed neutrino field and C is the charge-conjugation matrix. Throughout this work, we neglect interference between the LNC and LNV amplitudes and treat the LNC and LNV contributions separately in the rate.

After response expansion, the one-body kinematic terms can be written (expanded to the \mathbf{q}/m_A and $(\mathbf{q}/m_N)^2$ order)

$$\begin{aligned}
R_{MM}^{\tau\tau'} &= \left(4E_\nu^2 - \mathbf{q}^2 - \frac{2E_\nu\mathbf{q}^2}{m_A}\right) (c_1^{\tau\dagger} c_1^{\tau'}) + (16E_\nu^4 - 4E_\nu^2\mathbf{q}^2) (c_{13}^{\tau\dagger} c_{13}^{\tau'}) \\
&\quad + \left(-\frac{16E_\nu^3\mathbf{q}^2}{m_A} + \frac{2E_\nu\mathbf{q}^4}{m_A}\right) (c_{13}^{\tau\dagger} c_{13}^{\tau'}) + \mathbf{q}^2 (c_3^{\tau\dagger} c_3^{\tau'}) \\
&\quad + \left(8E_\nu^3 - 2E_\nu\mathbf{q}^2 - \frac{6E_\nu^2\mathbf{q}^2}{m_A} + \frac{\mathbf{q}^4}{2m_A}\right) \left[(c_1^{\tau\dagger} c_{13}^{\tau'}) + (c_{13}^{\tau\dagger} c_1^{\tau'}) \right] \\
&\quad + \left(\frac{2iE_\nu\mathbf{q}^2}{m_N} - \frac{i\mathbf{q}^4}{2m_A m_N}\right) \left[(c_9^{\tau\dagger} c_3^{\tau'}) - (c_3^{\tau\dagger} c_9^{\tau'}) \right] + \left(\frac{4E_\nu^2\mathbf{q}^2}{m_N^2} - \frac{2E_\nu\mathbf{q}^4}{m_A m_N^2}\right) (c_9^{\tau\dagger} c_9^{\tau'}), \\
R_{\Sigma''\Sigma''}^{\tau\tau'} &= \left(\frac{E_\nu^2\mathbf{q}^2}{m_N^2} - \frac{E_\nu\mathbf{q}^4}{2m_A m_N^2} - \frac{\mathbf{q}^4}{4m_N^2}\right) (c_{11}^{\tau\dagger} c_{11}^{\tau'}) + \frac{\mathbf{q}^4}{4m_N^2} (c_{10}^{\tau\dagger} c_{10}^{\tau'}) \\
&\quad + \left(\frac{E_\nu^2}{2m_A} - \frac{E_\nu\mathbf{q}^2}{2m_N}\right) (c_4^{\tau\dagger} c_4^{\tau'}) + \left(\frac{iE_\nu\mathbf{q}^2}{2m_N} - \frac{i\mathbf{q}^4}{8m_A m_N}\right) \left[(c_{10}^{\tau\dagger} c_4^{\tau'}) - (c_4^{\tau\dagger} c_{10}^{\tau'}) \right] \\
&\quad + \left(\frac{E_\nu^3\mathbf{q}^2}{m_A m_N} - \frac{E_\nu\mathbf{q}^4}{4m_A m_N}\right) \left[(c_{11}^{\tau\dagger} c_{14}^{\tau'}) + (c_{14}^{\tau\dagger} c_{11}^{\tau'}) \right] \\
&\quad + \left(\frac{E_\nu^2\mathbf{q}^2}{2m_A m_N} - \frac{\mathbf{q}^4}{8m_A m_N}\right) \left[(c_2^{\tau\dagger} c_{11}^{\tau'}) + (c_{11}^{\tau\dagger} c_2^{\tau'}) \right], \\
R_{\Sigma'\Sigma'}^{\tau\tau'} &= \left(2E_\nu^4 + \frac{1}{2}E_\nu^2\mathbf{q}^2 - \frac{2E_\nu^3\mathbf{q}^2}{m_A} - \frac{E_\nu\mathbf{q}^4}{4m_A}\right) (c_{14}^{\tau\dagger} c_{14}^{\tau'}) \\
&\quad + \left(E_\nu^3 + \frac{1}{4}E_\nu\mathbf{q}^2 - \frac{3E_\nu^2\mathbf{q}^2}{4m_A} - \frac{\mathbf{q}^4}{16m_A}\right) \left[(c_2^{\tau\dagger} c_{14}^{\tau'}) + (c_{14}^{\tau\dagger} c_2^{\tau'}) \right] \\
&\quad + \left(\frac{2iE_\nu^2\mathbf{q}^2}{m_N} - \frac{iE_\nu\mathbf{q}^4}{m_A m_N}\right) \left[(c_6^{\tau\dagger} c_{14}^{\tau'}) - (c_{14}^{\tau\dagger} c_6^{\tau'}) \right] \\
&\quad + \left(\frac{1}{2}E_\nu^2 + \frac{1}{8}\mathbf{q}^2 - \frac{E_\nu\mathbf{q}^2}{4m_A}\right) (c_2^{\tau\dagger} c_2^{\tau'}) + \left(\frac{iE_\nu\mathbf{q}^2}{m_N} - \frac{i\mathbf{q}^4}{4m_A m_N}\right) \left[(c_6^{\tau\dagger} c_2^{\tau'}) - (c_2^{\tau\dagger} c_6^{\tau'}) \right] \\
&\quad + \left(\frac{2E_\nu^2\mathbf{q}^2}{m_N^2} + \frac{\mathbf{q}^4}{2m_N^2} - \frac{E_\nu\mathbf{q}^4}{m_A m_N^2}\right) (c_6^{\tau\dagger} c_6^{\tau'}) + \left(\frac{1}{2}E_\nu^2 - \frac{E_\nu\mathbf{q}^2}{4m_A} - \frac{1}{8}\mathbf{q}^2\right) (c_4^{\tau\dagger} c_4^{\tau'}), \\
R_{\Phi''\Phi''}^{\tau\tau'} &= \left(4E_\nu^2 - \frac{2E_\nu\mathbf{q}^2}{m_A}\right) (c_8^{\tau\dagger} c_8^{\tau'}), \\
R_{\tilde{\Phi}\tilde{\Phi}'}^{\tau\tau'} &= \left(2E_\nu^2 - \frac{1}{2}\mathbf{q}^2 - \frac{E_\nu\mathbf{q}^2}{m_A}\right) (c_8^{\tau\dagger} c_8^{\tau'}), \\
R_{\Delta\Delta}^{\tau\tau'} &= \left(2E_\nu^2 + \frac{1}{2}\mathbf{q}^2 - \frac{E_\nu\mathbf{q}^2}{m_A}\right) (c_5^{\tau\dagger} c_5^{\tau'}), \\
R_{\Phi''M}^{\tau\tau'} &= \left(-2E_\nu|\mathbf{q}| + \frac{|\mathbf{q}|^3}{2m_A}\right) (c_3^{\tau\dagger} c_8^{\tau'}) + \left(-\frac{4iE_\nu^2|\mathbf{q}|}{m_N} + \frac{2iE_\nu|\mathbf{q}|^3}{m_A m_N}\right) (c_9^{\tau\dagger} c_8^{\tau'}), \tag{5.39}
\end{aligned}$$

where m_N is the mass of nucleon, the nuclear recoil energy $T_{\text{nr}} = \mathbf{q}^2/(2m_A)$. The isospin

$\tau, \tau' = 0, 1$,

$$c_i^0 = \frac{1}{2}(c_{i,p} + c_{i,n}), \quad c_i^1 = \frac{1}{2}(c_{i,p} - c_{i,n}). \quad (5.40)$$

These kinematic factors, together with the nuclear response functions discussed above, will be used to constrain the LEFT Wilson coefficients and the associated new-physics scales.

6 Experimental Constraints

Having derived the $\text{CE}\nu\text{NS}$ differential cross section via the multipole expansion and expressed the neutrino-nucleus amplitude in terms of nuclear response functions, the next step is to confront these predictions with data and extract constraints on new physics. The amplitude are applied to the experimental analyses by providing the expected event yields for the different measurements and performing the corresponding χ^2 fits. The experimental data are further used to set lower bounds on the effective scales and to constrain the electron-flavor NSI parameters.

6.1 Experiments

The experimental inputs employed in this analysis originate from accelerator-, solar-, and reactor-based $\text{CE}\nu\text{NS}$ measurements, which differ both in their neutrino sources and in the detector-level observables used to report the data. Specifically, the COHERENT experiment detects neutrinos from the Spallation Neutron Source (SNS) using a CsI[Na] scintillator [29, 40] and Ar [41, 42]. PandaX-4T and XENONnT probe $\text{CE}\nu\text{NS}$ from solar ${}^8\text{B}$ neutrinos in liquid xenon [44, 45], while CONUS+ measures reactor $\bar{\nu}_e$ -induced $\text{CE}\nu\text{NS}$ using high-purity germanium detectors [31, 46, 47]. To treat these different data sets within a common statistical framework, we first define a universal recoil-energy rate in terms of the nuclear recoil T_{nr} , and subsequently specify, for each experiment, the appropriate detector response, binning prescription, and χ^2 function adopted in the fit, following the conventions of Ref. [26].

For an incident (anti)neutrino flux $\Phi_{\nu_\alpha}(E_\nu)$ at the detector, the differential recoil rate per target nucleus is

$$\frac{dR_{\nu_\alpha}}{dT_{\text{nr}}} = \int_{E_{\nu,\text{min}}(T_{\text{nr}})}^{E_{\nu,\text{max}}} dE_\nu \Phi_{\nu_\alpha}(E_\nu) \frac{d\sigma}{dT_{\text{nr}}}(E_\nu, T_{\text{nr}}), \quad (6.1)$$

where T_{nr} is the nuclear recoil energy, $E_{\nu,\text{min}}(T_{\text{nr}})$ and $E_{\nu,\text{max}}$ are fixed by source and kinematics. The exposure amounts of different experiments included in flux $\Phi_{\nu_\alpha}(E_\nu)$. In the following, we apply this common recoil-rate definition to the three experiment considered in this work, specifying in each case the corresponding detector response and statistical treatment.

For COHERENT (SNS) experiment, We consider the CsI[Na] [40] and Ar [41] detector. The predicted $\text{CE}\nu\text{NS}$ counts in the i -th experimental bin are obtained by folding $dR_{\nu_\alpha}/dT_{\text{nr}}$ with the detector response and efficiency,

$$N_{\text{CE}\nu\text{NS}}^i = n_N \sum_{\nu_\alpha=\nu_e, \nu_\mu, \bar{\nu}_\mu} \int_i dn_{\text{PE}} \epsilon(n_{\text{PE}}) \int dT_{\text{nr}} P(n_{\text{PE}} | T_{\text{nr}}) \frac{dR_{\nu_\alpha}}{dT_{\text{nr}}}, \quad (6.2)$$

here n_N is the number of target nuclei, n_{PE} the photoelectron variable, $\epsilon(n_{\text{PE}})$ the detection efficiency, and $P(n_{\text{PE}}|T_{\text{nr}})$ denotes the energy resolution function (including quenching and energy smearing). The SNS flux components and the COHERENT energy resolution function inputs are taken from Refs. [3, 40, 42, 106].

We adopt a binned least-squares function with correlated normalization nuisances for signal and beam-related background [10, 107],

$$\chi^2_{\text{COHERENT}} = \sum_{i=1}^{N_{\text{bin}}} \frac{\left[N_{\text{meas}}^i - (1 + \alpha) N_{\text{CE}\nu\text{NS}}^i - (1 + \beta) N_{\text{bkg}}^i \right]^2}{(\sigma_i)^2} + \left(\frac{\alpha}{\sigma_\alpha} \right)^2 + \left(\frac{\beta}{\sigma_\beta} \right)^2, \quad (6.3)$$

where N_{meas}^i are the measured counts, $N_{\text{CE}\nu\text{NS}}^i$ the theoretical calculating value, N_{bkg}^i the beam-related background prediction, and σ_i the per-bin uncertainty. The numerical values of $\sigma_\alpha = 0.125, \sigma_\beta = 0.35$ for CsI [24, 26, 40] and $\sigma_\alpha = 0.12, \sigma_\beta = 0.146$ for Ar [108, 109].

For solar- ${}^8\text{B}$ CE ν NS in liquid xenon (PandaX-4T + XENONnT), we include $\nu_\alpha \in \{\nu_e, \nu_\mu, \nu_\tau\}$ and use Eq. (6.1) with the solar- ${}^8\text{B}$ flux and oscillation-averaged flavor composition as in Ref. [26]. Given the publicly available information for the solar- ${}^8\text{B}$ analyses, we model both PandaX-4T (paired + US2) and XENONnT as single-bin counting measurements in reconstructed recoil energy, following the treatment in Refs. [26, 27].

$$N_{\text{CE}\nu\text{NS}}^{(k)} = n_N^{(k)} \sum_{\alpha=e,\mu,\tau} \int_{T_{\text{nr},\text{min}}^{(k)}}^{T_{\text{nr},\text{max}}^{(k)}} dT_{\text{nr}} \epsilon^{(k)}(T_{\text{nr}}) \frac{dR_{\nu_\alpha}}{dT_{\text{nr}}}, \quad k \in \{\text{paired, US2, XENONnT}\}, \quad (6.4)$$

where the $\epsilon(n_{\text{PE}})$ is the detection efficiency. The combined χ^2 is a sum of three independent single-bin contributions,

$$\chi^2_{\text{Solar}{}^8\text{B}} = \sum_k \chi_k^2, \quad \chi_k^2 = \frac{\left[N_{\text{meas}}^{(k)} - (1 + \alpha_k) N_{\text{CE}\nu\text{NS}}^{(k)} \right]^2}{(\sigma^{(k)})^2} + \left(\frac{\alpha_k}{\sigma_{\alpha_k}} \right)^2, \quad (6.5)$$

where k denotes the experiments paired and US2 in PandaX-4T and XENONnT. The N_{meas} is the measured counts, $N_{\text{CE}\nu\text{NS}}$ the theoretical calculating value. α_k accounts for the correlated normalization uncertainty. The systematic uncertainty $\sigma_{\alpha_k} = 0.12$ and the statistical uncertainties are [26, 27, 110]

$$\sigma^{(\text{US2})} = 37.3, \quad \sigma^{(\text{paired})} = 37.1, \quad \sigma^{(\text{XENONnT})} = 36.9, \quad (6.6)$$

with experimental details in Refs. [44, 45].

For CONUS+ (reactor $\bar{\nu}_e$, Ge), the reactor CE ν NS, we use Eq. (6.1) with $\nu_\alpha = \bar{\nu}_e$ [31, 46] and the reactor flux model (see Refs. [111–113]). The comparison is performed in reconstructed electron-equivalent energy $E_{\text{ee}}^{\text{reco}}$; the predicted binned counts are obtained by folding the recoil spectrum with quenching and resolution,

$$N_i^{\text{th}} = \int_{E_{\text{ee}}^i}^{E_{\text{ee}}^{i+1}} dE_{\text{ee}}^{\text{reco}} \left[n_N \int dT_{\text{nr}} G(E_{\text{ee}}^{\text{reco}}, E_{\text{ee}}(T_{\text{nr}})) \frac{dR}{dT_{\text{nr}}} \right], \quad (6.7)$$

where the $E_{\text{ee}}(T_{\text{nr}})$ is defined through the adopted quenching model. the $G(E_{\text{ee}}^{\text{reco}}, E_{\text{ee}}(T_{\text{nr}}))$ is the energy resolution function. All detector-response inputs (threshold, resolution, quenching) are taken from the CONUS+ analyses in Refs. [47, 113].

For binned excess-count data, we adopt a profiled least-squares function with a global normalization nuisance parameter α ,

$$\chi_{\text{CONUS+}}^2 = \sum_{i=1}^{N_{\text{bin}}} \frac{[N_i^{\text{meas}} - (1 + \alpha) N_i^{\text{th}}]^2}{\sigma_i^2} + \left(\frac{\alpha}{\sigma_\alpha} \right)^2, \quad (6.8)$$

where N_i^{meas} and σ_i are the reported excess counts and uncertainties [47], and $\sigma_\alpha = 0.169$ summarizes statistical uncertainties [113].

6.2 Constraints on NP scales and NSI parameters

We now recast the CE ν NS measurements into constraints on the LEFT parameter space. Following the standard normalization, the dimensionful Wilson coefficients are parametrized in terms of a dimensionless coupling \mathcal{C}_a^d and an effective NP scale Λ_a as

$$\hat{\mathcal{C}}_a^d \equiv \frac{\mathcal{C}_a^d}{\Lambda_a^{d-4}}. \quad (6.9)$$

Setting $|\mathcal{C}_a^d| = 1$, the experimental bound on Wilson coefficients is converted into a limit on Λ_a . In this convention, a larger lower bound on Λ_a corresponds to a stronger suppression of the corresponding NP interaction and therefore a more stringent constraint from CE ν NS data.

To derive limits, we adopt the single-operator approach: for a given operator \mathcal{O}_a^d we switch on only $\hat{\mathcal{C}}_a^d$ while setting all other coefficients to zero, and we perform a one-parameter fit to the combined CE ν NS data. The 90% C.L. lower bound on Λ_a is then obtained by requiring the appropriate one-dimensional likelihood criterion,

$$\Delta\chi^2(\Lambda_a) \equiv \chi^2(\Lambda_a) - \chi_{\text{min}}^2 \leq 2.71, \quad (6.10)$$

where χ_{min}^2 denotes the minimum of the profiled χ^2 for that operator.

The resulting bounds are summarized in Fig. 3, where we compare the constraints from the CONUS+, COHERENT CsI combined with Ar measurement, and those obtained from solar ${}^8\text{B}$ CE ν NS in liquid xenon (PandaX-4T and XENONnT). The source of CONUS+ experiment is electronic antineutrino, so we constrain the process that the incident neutrino is e flavor. Presenting the results in terms of Λ_a provides an intuitive measure of the reach of each experiment in the LEFT framework and highlights the complementarity between reactor, accelerator-based and solar-neutrino CE ν NS data sets across different operator structures.

In general, operators that contribute to the coherently enhanced channel and interfere with the SM amplitude lead to more strong bounds, whereas operators that are dominated by spin-dependent responses or lack coherent enhancement are constrained more weakly. This behavior can be understood in terms of nuclear response scaling in the long-wavelength limit:

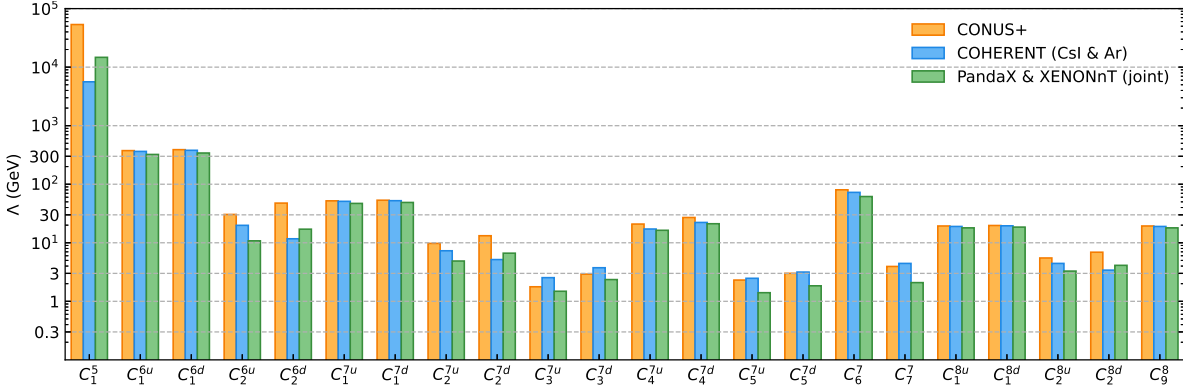


Figure 3: For CE ν NS processes initiated by an electron-flavor neutrino, we present lower bounds at 90% C.L. on the effective scale Λ (in GeV) associated with individual LEFT Wilson coefficients \hat{C}_1^5 , \hat{C}_a^6 , \hat{C}_a^6 , \hat{C}_a^7 , \hat{C}_a^7 , \hat{C}_6 , \hat{C}_7 , \hat{C}_a^8 , \hat{C}_a^8 and \hat{C}_9^8 . The limits are obtained by turning on one operator at a time. The orange, blue and green bars correspond to constraints from CONUS+, COHERENT (CsI and Ar combination), PandaX-4T and XENONnT combination, respectively.

the coherent (spin-independent) response scales as $W_M \sim \mathcal{O}(A^2)$ due to the in-phase addition of nucleon amplitudes, while spin-dependent responses scale only as $W_\Sigma \sim \mathcal{O}(1)$ and therefore do not benefit from the same parametric enhancement, as discussed in Tab. 4. For instance, the vector-current dimension-6 operator $\mathcal{O}_1^{6u/d}$ couples to the coherent charge response and thus scales as $\sim A^2$, whereas the axial operator $\mathcal{O}_2^{6u/d}$ is spin-dependent and non-coherent, without A^2 enhancement.

The comparison among experiments further highlights their complementarity. COHERENT provides spectral information in multiple bins and thus yields robust constraints on a broad set of coefficients. The solar- 8 B liquid-xenon measurements (PandaX-4T and XENONnT) probe a different neutrino source and recoil-energy regime, and their combined analysis offers competitive sensitivity for operators that primarily affect low-energy nuclear recoils. For instance, dipole-like contributions can be enhanced at low momentum transfer, so low-threshold recoil measurements can become particularly sensitive in that direction. For higher-dimensional operators (dimension-7 and 8), the overall reach in Λ is generically reduced, as additional powers of E_ν/Λ or q/Λ suppress their impact in MeV-scale CE ν NS, requiring higher statistics and tighter systematics to achieve comparable sensitivity.

We also perform an analysis in terms of neutrino non-standard interactions (NSIs). At the quark level, neutral-current (NC) NSIs can be parameterized as [21, 48, 114–116]

$$\mathcal{L}_{\text{NC}} \supset -2\sqrt{2} G_F \left[\epsilon_{\alpha\beta}^{qL} (\bar{\nu}_\alpha \gamma^\mu P_L \nu_\beta) (\bar{q} \gamma_\mu P_L q) + \epsilon_{\alpha\beta}^{qR} (\bar{\nu}_\alpha \gamma^\mu P_L \nu_\beta) (\bar{q} \gamma_\mu P_R q) \right], \quad (6.11)$$

where $P_{L/R} = (1 \mp \gamma_5)/2$, α, β denote neutrino flavors, $q \in \{u, d\}$, and G_F is the Fermi constant.

In the LEFT notation adopted in Eq. (2.2), the NSI parameters $\epsilon_{\alpha\beta}^{qL(R)}$ are related to the dimension-6 Wilson coefficients $\hat{\mathcal{C}}_{1,q}^{(6)}$ and $\hat{\mathcal{C}}_{2,q}^{(6)}$ via

$$\epsilon_{\alpha\beta}^{qL/R} = -\frac{1}{2\sqrt{2}G_F} \left(\hat{\mathcal{C}}_{1,q}^{(6)} \mp \hat{\mathcal{C}}_{2,q}^{(6)} \right). \quad (6.12)$$

Accordingly, when NSI effects are present we decompose the Wilson coefficients as

$$\hat{\mathcal{C}}_i^{(6)} = \hat{\mathcal{C}}_i^{(6)} \Big|_{\text{SM}} + \hat{\mathcal{C}}_i^{(6)} \Big|_{\text{NSI}}. \quad (6.13)$$

For comparison with existing CE ν NS NSI studies, we focus on the vector combinations ϵ_{ee}^{qV} (with $q = u, d$), defined as [28]

$$\epsilon_{ee}^{qV} = -\frac{1}{\sqrt{2}G_F} \hat{\mathcal{C}}_{1,q}^{(6)} \Big|_{\text{NSI}}. \quad (6.14)$$

Fig. 4 shows the 90% C.L. allowed regions in the $(\epsilon_{ee}^{uV}, \epsilon_{ee}^{dV})$ plane derived from COHERENT (CsI), CONUS+, and the combined solar- ${}^8\text{B}$ (PandaX-4T+XENONnT) analysis. The contours are obtained using the two-parameter criterion $\Delta\chi^2 \leq 4.61$ (2 degrees of freedom). The resulting regions exhibit the characteristic elongated, band-like structure, reflecting the strong correlation between ϵ_{ee}^{uV} and ϵ_{ee}^{dV} in CE ν NS. For a given nuclear target (Z, N) , the event rate is primarily sensitive to an approximately linear combination of the up- and down-quark vector NSIs entering the effective weak charge, while the orthogonal combination remains only weakly constrained. Consequently, the allowed parameter space extends along a diagonal direction in the $(\epsilon_{ee}^{uV}, \epsilon_{ee}^{dV})$ plane rather than forming a compact elliptical region.

Comparing the widths of the allowed bands, CONUS+ yields the tightest constraint, followed by COHERENT, while the solar- ${}^8\text{B}$ liquid-xenon combination is comparatively weaker in the present treatment. This pattern is driven by the relative fluxes, thresholds, and dominant systematics: CONUS+ benefits from the intense reactor flux and low recoil thresholds, COHERENT is limited by SNS statistics and flux/background uncertainties, and the solar- ${}^8\text{B}$ liquid-xenon analyses are further weakened by the broad neutrino-energy spectrum and detector-response systematics [113, 117].

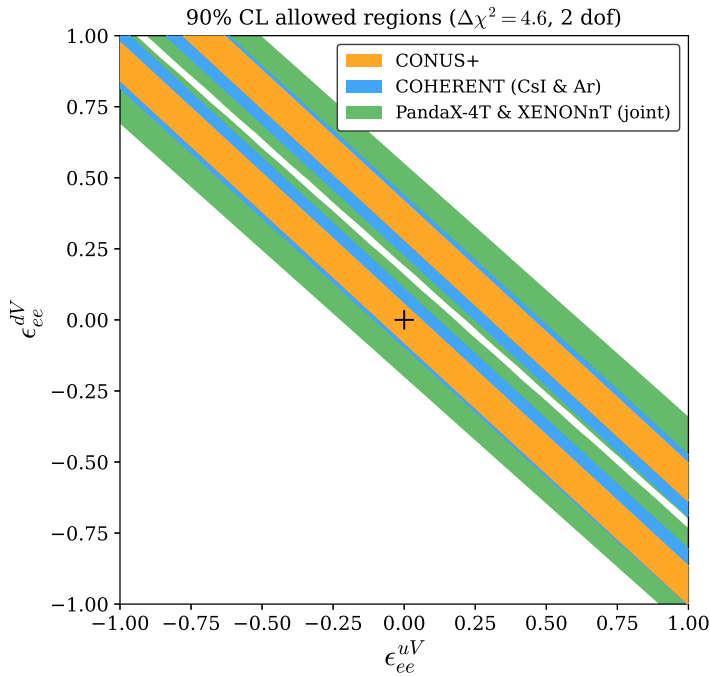


Figure 4: The 90% C.L. allowed regions in the $(\epsilon_{ee}^{uV}, \epsilon_{ee}^{dV})$ plane derived from the CONUS+ (orange) and COHERENT (blue) CE ν NS measurements, together with the combined constraint from the PandaX-4T + XENONnT (green) solar- ${}^8\text{B}$ analysis.

7 SMEFT Operators and UV Completions

Having established the low-energy description of CE ν NS in the LEFT and carried it through chiral EFT to the nuclear response and differential cross section (see Fig. 1), we now turn to the ultraviolet side of the same EFT chain. In particular, when the NP scale Λ lies above the electroweak scale, the appropriate starting point is the SMEFT, defined between Λ and Λ_{EW} with $SU(3)_C \times SU(2)_L \times U(1)_Y$ gauge invariance. The SMEFT operators are first evolved and matched at Λ_{EW} onto LEFT operators, which then are incorporated into the hadronic and nuclear matching steps already developed in the previous sections. This section therefore completes the top part of Fig. 1 by organizing the relevant SMEFT operator basis (up to dimension 8) and illustrating representative UV completions that generate them.

7.1 SMEFT Operators

The LEFT describes the theory below the electroweak scale with the gauge group of $SU(3)_C \times U(1)_{\text{em}}$. When the NP is heavier than the electroweak scale and contains the properties of the SM group $SU(3)_C \times SU(2)_L \times U(1)_Y$, the SMEFT comes into play to characterize the EFT valid between the NP scale Λ and the electroweak scale Λ_{EW} .

The SMEFT Lagrangian comprises the SM Lagrangian of dimension 4, together with a

complete set of independent higher-dimensional operators.

$$\mathcal{L}_{\text{SMEFT}} = \mathcal{L}_{\text{SM}} + \sum_{D \geq 5} \sum_a \frac{C_a^D}{\Lambda^{D-4}} \mathcal{O}_a^D , \quad (7.1)$$

where D denotes the mass dimension for the a -th operator \mathcal{O}_a^D .

The SM Lagrangian in unbroken phase is

$$\begin{aligned} \mathcal{L}_{\text{SM}} = & -\frac{1}{4} G_{\mu\nu}^A G^{A\mu\nu} - \frac{1}{4} W_{\mu\nu}^I W^{I\mu\nu} - \frac{1}{4} B_{\mu\nu} B^{\mu\nu} \\ & + \sum_{\psi=Q,u_R,d_R,\ell,e_R} \bar{\psi} i \not{D} \psi + (D_\mu H)^\dagger (D^\mu H) - \lambda \left(H^\dagger H - \frac{1}{2} v^2 \right)^2 \\ & - \left[\bar{\ell} e_R (Y_e) H + \bar{Q} u_R (Y_u) \tilde{H} + \bar{Q} d_R (Y_d) H + \text{h.c.} \right] \\ & + \frac{\theta_3 g_s^2}{32\pi^2} G_{\mu\nu}^A \tilde{G}^{A\mu\nu} + \frac{\theta_2 g^2}{32\pi^2} W_{\mu\nu}^I \tilde{W}^{I\mu\nu} + \frac{\theta_1 g'^2}{32\pi^2} B_{\mu\nu} \tilde{B}^{\mu\nu} . \end{aligned} \quad (7.2)$$

The gauge covariant derivatives is $D_\mu = \partial_\mu + i g_1 Y B_\mu + i g_2 t^I W_\mu^I + i g_3 T^A G_\mu^A$. Here, $T^A = \lambda^A/2$ and $t^I = \tau^I/2$ are the $SU(3)_C$ and $SU(2)_L$ generators while the λ^A and τ^I are the Gell-Mann and Pauli matrices, and Y is the $U(1)_Y$ generator. The complex conjugate of the Higgs field becomes either as H^\dagger or \tilde{H} . The \tilde{H} is defined by $\tilde{H}_i = \epsilon_{ij} H^{\dagger j}$ where the ϵ_{ij} is totally antisymmetric with $\epsilon_{12} = 1$. Fermion fields Q and ℓ are left-handed doublet fields $(u_L, d_L)^T$ and $(\nu_L, e_L)^T$. The right-handed fermion fields are u_R, d_R and e_R . In addition, the fermion fields have weak-eigenstate indices $r = 1, 2, 3$ and the Yukawa couplings Y_e, Y_u and Y_d are 3×3 matrices. However, only the u and d quarks are considered in the LEFT operators, such that quark flavor degrees of freedom are not taken into account; by contrast, the three flavor indices associated with neutrinos are considered in the analysis.

The relevant SMEFT operators up to dimension 8 are listed in Tab. 5. For convenience, the index D is omitted. The dimension-5 Weinberg operator \mathcal{O}_5 can contribute to the LNV process and has been constrained by the mass of neutrino. Thus, we neglect the contribution of \mathcal{O}_5 in this work. For the LNC dimension-6 and dimension-7 LEFT operators, we only consider contributions from dimension-6 SMEFT operators, as those from dimension-8 SMEFT operators are highly suppressed. Separately, dimension-8 LEFT operators receive contributions only from dimension-8 SMEFT operators at tree-level matching; we therefore incorporate dimension-8 SMEFT operators in our analysis. For LNV LEFT operators, by contrast, we restrict our consideration to SMEFT operators up to dimension 7. The full set of matching conditions is presented in App. E.

After the $SU(2)_L$ symmetry breaking, we can obtain the matching from SMEFT operator to LEFT operators as the Ref [66].

Similarly, the QCD RGEs of the SMEFT operators are also concluded and only these Wilson coefficients $C_{uB}, C_{uW}, C_{dB}, C_{dW}, C_{QuLLH}, C_{dLQLH1}, C_{dLQLH2}$ are needed to consid-

ered. The REG of the SMEFT operators are given by [118–122]

$$\frac{d}{d \ln \mu} C_{u(d)B(W)} = 2C_F \frac{\alpha_s}{4\pi} C_{u(d)B(W)}, \quad (7.3)$$

$$\frac{d}{d \ln \mu} C_{QuLLH} = -6C_F \frac{\alpha_s}{4\pi} C_{QuLLH}, \quad (7.4)$$

$$\frac{d}{d \ln \mu} \begin{pmatrix} C_{dLQLH1} \\ C_{dLQLH2} \end{pmatrix} = \frac{\alpha_s}{4\pi} \begin{pmatrix} -6C_F & 0 \\ 4C_F & -6C_F \end{pmatrix} \begin{pmatrix} C_{dLQLH1} \\ C_{dLQLH2} \end{pmatrix}, \quad (7.5)$$

$$\frac{d}{d \ln \mu} C_{\ell^2 q^2 D^2}^{(2)(4)} = C_F \frac{\alpha_s}{3\pi} C_{\ell^2 q^2 D^2}^{(2)(4)}, \quad (7.6)$$

$$\frac{d}{d \ln \mu} C_{\ell^2 [u(d)]^2 D^2} = C_F \frac{\alpha_s}{3\pi} C_{\ell^2 [u(d)]^2 D^2}. \quad (7.7)$$

Dimension-6		Dimension-5	
\mathcal{O}_H	$(H^\dagger H)^3$	\mathcal{O}_5	$\epsilon^{ik} \epsilon^{jl} (\ell_i^T C \ell_j) H_k H_l$
\mathcal{O}_{HW}	$H^\dagger H W_{\mu\nu}^I W^{I\mu\nu}$	Dimension-7	
\mathcal{O}_{HB}	$H^\dagger H B_{\mu\nu} B^{\mu\nu}$	\mathcal{O}_{QuLLH}	$\epsilon^{ij} (\bar{Q}^k u_R) (\ell_k^T C \ell_i) H_j$
\mathcal{O}_{HWB}	$H^\dagger \tau^I H W_{\mu\nu}^I B^{\mu\nu}$	\mathcal{O}_{dLQLH1}	$\epsilon^{ij} \epsilon^{kl} (\bar{d}_R \ell_i) (Q_j^T C \ell_k) H_l$
\mathcal{O}_{HD}	$(H^\dagger D^\mu H)^* (H^\dagger D^\mu H)$	\mathcal{O}_{dLQLH2}	$\epsilon^{ik} \epsilon^{jl} (\bar{d}_R \ell_i) (Q_j^T C \ell_k) H_l$
$\mathcal{O}_{H\ell}^{(1)}$	$(H^\dagger i \bar{D}_\mu H) (\bar{\ell} \gamma^\mu \ell)$	Dimension-8	
$\mathcal{O}_{H\ell}^{(3)}$	$(H^\dagger i \bar{D}_\mu^I H) (\bar{\ell} \tau^I \gamma^\mu \ell)$	$\mathcal{O}_{l^2 G^2 D}$	$(\bar{\ell} \gamma^\mu i \bar{D}^\nu \ell) G_{\mu\rho}^A G_\nu^{A\rho}$
$\mathcal{O}_{Hq}^{(1)}$	$(H^\dagger i \bar{D}_\mu H) (\bar{Q} \gamma^\mu Q)$	$\mathcal{O}_{l^2 q^2 G}^{(1)}$	$(\bar{\ell} \gamma^\mu \ell) (\bar{Q} \gamma^\nu T^A Q) G_{\mu\nu}^A$
$\mathcal{O}_{Hq}^{(3)}$	$(H^\dagger i \bar{D}_\mu^I H) (\bar{Q} \tau^I \gamma^\mu Q)$	$\mathcal{O}_{l^2 q^2 G}^{(2)}$	$(\bar{\ell} \gamma^\mu \ell) (\bar{Q} \gamma^\nu T^A Q) \tilde{G}_{\mu\nu}^A$
\mathcal{O}_{Hu}	$(H^\dagger i \bar{D}_\mu H) (\bar{u}_R \gamma^\mu u_R)$	$\mathcal{O}_{l^2 q^2 G}^{(3)}$	$(\bar{\ell} \gamma^\mu \tau^I \ell) (\bar{Q} \gamma^\nu T^A \tau^I Q) G_{\mu\nu}^A$
\mathcal{O}_{Hd}	$(H^\dagger i \bar{D}_\mu H) (\bar{d}_R \gamma^\mu d_R)$	$\mathcal{O}_{l^2 q^2 G}^{(4)}$	$(\bar{\ell} \gamma^\mu \tau^I \ell) (\bar{Q} \gamma^\nu T^A \tau^I Q) \tilde{G}_{\mu\nu}^A$
\mathcal{O}_{uB}	$(\bar{Q} \sigma^{\mu\nu} u_R) \tilde{H} B_{\mu\nu}$	$\mathcal{O}_{l^2 u^2 G}^{(1)}$	$(\bar{\ell} \gamma^\mu \ell) (\bar{u}_R \gamma^\nu T^A u_R) G_{\mu\nu}^A$
\mathcal{O}_{uW}	$(\bar{Q} \sigma^{\mu\nu} u_R) \tau^I \tilde{H} W_{\mu\nu}^I$	$\mathcal{O}_{l^2 u^2 G}^{(2)}$	$(\bar{\ell} \gamma^\mu \ell) (\bar{u}_R \gamma^\nu T^A u_R) \tilde{G}_{\mu\nu}^A$
\mathcal{O}_{dB}	$(\bar{Q} \sigma^{\mu\nu} d_R) H B_{\mu\nu}$	$\mathcal{O}_{l^2 d^2 G}^{(1)}$	$(\bar{\ell} \gamma^\mu \ell) (\bar{d}_R \gamma^\nu T^A d_R) G_{\mu\nu}^A$
\mathcal{O}_{dW}	$(\bar{Q} \sigma^{\mu\nu} d_R) \tau^I H W_{\mu\nu}^I$	$\mathcal{O}_{l^2 d^2 G}^{(2)}$	$(\bar{\ell} \gamma^\mu \ell) (\bar{d}_R \gamma^\nu T^A d_R) \tilde{G}_{\mu\nu}^A$
$\mathcal{O}_{\ell q}^{(1)}$	$(\bar{\ell} \gamma^\mu \ell) (\bar{Q} \gamma_\mu Q)$	$\mathcal{O}_{l^2 q^2 D^2}^{(2)}$	$(\bar{\ell} \gamma^\mu \bar{D}^\nu \ell) (\bar{Q} \gamma_\mu \bar{D}_\nu Q)$
$\mathcal{O}_{\ell q}^{(3)}$	$(\bar{\ell} \gamma^\mu \tau^I \ell) (\bar{Q} \gamma_\mu \tau^I Q)$	$\mathcal{O}_{l^2 q^2 D^2}^{(4)}$	$(\bar{\ell} \gamma^\mu \bar{D}^I \ell) (\bar{Q} \gamma_\mu \bar{D}^I Q)$
$\mathcal{O}_{\ell u}$	$(\bar{\ell} \gamma^\mu \ell) (\bar{u}_R \gamma_\mu u_R)$	$\mathcal{O}_{l^2 u^2 D^2}^{(2)}$	$(\bar{\ell} \gamma^\mu \bar{D}^\nu \ell) (\bar{u}_R \gamma_\mu \bar{D}_\nu u_R)$
$\mathcal{O}_{\ell d}$	$(\bar{\ell} \gamma^\mu \ell) (\bar{d}_R \gamma_\mu d_R)$	$\mathcal{O}_{l^2 d^2 D^2}^{(2)}$	$(\bar{\ell} \gamma^\mu \bar{D}^\nu \ell) (\bar{d}_R \gamma_\mu \bar{D}_\nu d_R)$

Table 5: The SMEFT operators for CE ν NS process.

7.2 UV Completions

There are considerable numbers of the UV models which can contribute to the SMEFT operators. We derive the complete tree-level UV models and give the minimal Lagrangian of these models for CE ν NS. In the notation adopted in Refs. [123, 124], the (S , F , V , R , T)

correspond to the scalar particles, spin 1/2 fermion particles, vector particles, spin 3/2 fermion particles and spin 2 tensor particles. In addition, the representation of the SM group would be presented as $(SU(3)_C, SU(2)_L)_{U(1)_Y}$.

Dimension-6 UV Completions

The UV completions of dimension-6 SMEFT operators has been listed in Tab. 6. The corresponding gauge invariant UV Lagrangian for these particles can be obtained and the kinematic terms of the particles are

$$\begin{aligned}
\mathcal{L}_{\text{UV}}^{\text{kin}} = & -S_1^\dagger(D^2 + M_{S_1}^2)S_1 - S_4^{\dagger i}(D^2 + M_{S_4}^2)S_{4i} - S_5^{\dagger I}(D^2 + M_{S_5}^2)S_{5I} - S_6^{\dagger I}(D^2 + M_{S_6}^2)S_{6I} \\
& - S_7^{\dagger i}(D^2 + M_{S_7}^2)S_7^i - S_8^{\dagger i}(D^2 + M_{S_8}^2)S_8^i - S_{10}^{\dagger a}(D^2 + M_{S_{10}}^2)S_{10a} \\
& - S_{12}^{\dagger ai}(D^2 + M_{S_{12}}^2)S_{12ai} - S_{13}^{\dagger ai}(D^2 + M_{S_{13}}^2)S_{13ai} - S_{14}^{\dagger aI}(D^2 + M_{S_{14}}^2)S_{14aI} \\
& + \bar{F}_1(i\cancel{D} - M_{F_1})F_1 + \bar{F}_2(i\cancel{D} - M_{F_2})F_2 + \bar{F}_5^I(i\cancel{D} - M_{F_5})F_{5I} + \bar{F}_6^I(i\cancel{D} - M_{F_6})F_{6I} \\
& + \bar{F}_8^a(i\cancel{D} - M_{F_8})F_{8a} + \bar{F}_9^a(i\cancel{D} - M_{F_9})F_{9a} + \bar{F}_{10}^{ai}(i\cancel{D} - M_{F_{10}})F_{10ai} \\
& + \bar{F}_{11}^{ai}(i\cancel{D} - M_{F_{11}})F_{11ai} + \bar{F}_{12}^{ai}(i\cancel{D} - M_{F_{12}})F_{12ai} + \bar{F}_{13}^{aI}(i\cancel{D} - M_{F_{13}})F_{13aI} \\
& + V_1^{\dagger \mu}(g_{\mu\nu}D^2 - D_\nu D_\mu + g_{\mu\nu}M_{V_1}^2)V_1^\nu + V_2^{\dagger \mu}(g_{\mu\nu}D^2 - D_\nu D_\mu + g_{\mu\nu}M_{V_2}^2)V_2^\nu \\
& + V_4^{\dagger \mu}(g_{\mu\nu}D^2 - D_\nu D_\mu + g_{\mu\nu}M_{V_4}^2)V_4^\nu + V_5^{\dagger \mu}(g_{\mu\nu}D^2 - D_\nu D_\mu + g_{\mu\nu}M_{V_5}^2)V_5^\nu \\
& + V_7^{\dagger \mu}(g_{\mu\nu}D^2 - D_\nu D_\mu + g_{\mu\nu}M_{V_7}^2)V_7^\nu + V_8^{\dagger \mu}(g_{\mu\nu}D^2 - D_\nu D_\mu + g_{\mu\nu}M_{V_8}^2)V_8^\nu \\
& + V_9^{\dagger \mu}(g_{\mu\nu}D^2 - D_\nu D_\mu + g_{\mu\nu}M_{V_9}^2)V_9^\nu, \tag{7.8}
\end{aligned}$$

where $g_{\mu\nu}$ is the metric tensor, a is the $SU(3)_C$ triplet index, (ij) are $SU(2)_L$ doublet index and i is the $SU(2)_L$ quartet index. Moreover, the interactions of these particles with SM field are

$$\begin{aligned}
\mathcal{L}_{\text{UV}}^{\text{int}} = & \mathcal{C}_{S_1 H^2}(H^\dagger H)S_1 + \mathcal{C}_{S_1^3}(S_1 S_1 S_1) + \mathcal{D}_{S_1^2 H^2}(H^\dagger H)S_1 S_1 + \mathcal{D}_{S_4 H^3}(H^\dagger H)(H^{\dagger i} S_{4i}) \\
& + \mathcal{C}_{S_5 H^2}(H \tau^I H^\dagger)S_5^I + \mathcal{D}_{S_5^2 H^2 1}(H^\dagger H)S_{5I} S_5^I + \mathcal{D}_{S_5^2 H^2 2}(\tau^I)_k^i(\tau^J)_j^k H^{\dagger j} H_i S_5^I S_5^J \\
& + \mathcal{C}_{S_6 H^2} \epsilon^{kj} (\tau^I)_k^i H_i H_j S_6^{\dagger I} + \mathcal{D}_{S_6^2 H^2 1}(H^\dagger H)S_6^I S_6^{\dagger I} + \mathcal{D}_{S_6^2 H^2 2}(\tau^I)_k^i(\tau^J)_j^k H^{\dagger j} H_i S_6^I S_6^{\dagger J} \\
& + \mathcal{D}_{S_7 H^3} \epsilon_{kl} C_{i,jl}^{\dagger i} H_i H_j H^{\dagger k} S_7^{\dagger i} + \mathcal{D}_{S_8 H^3} C_{i,jk}^{\dagger i} H_i H_j H_k S_8^{\dagger i} + \mathcal{D}_{S_{10} \ell Q} \epsilon^{ij} (\ell_i^T C Q_{aj}) S_{10}^{\dagger a} \\
& + \mathcal{D}_{S_{12} \ell d} \epsilon^{ij} (\bar{d}_R^a \ell_i) S_{12aj} + \mathcal{D}_{S_{13} \ell u} \epsilon^{ij} (\bar{u}_R^a \ell_i) S_{13aj} + \mathcal{D}_{S_{14} L Q} \epsilon^{jk} (\tau)_k^i (\ell_i^T C Q_{aj}) S_{14}^{\dagger a I} \\
& + \mathcal{D}_{F_1 H \ell} \epsilon^{ij} (F_1^T C \ell_i) H_j + \mathcal{D}_{F_2 H \ell} (F_2^T C \ell_i) H^{\dagger i} + \mathcal{D}_{F_5 H \ell} \epsilon^{kj} (\tau^I)_k^i (F_5^I C \ell_i) H_j \\
& + \mathcal{D}_{F_6 H \ell} (\tau^I)_j^i (F_6^I C \ell_i) H^{\dagger j} + \mathcal{D}_{F_8 H Q} (\bar{F}_8^a Q_{ai}) H^{\dagger i} + \mathcal{D}_{F_9 H Q} \epsilon^{ij} (\bar{F}_9^a Q_{ai}) H_j \\
& + \mathcal{D}_{F_{10} H d} \epsilon^{ij} (\bar{d}_R^a F_{10ai}) H_j + \mathcal{D}_{F_{11} H d} (\bar{d}_R^a F_{11ai}) H^{\dagger i} + \mathcal{D}_{F_{11} H u} \epsilon^{ij} (\bar{u}_R^a F_{11ai}) H_j \\
& + \mathcal{D}_{F_{12} H u} (\bar{u}_R^a F_{12ai}) H^{\dagger i} + \mathcal{D}_{F_{13} H Q} (\tau^I)_j^i (\bar{F}_{13}^a Q_{ai}) H^{\dagger j} + \mathcal{D}_{F_{14} H Q} \epsilon^{kj} (\tau^I)_k^i (\bar{F}_{14}^a Q_{ai}) H_j \\
& + \mathcal{D}_{V_1 D H} (H^\dagger D_\mu H) V_1^\mu + \mathcal{D}_{V_1 \ell^2} (\bar{\ell} \gamma_\mu \ell) V_1^\mu + \mathcal{D}_{V_1 Q^2} (\bar{Q} \gamma_\mu Q) V_1^\mu + \mathcal{D}_{V_1 u^2} (\bar{u}_R \gamma_\mu u_R) V_1^\mu \\
& + \mathcal{D}_{V_1 d^2} (\bar{d}_R \gamma_\mu d_R) V_1^\mu + \mathcal{D}_{V_2 D H^2} \epsilon^{ij} (D_\mu H_i) H_j V_2^{\dagger \mu} + \mathcal{D}_{V_4 D H^2} (\tau^I)_j^i (\tau^I) H^{\dagger j} V_4^{\dagger \mu} \\
& + \mathcal{D}_{V_4 L^2} (\bar{\ell} \tau^I \ell) V_4^{I \mu} + \mathcal{D}_{V_4 Q^2} (\bar{Q} \tau^I Q) V_4^{I \mu} + \mathcal{D}_{V_5 \ell Q} (\ell \gamma_\mu Q_a) V_5^{\dagger a \mu} \\
& + \mathcal{D}_{V_7 \ell d} (\bar{d}_R^a \gamma_\mu C \ell^{\bar{i} T}) V_{7ai}^\mu + \mathcal{D}_{V_8 \ell u} (\bar{u}_R^a \gamma_\mu C \ell^{\bar{i} T}) V_{8ai}^\mu + \mathcal{D}_{V_9 \ell Q} (\bar{\ell} \tau^I Q_a) V_9^{\dagger a I \mu} + \text{h.c.}, \tag{7.9}
\end{aligned}$$

where the coupling constants \mathcal{C} s have the mass dimension and the coupling constants \mathcal{D} s are dimensionless. We define the C_i^{ijk} via the relation $C_i^{ijk} = \frac{1}{\sqrt{2}}(C_i)^{jk}(\epsilon\tau^J)^{ji}$ where the index i takes values $3/2, 1/2, -1/2, 3/2$, ϵ^{ij} denotes the $SU(2)$ -invariant antisymmetric tensor with indices $i, j = 1, 2$; τ^J ($J = 1, 2, 3$) are the Pauli matrices and C_i matrices are

$$(C_{3/2})^{Ij} = \frac{1}{\sqrt{2}} \begin{pmatrix} 1 & 0 \\ -i & 0 \\ 0 & 0 \end{pmatrix}, (C_{1/2})^{Ij} = \frac{1}{\sqrt{6}} \begin{pmatrix} 0 & 1 \\ 0 & -i \\ -2 & 0 \end{pmatrix},$$

$$(C_{-1/2})^{Ij} = -\frac{1}{\sqrt{6}} \begin{pmatrix} 1 & 0 \\ i & 0 \\ 0 & 2 \end{pmatrix}, (C_{-3/2})^{Ij} = -\frac{1}{\sqrt{2}} \begin{pmatrix} 0 & 1 \\ 0 & i \\ 0 & 0 \end{pmatrix}. \quad (7.10)$$

The SMEFT operator can be obtained through integrating out the UV particles. Here, we take the operator \mathcal{O}_{ld} as the example. As is shown in Fig. 5, the these three particles can contribute to \mathcal{O}_{ld} . The Wilson coefficient for \mathcal{O}_{ld} through the matching

$$\frac{C_{ld}}{\Lambda^2} = \frac{\mathcal{D}_{V_1 d^2} \mathcal{D}_{V_1 \ell^2}}{M_{V_1}^2} + \frac{\mathcal{D}_{d^\dagger L^\dagger V_7} \mathcal{D}_{d^\dagger L^\dagger V_7}}{M_{V_7}^2} + \frac{\mathcal{D}_{S_{12} \ell d} \mathcal{D}_{S_{12} \ell d}}{M_{S_{12}}^2}, \quad (7.11)$$

and the Wilson coefficients of any other SMEFT operators can be obtained through Eq. (7.9). The constraints of the coupling constants and mass would be deduced from the Wilson coefficients which contribute to the low energy experiments through the above framework.

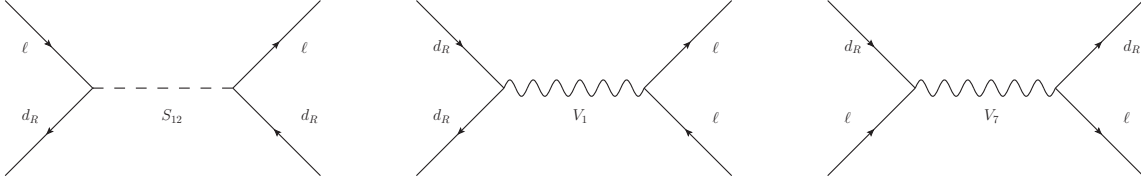


Figure 5: Contributions to \mathcal{O}_{ld} from the UV completions with S_{12} , V_1 and V_7 particles.

Dimension-7 UV Completions

The dimension-7 SMEFT operators would violate the lepton number. And three types of the seesaw $S_6(\mathbf{1}, \mathbf{3})_0$, $F_1(\mathbf{1}, \mathbf{1})_0$ and $F_5(\mathbf{1}, \mathbf{3})_0$ can contribute to the dimension-7 operators. However, these three types of the seesaw can contribute to dimension 5 and are highly suppressed. We exclude these three types of the seesaw models in the dimension-7 SMEFT operators UV completion. When considering other UV models, at least two particles should be added at tree level. We list the pairs of the UV models in Tab. 7.

\mathcal{O}_H	$S_1(\mathbf{1}, \mathbf{1})_0, S_4(\mathbf{1}, \mathbf{2})_{\frac{1}{2}}, S_5(\mathbf{1}, \mathbf{3})_0, S_6(\mathbf{1}, \mathbf{3})_1, S_7(\mathbf{1}, \mathbf{4})_{\frac{1}{2}}, S_8(\mathbf{1}, \mathbf{4})_{\frac{3}{2}}, V_2(\mathbf{1}, \mathbf{1})_1, V_4(\mathbf{1}, \mathbf{3})_0$
\mathcal{O}_{HD}	$S_5(\mathbf{1}, \mathbf{3})_0, S_6(\mathbf{1}, \mathbf{3})_1, V_1(\mathbf{1}, \mathbf{1})_0, V_2(\mathbf{1}, \mathbf{1})_1, V_4(\mathbf{1}, \mathbf{3})_0$
$\mathcal{O}_{H\ell}^{(1)}$	$F_1(\mathbf{1}, \mathbf{1})_0, F_2(\mathbf{1}, \mathbf{1})_1, F_5(\mathbf{1}, \mathbf{3})_0, F_6(\mathbf{1}, \mathbf{3})_1, V_1(\mathbf{1}, \mathbf{1})_0$
$\mathcal{O}_{H\ell}^{(3)}$	$F_1(\mathbf{1}, \mathbf{1})_0, F_2(\mathbf{1}, \mathbf{1})_1, F_5(\mathbf{1}, \mathbf{3})_0, F_6(\mathbf{1}, \mathbf{3})_1, V_4(\mathbf{1}, \mathbf{3})_0$
$\mathcal{O}_{Hq}^{(1)}$	$F_8(\mathbf{3}, \mathbf{1})_{-\frac{1}{3}}, F_9(\mathbf{3}, \mathbf{1})_{\frac{2}{3}}, F_{13}(\mathbf{3}, \mathbf{3})_{-\frac{1}{3}}, F_{14}(\mathbf{3}, \mathbf{3})_{\frac{2}{3}}, V_1(\mathbf{1}, \mathbf{1})_0$
$\mathcal{O}_{Hq}^{(3)}$	$F_8(\mathbf{3}, \mathbf{1})_{-\frac{1}{3}}, F_9(\mathbf{3}, \mathbf{1})_{\frac{2}{3}}, F_{13}(\mathbf{3}, \mathbf{3})_{-\frac{1}{3}}, F_{14}(\mathbf{3}, \mathbf{3})_{\frac{2}{3}}, V_4(\mathbf{1}, \mathbf{3})_0$
\mathcal{O}_{Hu}	$F_{11}(\mathbf{3}, \mathbf{2})_{\frac{1}{6}}, F_{12}(\mathbf{3}, \mathbf{2})_{\frac{7}{6}}, V_1(\mathbf{1}, \mathbf{1})_0$
\mathcal{O}_{Hd}	$F_{10}(\mathbf{3}, \mathbf{2})_{-\frac{5}{6}}, F_{11}(\mathbf{3}, \mathbf{2})_{\frac{1}{6}}, V_1(\mathbf{1}, \mathbf{1})_0$
$\mathcal{O}_{\ell q}^{(1)}$	$S_{10}(\mathbf{3}, \mathbf{1})_{-\frac{1}{3}}, S_{14}(\mathbf{3}, \mathbf{3})_{-\frac{1}{3}}, V_1(\mathbf{1}, \mathbf{1})_0, V_5(\mathbf{3}, \mathbf{1})_{\frac{2}{3}}, V_9(\mathbf{3}, \mathbf{1})_{\frac{2}{3}}$
$\mathcal{O}_{\ell q}^{(3)}$	$S_{10}(\mathbf{3}, \mathbf{1})_{-\frac{1}{3}}, S_{14}(\mathbf{3}, \mathbf{3})_{-\frac{1}{3}}, V_4(\mathbf{1}, \mathbf{3})_0, V_5(\mathbf{3}, \mathbf{1})_{\frac{2}{3}}, V_9(\mathbf{3}, \mathbf{3})_{\frac{2}{3}}$
$\mathcal{O}_{\ell u}$	$S_{13}(\mathbf{3}, \mathbf{2})_{\frac{7}{6}}, V_1(\mathbf{1}, \mathbf{1})_0, V_8(\mathbf{3}, \mathbf{2})_{\frac{1}{6}}$
$\mathcal{O}_{\ell d}$	$S_{12}(\mathbf{3}, \mathbf{2})_{\frac{1}{6}}, V_1(\mathbf{1}, \mathbf{1})_0, V_7(\mathbf{3}, \mathbf{2})_{-\frac{5}{6}}$

Table 6: The UV completions for dimension-6 SMEFT operators that contribute to CE ν NS.

\mathcal{O}_{QuLLH}	$\{S_2(\mathbf{1}, \mathbf{1})_1, S_4(\mathbf{1}, \mathbf{2})_{\frac{1}{2}}\} \quad \{S_2(\mathbf{1}, \mathbf{1})_1, F_8(\mathbf{3}, \mathbf{1})_{-\frac{1}{3}}\} \quad \{S_2(\mathbf{1}, \mathbf{1})_1, F_{12}(\mathbf{3}, \mathbf{2})_{\frac{7}{6}}\}$ $\{F_{12}(\mathbf{3}, \mathbf{2})_{\frac{7}{6}}, V_5(\mathbf{3}, \mathbf{1})_{\frac{2}{3}}\} \quad \{F_{12}(\mathbf{3}, \mathbf{2})_{\frac{7}{6}}, V_9(\mathbf{3}, \mathbf{3})_{\frac{2}{3}}\}$
\mathcal{O}_{dLQLH1}	$\{S_{12}(\mathbf{3}, \mathbf{2})_{\frac{1}{6}}, F_{14}(\mathbf{3}, \mathbf{3})_{\frac{2}{3}}\}$
\mathcal{O}_{dLQLH2}	$\{S_2(\mathbf{1}, \mathbf{1})_1, S_4(\mathbf{1}, \mathbf{2})_{\frac{1}{2}}\} \quad \{S_2(\mathbf{1}, \mathbf{1})_1, F_9(\mathbf{3}, \mathbf{1})_{\frac{2}{3}}\} \quad \{S_2(\mathbf{1}, \mathbf{1})_1, F_{10}(\mathbf{3}, \mathbf{2})_{-\frac{5}{6}}\}$ $\{S_{12}(\mathbf{3}, \mathbf{2})_{\frac{1}{6}}, F_9(\mathbf{3}, \mathbf{1})_{\frac{2}{3}}\} \quad \{S_{12}(\mathbf{3}, \mathbf{2})_{\frac{1}{6}}, F_{14}(\mathbf{3}, \mathbf{3})_{\frac{2}{3}}\}$

Table 7: The UV completions for dimension-7 SMEFT operators that contribute to CE ν NS.

Similarly, the gauge invariant UV Lagrangian involved for these particles becomes

$$\begin{aligned}
\mathcal{L}_{\text{UV}} = & \left\{ -S_2^\dagger(D^2 + M_{S_2}^2)S_2 - S_4^{\dagger i}(D^2 + M_{S_4}^2)S_{4i} - S_{12}^{\dagger ai}(D^2 + M_{S_{12}}^2)S_{12ai} \right. \\
& + \bar{F}_8^a(iD\cancel{D} - M_{F_8})F_{8a} + \bar{F}_9^a(iD\cancel{D} - M_{F_9})F_{9a} + \bar{F}_{12}^{ai}(iD\cancel{D} - M_{F_{12}})F_{12ai} \\
& + \bar{F}_{14}^{aI}(iD\cancel{D} - M_{F_{14}})F_{14a}^I + V_5^{\dagger \mu}(g_{\mu\nu}D^2 - D_\nu D_\mu + g_{\mu\nu}M_{V_5^2})V_5^\nu \\
& + V_9^{\dagger \mu}(g_{\mu\nu}D^2 - D_\nu D_\mu + g_{\mu\nu}M_{V_9^2})V_9^\nu \Big\} \\
& + \left\{ \mathcal{D}_{S_2 \ell^2} \epsilon^{ij}(\ell_i^T C \ell_j)S_2 + \mathcal{D}_{S_4 u Q} \epsilon^{ij}(\bar{u}_R Q_j)S_{4i} + \mathcal{D}_{S_4 Q d}(\bar{d}_R Q_i)S_4^{\dagger i} \right. \\
& + \mathcal{D}_{S_{12} \ell d} \epsilon^{ij}(\bar{d}_R^a \ell_j)S_{12ai} + \mathcal{D}_{F_8 H Q}(\bar{F}_8^a Q_{ai})H^{\dagger i} + \mathcal{D}_{F_9 H Q} \epsilon^{ij}(\bar{F}_9^a Q_{ai})H_j \\
& + \mathcal{D}_{F_{10} H d} \epsilon^{ij}(\bar{d}_R^a F_{10ai})H_j + \mathcal{D}_{F_{12} H u}(\bar{u}_R^a F_{12ai})H^{\dagger i} + \mathcal{D}_{F_{14} H Q} \epsilon^{kj}(\tau^I)_k^i(\bar{F}_{14}^{aI} Q_{ai})H_j, \\
& + \mathcal{D}_{V_5 \ell Q}(\bar{\ell} \gamma_\mu Q)V_5^{\dagger a \mu} - \sqrt{2} \mathcal{D}_{V_9 \ell Q}(\bar{\ell} \tau^I Q)V_9^{\dagger a I \mu} + \text{h.c.} \Big\} \\
& + \left\{ \mathcal{C}_{S_2 S_4 H} \epsilon^{ij} H_j S_{4i} S_2^\dagger + \mathcal{D}_{S_2 F_8 u}(\bar{u}_R^a F_{8a})S_2 + \mathcal{D}_{S_2 F_9 d}(\bar{d}_R^a F_{9a})S_2^\dagger \right. \\
& + \mathcal{D}_{S_2 F_{10} Q} (F_{10}^{aiT} C Q_{ai})S_2^\dagger + \mathcal{D}_{S_2 F_{12} Q} (F_{12ai}^T C Q^{ai})S_2 + \mathcal{D}_{S_{12} F_9 \ell} (F_{9a}^T C \ell_i)S_{12}^{\dagger ai} \\
& + \mathcal{D}_{S_{12} F_{14} \ell} (\tau^I)_j^i (F_{14a}^{iT} C \ell_j)S_{12}^{\dagger ai} + \mathcal{D}_{F_{12} V_5 \ell} \epsilon_{ij}(\ell^j \gamma_\mu F_{12a}^i)(V_5)^{a \mu} \\
& + \mathcal{D}_{F_{12} V_9 \ell} \epsilon_{kj}(\tau^I)_k^i (\ell^j \gamma_\mu F_{12a}^i) V_9^{a I \mu} + \text{h.c.} \Big\}, \tag{7.12}
\end{aligned}$$

where the first curly bracket contains the kinetic terms, the second one contains the interactions of new particles and SM particles and the last one contains the mixed term for new particles.

There are five pairs of the UV models which can contribute to \mathcal{O}_{QuLLH} . After integrating out the UV particles through the Fig. 6, the Wilson coefficient of \mathcal{O}_{QuLLH} can be obtained similarly

$$\begin{aligned} \frac{C_{QuLLH}}{\Lambda^3} = & \frac{\mathcal{C}_{S_2 S_4 H} \mathcal{D}_{S_2 \ell^2} \mathcal{D}_{S_4 uQ}}{M_{S_2}^2 M_{S_4}^2} + \frac{\mathcal{D}_{S_2 F_8 u} \mathcal{D}_{S_2 \ell^2} \mathcal{D}_{F_8 HQ}}{M_{S_2}^2 M_{F_8}} + \frac{\mathcal{D}_{S_2 F_{12} Q} \mathcal{D}_{S_2 \ell^2} \mathcal{D}_{F_{12} Hu}}{M_{S_2}^2 M_{F_{12}}} \\ & + \frac{\mathcal{D}_{F_{12} V_5 \ell} \mathcal{D}_{V_5 \ell Q} \mathcal{D}_{F_{12} Hu}}{M_{V_5}^2 M_{F_{12}}} + \frac{\mathcal{D}_{F_{12} V_9 \ell} \mathcal{D}_{V_9 \ell Q} \mathcal{D}_{F_{12} Hu}}{M_{V_9}^2 M_{F_{12}}}. \end{aligned} \quad (7.13)$$

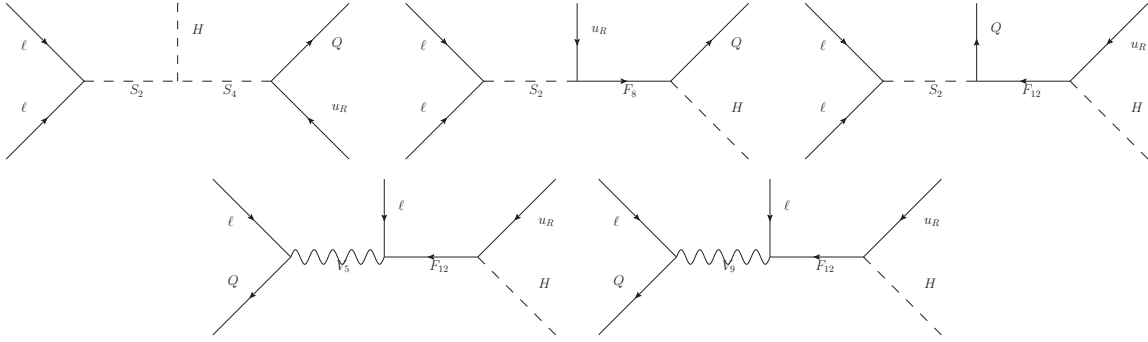


Figure 6: Contributions to \mathcal{O}_{QuLLH} from the UV completions with S_2 , S_4 , F_8 , F_{12} , V_5 and V_9 particles.

Dimension-8 UV Completions

When considering the SMEFT dimension-8 operators, there are considerable numbers of the UV models. Here, we only consider the UV models which will not generate the dimension-6 operators. In the dimension-8 UV completions, the spin 3/2 and spin 2 particles are concluded. Furthermore, the spin 3/2 and spin 2 particles are considered as Rarita-Schwinger [125] and Fierz-Pauli [126] fields. Similarly, the UV completions of the dimension-8 SMEFT operators which do not generate the dimension-6 operators has been listed in Tab. 8. Then the gauge

invariant UV Lagrangian is given by

$$\begin{aligned}
\mathcal{L}_{UV} = & \bar{F}_{26}^{Ai} (i \not{D} - M_{F_{26}}) F_{26i}^A + \mathcal{D}_{F_{16}\ell G} (\bar{F}_{18}^{Ai} \gamma^\mu \partial^\nu \ell_i) G_{\mu\nu}^A \\
& - \frac{1}{2} \left\{ g^{\mu\lambda} g^{\nu\rho} + g^{\nu\lambda} g^{\mu\rho} - \frac{2}{3} g^{\mu\nu} g^{\rho\lambda} \right\}^{-1} T_1^{\mu\nu} (\square - M_{T_1}) T_1^{\rho\lambda} \\
& + \bar{R}_{18\mu}^A \{ (\not{p} - M_{R_{18}}) g^{\mu\nu} - (\gamma^\mu p^\nu + p^\mu \gamma^\nu) + \gamma^\mu \not{p} \gamma^\nu + M_{R_{18}} \gamma^\mu \gamma^\nu \} R_{18\nu}^A \\
& + g_{T_1\ell^2} (\bar{\ell} \gamma_\mu \overleftrightarrow{\partial}_\nu \ell) T_1^{\mu\nu} + g_{T_2\ell^2} (\bar{\ell} \gamma_\mu \overleftrightarrow{\partial}_\nu \tau^I \ell) T_2^{I\mu\nu} \\
& + g_{T_1Q^2} (\bar{Q} \gamma_\mu \overleftrightarrow{\partial}_\nu Q) T_1^{\mu\nu} + g_{T_2Q^2} (\bar{Q} \gamma_\mu \overleftrightarrow{\partial}_\nu \tau^I Q) T_2^{I\mu\nu} \\
& + g_{T_1u^2} (\bar{u}_R \gamma_\mu \overleftrightarrow{\partial}_\nu u_R) T_1^{\mu\nu} + g_{T_1d^2} (\bar{d}_R \gamma_\mu \overleftrightarrow{\partial}_\nu \tau^I d_R) T_1^{\mu\nu} \\
& + g_{T_7\ell d} (\ell^T C \gamma_\mu \overleftrightarrow{\partial}_\nu d_R) T_7^{a\mu\nu} + g_{T_6\ell u} (\ell^T C \gamma_\mu \overleftrightarrow{\partial}_\nu u_R) T_6^{\dagger a\mu\nu} \\
& + g_{T_3\ell Q} (\bar{\ell} \gamma_\mu \overleftrightarrow{\partial}_\nu Q) T_3^{a\mu\nu} + g_{T_4\ell Q} (\bar{\ell} \gamma_\mu \overleftrightarrow{\partial}_\nu \tau^I Q) T_3^{aI\mu\nu} + g_{T_1G^2} G_{\mu\rho}^A G_\nu^{\rho A} T_1^{\mu\nu} \\
& + g_{R_{18}lG} \bar{R}_{18\mu}^A (g^{\mu\nu} + z \gamma^\mu \gamma^\nu) \gamma^\alpha \ell G_{\nu\alpha}^A,
\end{aligned} \tag{7.14}$$

where $g_{T_1\ell^2\dots}$ are the coupling constants, z is a constant and the dependence on z will vanish for the on-shell amplitudes. Moreover, the propagators of the Rarita-Schwinger and Fierz-Pauli field are

$$\Pi_{RS}^{\mu\nu} = (\not{p} + M) \left[g^{\mu\nu} - \frac{2}{3M^2} p^\mu p^\nu - \frac{1}{3} \gamma^\mu \gamma^\nu - \frac{1}{3M} (p^\nu \gamma^\mu - p^\mu \gamma^\nu) \right], \tag{7.15}$$

$$\Pi_{FP}^{\mu\nu\rho\lambda} = \frac{i}{2} \frac{(\mathcal{P}^{\mu\rho} \mathcal{P}^{\nu\lambda} + \mathcal{P}^{\mu\lambda} \mathcal{P}^{\nu\rho}) - \frac{2}{3} \mathcal{P}^{\mu\nu} \mathcal{P}^{\rho\lambda}}{p^2 - M^2}, \tag{7.16}$$

where $\mathcal{P}^{\mu\nu} = (g^{\mu\nu} - \frac{p^\mu p^\nu}{M^2})$. We take the operator $\mathcal{O}_{\ell^2 u^2 D^2}^{(2)}$ as the example. The Feynman diagrams show as Fig. 7 and effective Lagrangian can be evaluated

$$\mathcal{L}_{EFT} = \frac{g_{T_1\ell^2} g_{T_1u^2}}{2M_{T_1}^2} \left(g^{\mu\rho} g^{\nu\lambda} + g^{\mu\lambda} g^{\nu\rho} - \frac{2}{3} g^{\mu\nu} g^{\rho\lambda} \right) (\bar{\ell} \gamma_\mu \overleftrightarrow{\partial}_\nu \ell) (\bar{u}_R \gamma_\rho \overleftrightarrow{\partial}_\lambda u_R). \tag{7.17}$$

Through the matching procedure, the Wilson coefficient of the operator $\mathcal{O}_{\ell^2 u^2 D^2}^{(2)}$ is obtained

$$\frac{C_{\ell^2 u^2 D^2}}{\Lambda^4} = \frac{g_{T_1\ell^2} g_{T_1u^2}}{M_{T_1}^2}. \tag{7.18}$$

$\mathcal{O}_{\ell^2 G^2 D}$	$F_{18}(\mathbf{8}, \mathbf{2})_{-\frac{1}{2}}, R_{18}(\mathbf{8}, \mathbf{2})_{\frac{1}{2}}, T_1(\mathbf{1}, \mathbf{1})_0$
$\mathcal{O}_{\ell^2 q^2 D^2}^{(2)}$	$T_1(\mathbf{1}, \mathbf{1})_0, T_2(\mathbf{1}, \mathbf{3})_0, T_3(\bar{\mathbf{3}}, \mathbf{1})_{-\frac{2}{3}}, T_4(\bar{\mathbf{3}}, \mathbf{3})_{-\frac{2}{3}}$
$\mathcal{O}_{\ell^2 q^2 D^2}^{(4)}$	$T_1(\mathbf{1}, \mathbf{1})_0, T_2(\mathbf{1}, \mathbf{3})_0, T_3(\bar{\mathbf{3}}, \mathbf{1})_{-\frac{2}{3}}, T_4(\bar{\mathbf{3}}, \mathbf{3})_{-\frac{2}{3}}$
$\mathcal{O}_{\ell^2 u^2 D^2}^{(2)}$	$T_1(\mathbf{1}, \mathbf{1})_0, T_6(\mathbf{3}, \mathbf{2})_{\frac{1}{6}}$
$\mathcal{O}_{\ell^2 d^2 D^2}^{(2)}$	$T_1(\mathbf{1}, \mathbf{1})_0, T_7(\bar{\mathbf{3}}, \mathbf{2})_{\frac{5}{6}}$

Table 8: The UV completions for dimension-8 SMEFT operators that contribute to CE ν NS.

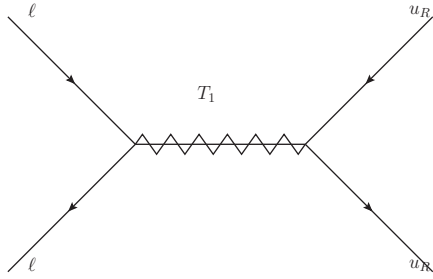


Figure 7: Contribution to $\mathcal{O}_{\ell^2 u^2 D^2}^{(2)}$ from the UV completions with T_1 particle.

8 Conclusion

In this work, we established a comprehensive end-to-end EFT framework for CE ν NS studies, covering the full energy scale hierarchy from NP scale to the nuclear scale. We accomplished complete EFT matching across relevant scales with QCD RG running effects included, developed systematic power counting to clarify the contributions of one-body and two-body currents, and provided full tree-level UV completions for SMEFT operators, bridging the NP with low-energy observations. Building on a broad set of CE ν NS experimental data—including the latest observation from CONUS+, multi-target-nucleus results from COHERENT, and first indications of solar 8 B neutrinos via CE ν NS from ton-scale PandaX and XENON detectors—we derived stringent and comprehensive new constraints on the scales of LEFT operators up to dimension 8 and neutrino NSI parameters.

Building on previous systematic studies of CE ν NS, this work presents several methodological innovations to further advance the field, with key contributions summarized as follows:

- The LEFT operators up to dimension 8 and their RG running effects are incorporated, with hadronic matching achieved via the systematic spurion method.
- A comprehensive power counting analysis for nuclear response functions is performed, assessing all relevant LEFT operator up to dimension 8 contributions and CE ν NS coherent enhancement.

- The SMEFT operator up to dimension 8 contributions at high scales are incorporated, with full tree-level UV completions to establish a comprehensive top-down framework.

Looking ahead to future directions, this framework can be extended to incorporate an expanded suite of experimental data, including additional measurements from ton-scale xenon detectors and results from upcoming accelerator-based neutrino experiments; such expansions will further tighten constraints on NP scenarios. Furthermore, synergizing with state-of-the-art lattice QCD calculations to refine the currently unknown LECs and extending the analysis to LNV scenarios will yield deeper insights into the fundamental nature of neutrino interactions and their broader implications for NP frameworks.

Acknowledgments

This work is supported by the National Science Foundation of China under Grants No. 12347105, No. 12375099, No. 12047503, and No. 12505127, and the National Key Research and Development Program of China Grant No. 2020YFC2201501, No. 2021YFA0718304. GL is also supported by the Guangdong Basic and Applied Basic Research Foundation (2024A1515012668).

A Expansion of Chiral Operators in Pion Fields

Using $u = e^X$ in Eq. (3.1), with $X \equiv \frac{i}{2f} \Pi$ and Π defined in Eq. (3.2), one has $X^\dagger = -X$ and thus $u^\dagger = e^{-X}$. The chiral building blocks introduced in Eq. (3.3) take the form

$$\begin{aligned} u_\mu &= i(e^{-X} \partial_\mu e^X - e^X \partial_\mu e^{-X}), \\ \chi_\pm &= e^{-X} \chi e^{-X} \pm e^X \chi^\dagger e^X, \\ \Sigma_\pm &= e^{-X} \tau e^{-X} \pm e^X \tau e^X, \\ Q_\pm &= e^{-X} \tau e^X \pm e^X \tau e^{-X}, \\ \nabla_\mu &= \partial_\mu + \frac{1}{2} (e^{-X} \partial_\mu e^X + e^X \partial_\mu e^{-X}). \end{aligned} \quad (\text{A.1})$$

Here τ denotes the spurion associated with the flavor matrices appearing in the LEFT operators. For bookkeeping, a generic 2×2 spurion matrix is expanded in the basis

$$\tau = \sum_{I=1}^4 \tau_I \mathbf{t}_I, \quad \mathbf{t}_1 = \begin{pmatrix} 1 & 0 \\ 0 & 0 \end{pmatrix}, \quad \mathbf{t}_2 = \begin{pmatrix} 0 & 1 \\ 0 & 0 \end{pmatrix}, \quad \mathbf{t}_3 = \begin{pmatrix} 0 & 0 \\ 1 & 0 \end{pmatrix}, \quad \mathbf{t}_4 = \begin{pmatrix} 0 & 0 \\ 0 & 1 \end{pmatrix}. \quad (\text{A.2})$$

According to the Baker-Campbell-Hausdorff formula,

$$e^X A e^{-X} = \sum_{n=0}^{\infty} \frac{1}{n!} [A]_X^{(n)}, \quad (\text{A.3})$$

and

$$e^{-X} A e^X = \sum_{n=0}^{\infty} \frac{1}{n!} [A]_{-X}^{(n)} = \sum_{n=0}^{\infty} \frac{(-1)^n}{n!} [A]_X^{(n)}, \quad (\text{A.4})$$

where

$$[A]_X^{(n)} \equiv \underbrace{[X, [X, \dots, [X, A] \dots]]}_n. \quad (\text{A.5})$$

Therefore Q_{\pm} admit the exact expansions

$$\begin{aligned} Q_+ &= \sum_{n=0}^{\infty} \frac{2}{(2n)!} [\tau]_X^{(2n)}, \\ Q_- &= - \sum_{n=0}^{\infty} \frac{2}{(2n+1)!} [\tau]_X^{(2n+1)}. \end{aligned} \quad (\text{A.6})$$

For the derivative term, one uses

$$e^{-X} \partial_{\mu} e^X = \sum_{n=0}^{\infty} \frac{(-1)^n}{(n+1)!} [\partial_{\mu} X]_X^{(n)}, \quad [\partial_{\mu} X]_X^{(n)} \equiv \underbrace{[X, [X, \dots, [X, \partial_{\mu} X] \dots]]}_n, \quad (\text{A.7})$$

and

$$e^X \partial_{\mu} e^{-X} = - \sum_{n=0}^{\infty} \frac{1}{(n+1)!} [\partial_{\mu} X]_X^{(n)}. \quad (\text{A.8})$$

It follows that

$$\begin{aligned} u_{\mu} &= i \sum_{n=0}^{\infty} \frac{2}{(2n+1)!} [\partial_{\mu} X]_X^{(2n)}, \\ \nabla_{\mu} &= \partial_{\mu} - \sum_{n=0}^{\infty} \frac{1}{(2n+2)!} [\partial_{\mu} X]_X^{(2n+1)}. \end{aligned} \quad (\text{A.9})$$

For $e^{\pm X} A e^{\pm X}$, the Taylor expansion gives

$$\begin{aligned} e^X A e^X &= \sum_{n,m \geq 0} \frac{1}{n! m!} X^n A X^m = \sum_{k=0}^{\infty} \frac{1}{k!} \{A\}_X^{(k)}, \\ e^{-X} A e^{-X} &= \sum_{n,m \geq 0} \frac{(-1)^{n+m}}{n! m!} X^n A X^m = \sum_{k=0}^{\infty} \frac{(-1)^k}{k!} \{A\}_X^{(k)}, \end{aligned} \quad (\text{A.10})$$

where

$$\{A\}_X^{(k)} \equiv \underbrace{\{X, \{X, \dots, \{X, A\} \dots\}\}}_k. \quad (\text{A.11})$$

Hence,

$$\begin{aligned}\Sigma_+ &= \sum_{k=0}^{\infty} \frac{2}{(2k)!} \{\tau\}_X^{(2k)}, \\ \Sigma_- &= - \sum_{k=0}^{\infty} \frac{2}{(2k+1)!} \{\tau\}_X^{(2k+1)}.\end{aligned}\quad (\text{A.12})$$

The expansions for χ_{\pm} are completely analogous. Retaining terms with at most three pion fields yields

$$u_{\mu} = 2i \partial_{\mu} X + \frac{i}{3} [X, [X, \partial_{\mu} X]] + \dots, \quad (\text{A.13})$$

$$\Sigma_+ = 2\tau + \{X, \{X, \tau\}\} + \dots, \quad (\text{A.14})$$

$$\Sigma_- = -2\{X, \tau\} - \frac{1}{3} \{X, \{X, \{X, \tau\}\}\} + \dots, \quad (\text{A.15})$$

$$Q_+ = 2\tau + [X, [X, \tau]] + \dots, \quad (\text{A.16})$$

$$Q_- = -2[X, \tau] - \frac{1}{3} [X, [X, [X, \tau]]] + \dots, \quad (\text{A.17})$$

$$\chi_+ = 2\chi + \{X, \{X, \chi\}\} + \dots, \quad (\text{A.18})$$

$$\chi_- = -2\{X, \chi\} - \frac{1}{3} \{X, \{X, \{X, \chi\}\}\} + \dots, \quad (\text{A.19})$$

$$\nabla_{\mu} = \partial_{\mu} - \frac{1}{2} [X, \partial_{\mu} X] + \dots. \quad (\text{A.20})$$

At leading chiral order, these expansions imply that u_{μ} , Σ_- , Q_- , and χ_- start at $\mathcal{O}(\pi)$ and therefore contain an odd number of pion fields (i.e. 1, 3, ...). In contrast, Σ_+ , Q_+ , χ_+ , and ∇_{μ} contain an even number of pion fields (i.e. 0, 2, ...).

B Naive Dimension Analysis

The matching between the LEFT operators and the chiral Lagrangian is not a one-to-one procedure, which means that every LEFT operator can be matched to several χ PT operators, and each χ PT operator receives contributions from several LEFT operators (will be clarified in the subsequent examples). Thus, we need a method to assess all these contributions systematically. In detail, we want to distinguish which one is more dominant among the LEFT operators matching to the same χ PT operator, and which one is more dominant among the χ PT operators matched from the same LEFT operator. In this section, we use the NDA [74–76, 127, 128] of the effective operators to organize them, an approach consistent with that adopted in Ref. [73].

The LEFT Lagrangian is organized as an expansion in powers of the electroweak scale inverse $1/\Lambda_{\text{EW}}$. The NDA master formula [74, 75] in the 4-dimensional spacetime states that the operators in the Lagrangian are normalized as

$$\frac{\Lambda_{\text{EW}}^4}{16\pi^2} \left[\frac{\partial}{\Lambda_{\text{EW}}} \right]^{N_p} \left[\frac{4\pi\phi}{\Lambda_{\text{EW}}} \right]^{N_{\phi}} \left[\frac{4\pi A}{\Lambda_{\text{EW}}} \right]^{N_A} \left[\frac{4\pi\psi}{\Lambda_{\text{EW}}^{3/2}} \right]^{N_{\psi}} \left[\frac{g}{4\pi} \right]^{N_g} \left[\frac{y}{4\pi} \right]^{N_y} \left[\frac{\lambda}{16\pi^2} \right]^{N_{\lambda}}. \quad (\text{B.1})$$

For convenience, we express the master formula by replacing the vector field A with the field-strength tensor $F \sim \partial A$ and omitting the renormalizable coupling constants g, y, λ ,

$$\text{LEFT: } \frac{\Lambda_{\text{EW}}^4}{16\pi^2} \left[\frac{\partial}{\Lambda_{\text{EW}}} \right]^{N_p} \left[\frac{4\pi F}{\Lambda_{\text{EW}}^2} \right]^{N_F} \left[\frac{4\pi\psi}{\Lambda_{\text{EW}}^{3/2}} \right]^{N_\psi}, \quad (\text{B.2})$$

which implies that the 4-fermion operators of dimension-6, 7, and 8 are normalized as

$$\frac{(4\pi)^2}{\Lambda_{\text{EW}}^2} \psi^4, \quad \frac{(4\pi)^2}{\Lambda_{\text{EW}}^2} \frac{\partial}{\Lambda_{\text{EW}}} \psi^4, \quad \frac{(4\pi)^2}{\Lambda_{\text{EW}}^2} \frac{\partial^2}{\Lambda_{\text{EW}}^2} \psi^4. \quad (\text{B.3})$$

In particular, the spurions are dimensionless in the NDA. On the other hand, the NDA master formula for the χ PT is

$$\chi\text{PT: } f^2 \Lambda_\chi^2 \left[\frac{\partial}{\Lambda_\chi} \right]^{N_p} \left[\frac{\psi}{f\sqrt{\Lambda_\chi}} \right]^{N_\psi} \left[\frac{F}{\Lambda_\chi f} \right]^{N_A}, \quad (\text{B.4})$$

where $4\pi f \sim \Lambda_\chi$. To relate these two NDA formulae we first replace all occurrences of the scale Λ_{EW} in Eq. (B.1) by the scale Λ_χ ,

$$\begin{aligned} & \frac{\Lambda_{\text{EW}}^4}{16\pi^2} \left[\frac{\Lambda_\chi}{\Lambda_{\text{EW}}} \right]^{N_p+2N_F+\frac{3}{2}N_\psi} \left[\frac{\partial}{\Lambda_\chi} \right]^{N_p} \left[\frac{F}{\Lambda_\chi^2} \right]^{N_F} \left[\frac{\psi}{\sqrt{\Lambda_\chi} f} \right]^{N_\psi} \\ &= \left[\frac{\Lambda_\chi}{\Lambda_{\text{EW}}} \right]^\mathcal{D} \left(f^2 \Lambda_\chi^2 \left[\frac{\partial}{\Lambda_\chi} \right]^{N_p} \left[\frac{F}{\Lambda_\chi^2} \right]^{N_F} \left[\frac{\psi}{\sqrt{\Lambda_\chi} f} \right]^{N_\psi} \right), \end{aligned} \quad (\text{B.5})$$

where $\mathcal{D} = N_p + 2N_F + \frac{3}{2}N_\psi - 4$. The expression inside the parentheses is similar to the NDA formula in the χ PT, so we replace it by the χ PT NDA formula in Eq. (B.4) and obtain the NDA formula for the matching,

$$\begin{aligned} \text{matching: } & \frac{\Lambda_{\text{EW}}^4}{16\pi^2} \left[\frac{\partial}{\Lambda_{\text{EW}}} \right]^{N_p} \left[\frac{4\pi F}{\Lambda_{\text{EW}}^2} \right]^{N_F} \left[\frac{4\pi\psi}{\Lambda_{\text{EW}}^{3/2}} \right]^{N_\psi} \\ & \sim \left[\frac{\Lambda_\chi}{\Lambda_{\text{EW}}} \right]^\mathcal{D} \left(f^2 \Lambda_\chi^2 \left[\frac{\partial}{\Lambda_\chi} \right]^{N_p} \left[\frac{\psi}{f\sqrt{\Lambda_\chi}} \right]^{N_\psi} \left[\frac{F}{\Lambda_\chi f} \right]^{N_A} \right). \end{aligned} \quad (\text{B.6})$$

C Values of Low Energy Constants

The numerical values of the LECs $L_{1\sim 14}$ have been calculated in this appendix. The LECs L_1 and L_2 are fixed by the proton and neutron magnetic moments [129]

$$2 + 2L_1 + 2L_2 = 2(\mu_p - 1) + \mu_n = 1.64(2), \quad (\text{C.1})$$

$$1 + 2L_2 = 2\mu_n + (\mu_p - 1) = -2.07(2), \quad (\text{C.2})$$

and the two LECs are obtained as

$$L_1 = 1.355(14), \quad L_2 = -1.535(10). \quad (\text{C.3})$$

The LECs L_3 and L_4 can be obtained through the axial vector currents constants

$$2L_3 = g_A = 1.2754(13), \quad 2L_3 + 4L_4 = \Sigma_{ud} = 0.397(40), \quad (\text{C.4})$$

where g_A is determined very precisely from nuclear β decay [129] and the values for Σ_{ud} follow from averages of the lattice QCD results [130, 131]. Thus, the LECs L_3 and L_4 become

$$L_3 = 0.6377(7), \quad L_4 = -0.220(10). \quad (\text{C.5})$$

The LECs L_5 , L_6 , L_7 and L_8 can be related to the generalized tensor form factors [132], and the relationship can be obtained

$$2(L_5 + L_6) = m_u F_{T,0}^{u/p} = 1.79(30) \text{ MeV}, \quad (\text{C.6})$$

$$2L_6 = m_d F_{T,0}^{d/p} = 0.97(15) \text{ MeV}, \quad (\text{C.7})$$

$$2(L_5 + L_6 + L_7 + L_8) = m_u F_{T,1}^{u/p} = 0.184(70) \text{ MeV}, \quad (\text{C.8})$$

$$2(L_6 + L_8) = m_d F_{T,1}^{d/p} = 2.74(37) \text{ MeV}. \quad (\text{C.9})$$

The values of LECs L_5 , L_6 , L_7 and L_8 are

$$L_5 = 0.41(17) \text{ MeV}, \quad L_6 = 0.49(80) \text{ MeV}, \quad L_7 = -1.68(25) \text{ MeV}, \quad L_8 = 0.88(20) \text{ MeV}. \quad (\text{C.10})$$

The LECs L_9 and L_{10} are related to the LECs c_1 and c_5 in Ref. [91]. The relations can be obtained [102, 133]

$$L_{10} = B_0 c_1 (m_d + m_u) = 24.05(48) \text{ MeV}, \quad (\text{C.11})$$

$$L_9 - \frac{1}{2} L_{10} = B_0 c_5 (m_d - m_u) = -0.51(8) \text{ MeV}. \quad (\text{C.12})$$

Thus, the numerical values of the LECs become

$$L_9 = 11.52(25) \text{ MeV}, \quad L_{10} = 24.05(48) \text{ MeV}. \quad (\text{C.13})$$

Similarly, the LECs L_{11} and L_{12} are related to the LECs d_{18} and d_{19} in Refs. [91, 133]

$$L_{11} = m_N B_0 d_{18} (m_d + m_u) = -42.96(24) \text{ MeV}, \quad (\text{C.14})$$

$$L_{12} = m_N B_0 d_{19} (m_d + m_u) = -36.75(36) \text{ MeV}, \quad (\text{C.15})$$

Moreover, the LECs of gluonic current interaction have been obtained [103]

$$L_{13} = F_G^N = -50.4(6) \text{ MeV}, \quad L_{14} = F_{\tilde{G}}^N = -0.306(28) \text{ GeV}. \quad (\text{C.16})$$

D Nuclear Response

In the eigenstate of nuclear angular momentum, we can expand the nuclear matrix element in Eq. (5.28) using a multipole expansion [98, 99]. We define the operators

$$M_{JM}(|\mathbf{q}|\mathbf{x}) \equiv j_J(|\mathbf{q}|x)Y_{JM}(\Omega_x), \quad (\text{D.1})$$

$$\mathbf{M}_{JL}^M(|\mathbf{q}|\mathbf{x}) \equiv j_L(|\mathbf{q}|x)\mathbf{Y}_{JLM}, \quad (\text{D.2})$$

where j_J is the spherical Bessel function, Y_{JM} is the spherical harmonic, and \mathbf{Y}_{JLM} is the vector spherical harmonic.

To arrive at the nuclear response basis, expressing the one-body operators in coordinate space and Fourier transform them to momentum space. Expanding the plane wave (and its vector counterpart) in scalar and vector spherical harmonics projects the charge and current onto definite multipoles, and the nucleon momentum in Eq. (5.26) is replaced by gradients acting on the nuclear wave function, $\mathbf{p} \rightarrow -i\nabla$. For elastic ground-state matrix elements, parity and time-reversal selection rules allow the multipole operators to be organized into six independent response operators $\{M_{JM}, \Delta_{JM}, \Sigma'_{JM}, \Sigma''_{JM}, \tilde{\Phi}'_{JM}, \Phi''_{JM}\}$, where M_{JM} is defined above and the remaining five are given below

$$\Delta_{JM}(|\mathbf{q}|\mathbf{x}) \equiv \mathbf{M}_{JJ}^M(|\mathbf{q}|\mathbf{x}) \cdot \frac{1}{|\mathbf{q}|}\nabla, \quad (\text{D.3})$$

$$\Sigma'_{JM}(|\mathbf{q}|\mathbf{x}) \equiv -i \left\{ \frac{1}{|\mathbf{q}|}\nabla \times \mathbf{M}_{JJ}^M(|\mathbf{q}|\mathbf{x}) \right\} \cdot \sigma, \quad (\text{D.4})$$

$$\Sigma''_{JM}(|\mathbf{q}|\mathbf{x}) \equiv \left\{ \frac{1}{|\mathbf{q}|}\nabla M_{JM}(|\mathbf{q}|\mathbf{x}) \right\} \cdot \sigma, \quad (\text{D.5})$$

$$\tilde{\Phi}'_{JM}(|\mathbf{q}|\mathbf{x}) \equiv \left(\frac{1}{|\mathbf{q}|}\nabla \times \mathbf{M}_{JJ}^M(|\mathbf{q}|\mathbf{x}) \right) \cdot \left(\sigma \times \frac{1}{|\mathbf{q}|}\nabla \right) + \frac{1}{2}\mathbf{M}_{JJ}^M(|\mathbf{q}|\mathbf{x}) \cdot \sigma, \quad (\text{D.6})$$

$$\Phi''_{JM}(|\mathbf{q}|\mathbf{x}) \equiv i \left(\frac{1}{|\mathbf{q}|}\nabla M_{JM}(|\mathbf{q}|\mathbf{x}) \right) \cdot \left(\sigma \times \frac{1}{|\mathbf{q}|}\nabla \right), \quad (\text{D.7})$$

which are the response operators in Eq.(5.30).

The many-body nuclear matrix element can be written as a sum over one-body density matrices. Using the nuclear angular momentum (j_N) and isospin (T, M_T) to label the nuclear state, we have

$$\langle j_N; TM_T | \sum_{i=1}^A O_{J;\tau;i} | j_N; TM_T \rangle = (-1)^{T-M_T} \begin{pmatrix} T & \tau & T \\ -M_T & 0 & M_T \end{pmatrix} \sum_{|\alpha|, |\beta|, i} \Psi_{|\alpha|, |\beta|}^{J;\tau} \langle |\alpha| \ddot{\cdot} O_{J;\tau;i} \ddot{\cdot} |\beta| \rangle, \quad (\text{D.8})$$

where $|\alpha|$ and $|\beta|$ denote the quantum numbers of the single-particle basis, Ψ is the one-body density matrix for the transition between the ground states $|\alpha|$ and $|\beta|$, and $\ddot{\cdot}$ indicates the reduced matrix element in spin and isospin space. The one-body density matrix Ψ can be obtained from a nuclear structure model, such as the shell model [99].

For the single-particle matrix elements $\langle |\alpha| \langle O_{J;\tau;i} | \beta | \rangle \rangle$, the harmonic oscillator model provides a convenient framework for calculation. With the harmonic oscillator as the single-particle basis, these matrix elements can be related to the response operators $O_J \rightarrow \{M_J, \Delta_J, \Sigma'_J, \Sigma''_J, \tilde{\Phi}'_J, \Phi''_J\}$, as presented in Eq. (5.32)

$$\begin{aligned}
W_{MM}^{\tau\tau'}(y) &= \sum_{J=0,2,\dots}^{\infty} \langle j_N | | M_{J;\tau} | | j_N \rangle \langle j_N | | M_{J;\tau'} | | j_N \rangle, \\
W_{\Sigma''\Sigma''}^{\tau\tau'}(y) &= \sum_{J=1,3,\dots}^{\infty} \langle j_N | | \Sigma''_{J;\tau} | | j_N \rangle \langle j_N | | \Sigma''_{J;\tau'} | | j_N \rangle, \\
W_{\Sigma'\Sigma'}^{\tau\tau'}(y) &= \sum_{J=1,3,\dots}^{\infty} \langle j_N | | \Sigma'_{J;\tau} | | j_N \rangle \langle j_N | | \Sigma'_{J;\tau'} | | j_N \rangle, \\
W_{\Phi''\Phi''}^{\tau\tau'}(y) &= \sum_{J=0,2,\dots}^{\infty} \langle j_N | | \Phi''_{J;\tau} | | j_N \rangle \langle j_N | | \Phi''_{J;\tau'} | | j_N \rangle, \\
W_{\Phi''M}^{\tau\tau'}(y) &= \sum_{J=0,2,\dots}^{\infty} \langle j_N | | \Phi''_{J;\tau} | | j_N \rangle \langle j_N | | M_{J;\tau'} | | j_N \rangle, \\
W_{\tilde{\Phi}'\tilde{\Phi}'}^{\tau\tau'}(y) &= \sum_{J=2,4,\dots}^{\infty} \langle j_N | | \tilde{\Phi}'_{J;\tau} | | j_N \rangle \langle j_N | | \tilde{\Phi}'_{J;\tau'} | | j_N \rangle, \\
W_{\Delta\Delta}^{\tau\tau'}(y) &= \sum_{J=1,3,\dots}^{\infty} \langle j_N | | \Delta_{J;\tau} | | j_N \rangle \langle j_N | | \Delta_{J;\tau'} | | j_N \rangle, \\
W_{\Delta\Sigma'}^{\tau\tau'}(y) &= \sum_{J=1,3,\dots}^{\infty} \langle j_N | | \Delta_{J;\tau} | | j_N \rangle \langle j_N | | \Sigma'_{J;\tau'} | | j_N \rangle. \tag{D.9}
\end{aligned}$$

In the harmonic oscillator basis, the reduced matrix element $\langle j_N | | O_J | | j_N \rangle$ can be expressed as a polynomial in the variable y

$$\langle j_N | | O_J | | j_N \rangle \propto y^{(J-K)/2} e^{-y} p(y), \tag{D.10}$$

where the operators $(\Delta, \Sigma', \Sigma'')$ have abnormal parity ($K = 1$), while $(M, \tilde{\Phi}', \Phi'')$ have normal parity ($K = 2$). Consequently, the nuclear responses $W(y)$ can be expressed as functions of y .

E Operator Matching: From SMEFT to LEFT

In this appendix, we give the matching between SMEFT and LEFT. We only consider the dimension-6 SMEFT operators contribution for the Higgs and electroweak gauge boson sector which has been obtained in Ref. [66]. The Higgs field can be written in unitary gauge as

$$H = \frac{1}{\sqrt{2}} \begin{pmatrix} 0 \\ [1 + c_{H,\text{kin}}] h + v_T \end{pmatrix}, \tag{E.1}$$

where

$$c_{H,\text{kin}} \equiv \left(C_{H\square} - \frac{1}{4} C_{HD} \right) v^2, \quad v_T \equiv \left(1 + \frac{3C_H v^2}{8\lambda} \right) v, \quad (\text{E.2})$$

where $c_{H,\text{kin}}$ parametrizes the Higgs kinetic-term and v_T is the vacuum expectation value (VEV) in SMEFT. the gauge field and coupling redefinitions for $SU(2)_L$ and $U(1)_Y$ read

$$\bar{g}_2 = g_2 (1 + C_{HW} v_T^2), \quad \bar{g}_1 = g_1 (1 + C_{HB} v_T^2), \quad (\text{E.3})$$

$$W_\mu^I = \mathcal{W}_\mu^I (1 + C_{HW} v_T^2), \quad B_\mu = \mathcal{B}_\mu (1 + C_{HB} v_T^2). \quad (\text{E.4})$$

Thus, the weak mixing of the two neutral gauge-bosons and the weak mixing angle $\bar{\theta}$ can be obtained

$$\begin{pmatrix} \mathcal{Z}^\mu \\ \mathcal{A}^\mu \end{pmatrix} = \begin{pmatrix} \bar{c} - \frac{\epsilon}{2} \bar{s} & -\bar{s} + \frac{\epsilon}{2} \bar{c} \\ \bar{s} + \frac{\epsilon}{2} \bar{c} & \bar{c} + \frac{\epsilon}{2} \bar{s} \end{pmatrix} \begin{pmatrix} \mathcal{W}_3^\mu \\ \mathcal{B}^\mu \end{pmatrix}, \quad \epsilon \equiv C_{HWB} v_T^2, \quad (\text{E.5})$$

$$\cos \bar{\theta} \equiv \bar{c} = \frac{\bar{g}_2}{\sqrt{\bar{g}_1^2 + \bar{g}_2^2}} \left[1 - \frac{\epsilon}{2} \frac{\bar{g}_1}{\bar{g}_2} \left(\frac{\bar{g}_2^2 - \bar{g}_1^2}{\bar{g}_1^2 + \bar{g}_2^2} \right) \right], \quad (\text{E.6})$$

$$\sin \bar{\theta} \equiv \bar{s} = \frac{\bar{g}_1}{\sqrt{\bar{g}_1^2 + \bar{g}_2^2}} \left[1 + \frac{\epsilon}{2} \frac{\bar{g}_2}{\bar{g}_1} \left(\frac{\bar{g}_2^2 - \bar{g}_1^2}{\bar{g}_1^2 + \bar{g}_2^2} \right) \right]. \quad (\text{E.7})$$

After the symmetry breaking, the mass of neutral charge massive gauge boson \mathcal{Z}^μ and the effective couplings to the \mathcal{Z}^μ boson become

$$M_{\mathcal{Z}}^2 = \frac{1}{4} (\bar{g}_2^2 + \bar{g}_1^2) v_T^2 \left(1 + \frac{1}{2} C_{HD} v_T^2 \right) + \frac{\epsilon}{2} \bar{g}_1 \bar{g}_2 v_T^2, \quad (\text{E.8})$$

$$\bar{g}_Z = \frac{\bar{g}_2 \bar{s} - \frac{1}{2} \bar{c} \bar{g}_2 v_T^2 C_{HWB}}{\bar{c} \bar{s}} \left[1 + \frac{\bar{g}_1^2 + \bar{g}_2^2}{2\bar{g}_1 \bar{g}_2} v_T^2 C_{HWB} \right]. \quad (\text{E.9})$$

In addition, the fermion couplings to the massive gauge bosons \mathcal{Z}^μ are

$$[Z_{\nu_L}]_{pr} = \left[\delta_{pr} \left(\frac{1}{2} \right) - \frac{1}{2} v_T^2 C_{Hlpr}^{(1)} + \frac{1}{2} v_T^2 C_{Hlpr}^{(3)} \right], \quad (\text{E.10})$$

$$[Z_{u_L}]_{pr} = \left[\delta_{pr} \left(\frac{1}{2} - \frac{2}{3} \bar{s}^2 \right) - \frac{1}{2} v_T^2 C_{Hqpr}^{(1)} + \frac{1}{2} v_T^2 C_{Hqpr}^{(3)} \right], \quad (\text{E.11})$$

$$[Z_{u_R}]_{pr} = \left[\delta_{pr} \left(-\frac{2}{3} \bar{s}^2 \right) - \frac{1}{2} v_T^2 C_{Hupr} \right], \quad (\text{E.12})$$

$$[Z_{d_L}]_{pr} = \left[\delta_{pr} \left(-\frac{1}{2} + \frac{1}{3} \bar{s}^2 \right) - \frac{1}{2} v_T^2 C_{Hqpr}^{(1)} - \frac{1}{2} v_T^2 C_{Hqpr}^{(3)} \right], \quad (\text{E.13})$$

$$[Z_{d_R}]_{pr} = \left[\delta_{pr} \left(+\frac{1}{3} \bar{s}^2 \right) - \frac{1}{2} v_T^2 C_{Hdpr} \right]. \quad (\text{E.14})$$

There are the direct and indirect contributions in the matching condition. The matching conditions for dimension-5, 6 and 7 LEFT operators have been obtained in Ref. [66, 67, 134]. Here, we give the matching conditions for relevant LEFT operators up to dimension-8. The relevant matching results for dimension-5, 6 and 7 LEFT operators are

$$\mathcal{C}_1^5 = \frac{ev_T^2}{2} (C_{LHB} + C_{LHW}) , \quad (\text{E.15})$$

$$\mathcal{C}_1^{6u} = \frac{\Lambda_{\text{EW}}^2}{\Lambda^2} \left[C_{lq}^{(1)\alpha\beta} + C_{lq}^{(3)\alpha\beta} + C_{lu}^{\alpha\beta} - \frac{\bar{g}_Z^2}{M_Z^2} \left([Z_\nu]^{\alpha\beta} [Z_{u_L}] + [Z_\nu]^{\alpha\beta} [Z_{u_R}] \right) \right] , \quad (\text{E.16})$$

$$\mathcal{C}_1^{6d} = \frac{\Lambda_{\text{EW}}^2}{\Lambda^2} \left[C_{lq}^{(1)\alpha\beta} - C_{lq}^{(3)\alpha\beta} + C_{ld}^{\alpha\beta} - \frac{\bar{g}_Z^2}{M_Z^2} \left([Z_\nu]^{\alpha\beta} [Z_{d_L}] + [Z_\nu]^{\alpha\beta} [Z_{d_R}] \right) \right] , \quad (\text{E.17})$$

$$\mathcal{C}_2^{6u} = \frac{\Lambda_{\text{EW}}^2}{\Lambda^2} \left[C_{lu}^{\alpha\beta} - C_{lq}^{(1)\alpha\beta} - C_{lq}^{(3)\alpha\beta} - \frac{\bar{g}_Z^2}{M_Z^2} \left([Z_\nu]^{\alpha\beta} [Z_{u_R}] - [Z_\nu]^{\alpha\beta} [Z_{u_L}] \right) \right] , \quad (\text{E.18})$$

$$\mathcal{C}_2^{6d} = \frac{\Lambda_{\text{EW}}^2}{\Lambda^2} \left[C_{ld}^{\alpha\beta} - C_{lq}^{(1)\alpha\beta} + C_{lq}^{(3)\alpha\beta} - \frac{\bar{g}_Z^2}{M_Z^2} \left([Z_\nu]^{\alpha\beta} [Z_{d_R}] - [Z_\nu]^{\alpha\beta} [Z_{d_L}] \right) \right] , \quad (\text{E.19})$$

$$\mathcal{C}_1^{7u} = \frac{\sqrt{2}\Lambda_{\text{EW}}^2}{M_Z\Lambda^2} \delta^{\alpha\beta} (\bar{c}C_{uW} - \bar{s}C_{uB}) , \quad \mathcal{C}_1^{7d} = -\frac{\sqrt{2}\Lambda_{\text{EW}}^2}{M_Z\Lambda^2} \delta^{\alpha\beta} (\bar{c}C_{dW} + \bar{s}C_{dB}) , \quad (\text{E.20})$$

$$\mathcal{C}_2^{7u} = \frac{\sqrt{2}\Lambda_{\text{EW}}^2}{M_Z\Lambda^2} \delta^{\alpha\beta} (\bar{s}C_{uB} - \bar{c}C_{uW}) , \quad \mathcal{C}_2^{7d} = \frac{\sqrt{2}\Lambda_{\text{EW}}^2}{M_Z\Lambda^2} \delta^{\alpha\beta} (\bar{c}C_{dW} + \bar{s}C_{dB}) , \quad (\text{E.21})$$

$$\mathcal{C}_4^{7u} = \frac{\sqrt{2}\Lambda_{\text{EW}}^2 v_T}{1\Lambda^3} C_{QuLLH}^{\alpha\beta} , \quad \mathcal{C}_4^{7d} = \frac{\sqrt{2}\Lambda_{\text{EW}}^2 v_T}{2\Lambda^3} C_{dLQLH1}^{\alpha\beta} , \quad (\text{E.22})$$

$$\mathcal{C}_5^{7u} = -\frac{\sqrt{2}\Lambda_{\text{EW}}^2 v_T}{2\Lambda^3} C_{QuLLH}^{\alpha\beta} , \quad \mathcal{C}_5^{7d} = -\frac{\sqrt{2}\Lambda_{\text{EW}}^2 v_T}{2\Lambda^3} C_{dLQLH1}^{\alpha\beta} , \quad (\text{E.23})$$

$$\mathcal{C}_3^{7d} = \frac{\sqrt{2}\Lambda_{\text{EW}}^2 v_T}{2\Lambda^3} C_{dLQLH2}^{\alpha\beta} . \quad (\text{E.24})$$

It should be emphasized that the operators \mathcal{O}_{LHB} and \mathcal{O}_{LHW} are not presented in this paper. Because only three types of the seesaw can contribute to the two operators at tree level which are constrained by Weinberg operators and neglected in this work. In addition, the SMEFT operators up to dimension-8 can not contribute to \mathcal{O}_3^{7u} at tree level.

Moreover, the matching conditions for LEFT dimension-8 operators become

$$\mathcal{C}_1^{8u} = \frac{\Lambda_{\text{EW}}^4}{\Lambda^4} \left[C_{l^2q^2D^2}^{(2)\alpha\beta} + C_{l^2q^2D^2}^{(4)\alpha\beta} + C_{l^2u^2D^2}^{(2)\alpha\beta} \right], \quad (\text{E.25})$$

$$\mathcal{C}_1^{8d} = \frac{\Lambda_{\text{EW}}^4}{\Lambda^4} \left[C_{l^2q^2D^2}^{(2)\alpha\beta} - C_{l^2q^2D^2}^{(4)\alpha\beta} + C_{l^2d^2D^2}^{(2)\alpha\beta} \right], \quad (\text{E.26})$$

$$\mathcal{C}_2^{8u} = \frac{\Lambda_{\text{EW}}^4}{\Lambda^4} \left[C_{l^2u^2D^2}^{(2)\alpha\beta} - C_{l^2q^2D^2}^{(2)\alpha\beta} - C_{l^2q^2D}^{(4)\alpha\beta} \right], \quad (\text{E.27})$$

$$\mathcal{C}_2^{8d} = \frac{\Lambda_{\text{EW}}^4}{\Lambda^4} \left[C_{l^2d^2D^2}^{(2)\alpha\beta} - C_{l^2q^2D^2}^{(2)\alpha\beta} + C_{l^2q^2D^2}^{(4)\alpha\beta} \right], \quad (\text{E.28})$$

$$\mathcal{C}_3^{8u} = \frac{\Lambda_{\text{EW}}^4}{\Lambda^4} \left[C_{l^2q^2G}^{(1)\alpha\beta} + C_{l^2q^2G}^{(3)\alpha\beta} + C_{l^2u^2G}^{(1)\alpha\beta} \right], \quad (\text{E.29})$$

$$\mathcal{C}_3^{8d} = \frac{\Lambda_{\text{EW}}^4}{\Lambda^4} \left[C_{l^2q^2G}^{(1)\alpha\beta} - C_{l^2q^2G}^{(3)\alpha\beta} + C_{l^2d^2G}^{(1)\alpha\beta} \right], \quad (\text{E.30})$$

$$\mathcal{C}_4^{8u} = \frac{\Lambda_{\text{EW}}^4}{\Lambda^4} \left[C_{l^2u^2G}^{(1)\alpha\beta} - C_{l^2q^2G}^{(1)\alpha\beta} - C_{l^2q^2G}^{(3)\alpha\beta} \right], \quad (\text{E.31})$$

$$\mathcal{C}_4^{8d} = \frac{\Lambda_{\text{EW}}^4}{\Lambda^4} \left[C_{l^2d^2G}^{(1)\alpha\beta} - C_{l^2q^2G}^{(1)\alpha\beta} + C_{l^2q^2G}^{(3)\alpha\beta} \right], \quad (\text{E.32})$$

$$\mathcal{C}_5^{8u} = \frac{\Lambda_{\text{EW}}^4}{\Lambda^4} \left[C_{l^2q^2D^2}^{(1)\alpha\beta} + C_{l^2q^2D^2}^{(3)\alpha\beta} + C_{l^2u^2D^2}^{(1)\alpha\beta} \right], \quad (\text{E.33})$$

$$\mathcal{C}_5^{8d} = \frac{\Lambda_{\text{EW}}^4}{\Lambda^4} \left[C_{l^2q^2D^2}^{(1)\alpha\beta} - C_{l^2q^2D^2}^{(3)\alpha\beta} + C_{l^2d^2D^2}^{(1)\alpha\beta} \right], \quad (\text{E.34})$$

$$\mathcal{C}_6^{8u} = \frac{\Lambda_{\text{EW}}^4}{\Lambda^4} \left[C_{l^2u^2D^2}^{(1)\alpha\beta} - C_{l^2q^2D^2}^{(1)\alpha\beta} - C_{l^2q^2D}^{(3)\alpha\beta} \right], \quad (\text{E.35})$$

$$\mathcal{C}_6^{8d} = \frac{\Lambda_{\text{EW}}^4}{\Lambda^4} \left[C_{l^2d^2D^2}^{(1)\alpha\beta} - C_{l^2q^2D^2}^{(1)\alpha\beta} + C_{l^2q^2D^2}^{(3)\alpha\beta} \right], \quad (\text{E.36})$$

$$\mathcal{C}_7^{8u} = \frac{\Lambda_{\text{EW}}^4}{\Lambda^4} \left[C_{l^2q^2G}^{(2)} + C_{l^2q^2G}^{(4)} + C_{l^2u^2G}^{(2)} \right], \quad (\text{E.37})$$

$$\mathcal{C}_7^{8d} = \frac{\Lambda_{\text{EW}}^4}{\Lambda^4} \left[C_{l^2q^2G}^{(2)} - C_{l^2q^2G}^{(4)} + C_{l^2d^2G}^{(2)} \right], \quad (\text{E.38})$$

$$\mathcal{C}_8^{8u} = \frac{\Lambda_{\text{EW}}^4}{\Lambda^4} \left[C_{l^2u^2G}^{(2)} - C_{l^2q^2G}^{(2)} - C_{l^2q^2G}^{(4)} \right], \quad (\text{E.39})$$

$$\mathcal{C}_8^{8d} = \frac{\Lambda_{\text{EW}}^4}{\Lambda^4} \left[C_{l^2d^2G}^{(2)} - C_{l^2q^2G}^{(2)} + C_{l^2q^2G}^{(4)} \right], \quad (\text{E.40})$$

$$\mathcal{C}_9^8 = \frac{\Lambda_{\text{EW}}^4}{\Lambda^4} [C_{l^2G^2D}], \quad (\text{E.41})$$

where some SMEFT operators are not presented in Tab. 5, as the corresponding dimension-8 LEFT operators either do not contribute to CE ν NS in the one-body state or are suppressed by dimension-6 LEFT operators with a similar form.

References

[1] D. Z. Freedman, *Coherent Neutrino Nucleus Scattering as a Probe of the Weak Neutral Current*, *Phys. Rev. D* **9** (1974) 1389–1392.

- [2] P. Coloma, M. C. Gonzalez-Garcia, M. Maltoni and T. Schwetz, *COHERENT Enlightenment of the Neutrino Dark Side*, *Phys. Rev. D* **96** (2017) 115007, [[1708.02899](#)].
- [3] J. Liao and D. Marfatia, *COHERENT constraints on nonstandard neutrino interactions*, *Phys. Lett. B* **775** (2017) 54–57, [[1708.04255](#)].
- [4] M. Cadeddu, C. Giunti, Y. F. Li and Y. Y. Zhang, *Average CsI neutron density distribution from COHERENT data*, *Phys. Rev. Lett.* **120** (2018) 072501, [[1710.02730](#)].
- [5] S.-F. Ge and I. M. Shoemaker, *Constraining Photon Portal Dark Matter with Texono and Coherent Data*, *JHEP* **11** (2018) 066, [[1710.10889](#)].
- [6] D. Aristizabal Sierra, N. Rojas and M. H. G. Tytgat, *Neutrino non-standard interactions and dark matter searches with multi-ton scale detectors*, *JHEP* **03** (2018) 197, [[1712.09667](#)].
- [7] E. Ciuffoli, J. Evslin, Q. Fu and J. Tang, *Extracting nuclear form factors with coherent neutrino scattering*, *Phys. Rev. D* **97** (2018) 113003, [[1801.02166](#)].
- [8] Y. Farzan, M. Lindner, W. Rodejohann and X.-J. Xu, *Probing neutrino coupling to a light scalar with coherent neutrino scattering*, *JHEP* **05** (2018) 066, [[1802.05171](#)].
- [9] J. Billard, J. Johnston and B. J. Kavanagh, *Prospects for exploring New Physics in Coherent Elastic Neutrino-Nucleus Scattering*, *JCAP* **11** (2018) 016, [[1805.01798](#)].
- [10] D. Aristizabal Sierra, V. De Romeri and N. Rojas, *COHERENT analysis of neutrino generalized interactions*, *Phys. Rev. D* **98** (2018) 075018, [[1806.07424](#)].
- [11] M. Cadeddu and F. Dordei, *Reinterpreting the weak mixing angle from atomic parity violation in view of the Cs neutron rms radius measurement from COHERENT*, *Phys. Rev. D* **99** (2019) 033010, [[1808.10202](#)].
- [12] W. Altmannshofer, M. Tammaro and J. Zupan, *Non-standard neutrino interactions and low energy experiments*, *JHEP* **09** (2019) 083, [[1812.02778](#)].
- [13] O. G. Miranda, G. Sanchez Garcia and O. Sanders, *Coherent elastic neutrino-nucleus scattering as a precision test for the Standard Model and beyond: the COHERENT proposal case*, *Adv. High Energy Phys.* **2019** (2019) 3902819, [[1902.09036](#)].
- [14] D. Aristizabal Sierra, V. De Romeri and N. Rojas, *CP violating effects in coherent elastic neutrino-nucleus scattering processes*, *JHEP* **09** (2019) 069, [[1906.01156](#)].
- [15] D. K. Papoulias, *COHERENT constraints after the COHERENT-2020 quenching factor measurement*, *Phys. Rev. D* **102** (2020) 113004, [[1907.11644](#)].
- [16] C. Giunti, *General COHERENT constraints on neutrino nonstandard interactions*, *Phys. Rev. D* **101** (2020) 035039, [[1909.00466](#)].
- [17] B. C. Canas, E. A. Garces, O. G. Miranda, A. Parada and G. Sanchez Garcia, *Interplay between nonstandard and nuclear constraints in coherent elastic neutrino-nucleus scattering experiments*, *Phys. Rev. D* **101** (2020) 035012, [[1911.09831](#)].
- [18] M. Hoferichter, J. Menéndez and A. Schwenk, *Coherent elastic neutrino-nucleus scattering: EFT analysis and nuclear responses*, *Phys. Rev. D* **102** (2020) 074018, [[2007.08529](#)].
- [19] W. Skiba and Q. Xia, *Electroweak constraints from the COHERENT experiment*, *JHEP* **10** (2022) 102, [[2007.15688](#)].

[20] M. Cadeddu, N. Cargioli, F. Dordei, C. Giunti, Y. F. Li, E. Picciano et al., *Constraints on light vector mediators through coherent elastic neutrino nucleus scattering data from COHERENT*, *JHEP* **01** (2021) 116, [[2008.05022](#)].

[21] Y. Du, H.-L. Li, J. Tang, S. Vihonen and J.-H. Yu, *Exploring SMEFT induced nonstandard interactions: From COHERENT to neutrino oscillations*, *Phys. Rev. D* **105** (2022) 075022, [[2106.15800](#)].

[22] A. Dasgupta, S. K. Kang and J. E. Kim, *Probing neutrino dipole portal at COHERENT experiment*, *JHEP* **11** (2021) 120, [[2108.12998](#)].

[23] M. Atzori Corona, M. Cadeddu, N. Cargioli, F. Dordei, C. Giunti, Y. F. Li et al., *Impact of the Dresden-II and COHERENT neutrino scattering data on neutrino electromagnetic properties and electroweak physics*, *JHEP* **09** (2022) 164, [[2205.09484](#)].

[24] V. De Romeri, O. G. Miranda, D. K. Papoulias, G. Sanchez Garcia, M. Tórtola and J. W. F. Valle, *Physics implications of a combined analysis of COHERENT CsI and LAr data*, *JHEP* **04** (2023) 035, [[2211.11905](#)].

[25] Y.-Y. Li, Y.-F. Li and S.-Y. Xia, *Neutrino magnetic dipole portal with low energy neutrino nucleus scattering data*, [2406.07477](#).

[26] G. Li, C.-Q. Song, F.-J. Tang and J.-H. Yu, *Constraints on neutrino nonstandard interactions from COHERENT, PandaX-4T and XENONnT*, *Phys. Rev. D* **111** (2025) 035002, [[2409.04703](#)].

[27] J. Liao, J. Tang and B.-L. Zhang, *Tensor interaction in coherent elastic neutrino-nucleus scattering*, *Phys. Rev. D* **112** (2025) 035036, [[2502.10702](#)].

[28] M. Abdullah et al., *Coherent elastic neutrino-nucleus scattering: Terrestrial and astrophysical applications*, [2203.07361](#).

[29] COHERENT collaboration, D. Akimov et al., *Observation of Coherent Elastic Neutrino-Nucleus Scattering*, *Science* **357** (2017) 1123–1126, [[1708.01294](#)].

[30] CONNIE collaboration, A. Aguilar-Arevalo et al., *Exploring low-energy neutrino physics with the Coherent Neutrino Nucleus Interaction Experiment*, *Phys. Rev. D* **100** (2019) 092005, [[1906.02200](#)].

[31] CONUS collaboration, H. Bonet et al., *Constraints on elastic neutrino nucleus scattering in the fully coherent regime from the CONUS experiment*, *Phys. Rev. Lett.* **126** (2021) 041804, [[2011.00210](#)].

[32] ν GEN collaboration, I. Alekseev et al., *First results of the ν GeN experiment on coherent elastic neutrino-nucleus scattering*, *Phys. Rev. D* **106** (2022) L051101, [[2205.04305](#)].

[33] J. Colaresi, J. I. Collar, T. W. Hossbach, C. M. Lewis and K. M. Yocum, *Measurement of Coherent Elastic Neutrino-Nucleus Scattering from Reactor Antineutrinos*, *Phys. Rev. Lett.* **129** (2022) 211802, [[2202.09672](#)].

[34] CLOVERS, CE ν NS@CSNS collaboration, C. Su, Q. Liu and T. Liang, *CE ν NS Experiment Proposal at CSNS* ‡, *Phys. Sci. Forum* **8** (2023) 19, [[2303.13423](#)].

[35] RICOCHET collaboration, C. Augier et al., *Results from a prototype TES detector for the Ricochet experiment*, *Nucl. Instrum. Meth. A* **1057** (2023) 168765, [[2304.14926](#)].

- [36] N. Ackermann et al., *Final CONUS results on coherent elastic neutrino nucleus scattering at the Brokdorf reactor*, [2401.07684](#).
- [37] L. T. Yang, Y. F. Liang and Q. Yue, *RECODE program for reactor neutrino CEvNS detection with PPC Germanium detector*, *PoS TAUP2023* (2024) 296.
- [38] C. Cai et al., *RELICS: a REactor neutrino LIquid xenon Coherent elastic Scattering experiment*, [2405.05554](#).
- [39] X. Xiao, *Cicenns: a 300-kg csi(na) detector for coherent elastic neutrino-nucleus scattering*, 2024.
- [40] COHERENT collaboration, D. Akimov et al., *Measurement of the Coherent Elastic Neutrino-Nucleus Scattering Cross Section on CsI by COHERENT*, *Phys. Rev. Lett.* **129** (2022) 081801, [\[2110.07730\]](#).
- [41] COHERENT collaboration, D. Akimov et al., *First Measurement of Coherent Elastic Neutrino-Nucleus Scattering on Argon*, *Phys. Rev. Lett.* **126** (2021) 012002, [\[2003.10630\]](#).
- [42] COHERENT collaboration, D. Akimov et al., *COHERENT Collaboration data release from the first detection of coherent elastic neutrino-nucleus scattering on argon*, [2006.12659](#).
- [43] COHERENT collaboration, S. Adamski et al., *First detection of coherent elastic neutrino-nucleus scattering on germanium*, [2406.13806](#).
- [44] PANDAX collaboration, Z. Bo et al., *First Measurement of Solar 8B Neutrino Flux through Coherent Elastic Neutrino-Nucleus Scattering in PandaX-4T*, [2407.10892](#).
- [45] XENON collaboration, E. Aprile et al., *First Measurement of Solar 8B Neutrinos via Coherent Elastic Neutrino-Nucleus Scattering with XENONnT*, [2408.02877](#).
- [46] (CONUS COLLABORATION)*, CONUS collaboration, N. Ackermann et al., *Final CONUS Results on Coherent Elastic Neutrino-Nucleus Scattering at the Brokdorf Reactor*, *Phys. Rev. Lett.* **133** (2024) 251802, [\[2401.07684\]](#).
- [47] N. Ackermann et al., *Direct observation of coherent elastic antineutrino-nucleus scattering*, *Nature* **643** (2025) 1229–1233, [\[2501.05206\]](#).
- [48] J. Barranco, O. G. Miranda and T. I. Rashba, *Probing new physics with coherent neutrino scattering off nuclei*, *JHEP* **12** (2005) 021, [\[hep-ph/0508299\]](#).
- [49] R. Calabrese, J. Gunn, G. Miele, S. Morisi, S. Roy and P. Santorelli, *Constraining scalar leptoquarks using COHERENT data*, *Phys. Rev. D* **107** (2023) 055039, [\[2212.11210\]](#).
- [50] V. De Romeri, V. M. Lozano and G. Sanchez Garcia, *Neutrino window to scalar leptoquarks: From low energy to colliders*, *Phys. Rev. D* **109** (2024) 055014, [\[2307.13790\]](#).
- [51] R. H. Helm, *Inelastic and Elastic Scattering of 187-Mev Electrons from Selected Even-Even Nuclei*, *Phys. Rev.* **104** (1956) 1466–1475.
- [52] S. Klein and J. Nystrand, *Exclusive vector meson production in relativistic heavy ion collisions*, *Phys. Rev. C* **60** (1999) 014903, [\[hep-ph/9902259\]](#).
- [53] R. Roth, S. Binder, K. Vobig, A. Calci, J. Langhammer and P. Navratil, *Ab Initio Calculations of Medium-Mass Nuclei with Normal-Ordered Chiral NN+3N Interactions*, *Phys. Rev. Lett.* **109** (2012) 052501, [\[1112.0287\]](#).

[54] S. R. Stroberg, J. D. Holt, A. Schwenk and J. Simonis, *AbInitio Limits of Atomic Nuclei*, *Phys. Rev. Lett.* **126** (2021) 022501, [[1905.10475](#)].

[55] C. G. Payne, S. Bacca, G. Hagen, W. Jiang and T. Papenbrock, *Coherent elastic neutrino-nucleus scattering on ^{40}Ar from first principles*, *Phys. Rev. C* **100** (2019) 061304, [[1908.09739](#)].

[56] P. Arthuis, C. Barbieri, M. Vorabbi and P. Finelli, *AbInitio Computation of Charge Densities for Sn and Xe Isotopes*, *Phys. Rev. Lett.* **125** (2020) 182501, [[2002.02214](#)].

[57] B. Hu et al., *Ab initio predictions link the neutron skin of ^{208}Pb to nuclear forces*, *Nature Phys.* **18** (2022) 1196–1200, [[2112.01125](#)].

[58] B. S. Hu, J. Padua-Argüelles, S. Leutheusser, T. Miyagi, S. R. Stroberg and J. D. Holt, *Ab Initio Structure Factors for Spin-Dependent Dark Matter Direct Detection*, *Phys. Rev. Lett.* **128** (2022) 072502, [[2109.00193](#)].

[59] S. Weinberg, *Baryon and Lepton Nonconserving Processes*, *Phys. Rev. Lett.* **43** (1979) 1566–1570.

[60] W. Buchmuller and D. Wyler, *Effective Lagrangian Analysis of New Interactions and Flavor Conservation*, *Nucl. Phys. B* **268** (1986) 621–653.

[61] B. Grzadkowski, M. Iskrzynski, M. Misiak and J. Rosiek, *Dimension-Six Terms in the Standard Model Lagrangian*, *JHEP* **10** (2010) 085, [[1008.4884](#)].

[62] L. Lehman, *Extending the Standard Model Effective Field Theory with the Complete Set of Dimension-7 Operators*, *Phys. Rev. D* **90** (2014) 125023, [[1410.4193](#)].

[63] Y. Liao and X.-D. Ma, *Renormalization Group Evolution of Dimension-seven Baryon- and Lepton-number-violating Operators*, *JHEP* **11** (2016) 043, [[1607.07309](#)].

[64] H.-L. Li, Z. Ren, J. Shu, M.-L. Xiao, J.-H. Yu and Y.-H. Zheng, *Complete set of dimension-eight operators in the standard model effective field theory*, *Phys. Rev. D* **104** (2021) 015026, [[2005.00008](#)].

[65] C. W. Murphy, *Dimension-8 operators in the Standard Model Effective Field Theory*, *JHEP* **10** (2020) 174, [[2005.00059](#)].

[66] E. E. Jenkins, A. V. Manohar and P. Stoffer, *Low-Energy Effective Field Theory below the Electroweak Scale: Operators and Matching*, *JHEP* **03** (2018) 016, [[1709.04486](#)].

[67] Y. Liao, X.-D. Ma and Q.-Y. Wang, *Extending low energy effective field theory with a complete set of dimension-7 operators*, *JHEP* **08** (2020) 162, [[2005.08013](#)].

[68] H.-L. Li, Z. Ren, M.-L. Xiao, J.-H. Yu and Y.-H. Zheng, *Operator bases in effective field theories with sterile neutrinos: $d \leq 9$* , *JHEP* **11** (2021) 003, [[2105.09329](#)].

[69] J. Gasser and H. Leutwyler, *Quark Masses*, *Phys. Rept.* **87** (1982) 77–169.

[70] J. Gasser and H. Leutwyler, *Chiral Perturbation Theory to One Loop*, *Annals Phys.* **158** (1984) 142.

[71] J. Gasser and H. Leutwyler, *Chiral Perturbation Theory: Expansions in the Mass of the Strange Quark*, *Nucl. Phys. B* **250** (1985) 465–516.

[72] G. Li, C.-Q. Song and J.-H. Yu, *Matching from quark to hadronic operators: external source vs spurion methods*, [2507.02538](#).

[73] C.-Q. Song, H. Sun and J.-H. Yu, *Systematic Spurion Matching between Low Energy EFT and Chiral Lagrangian*, [2501.09787](#).

[74] A. Manohar and H. Georgi, *Chiral Quarks and the Nonrelativistic Quark Model*, *Nucl. Phys. B* **234** (1984) 189–212.

[75] B. M. Gavela, E. E. Jenkins, A. V. Manohar and L. Merlo, *Analysis of General Power Counting Rules in Effective Field Theory*, *Eur. Phys. J. C* **76** (2016) 485, [[1601.07551](#)].

[76] E. E. Jenkins, A. V. Manohar and M. Trott, *Naive Dimensional Analysis Counting of Gauge Theory Amplitudes and Anomalous Dimensions*, *Phys. Lett. B* **726** (2013) 697–702, [[1309.0819](#)].

[77] A. L. Fitzpatrick, W. Haxton, E. Katz, N. Lubbers and Y. Xu, *The Effective Field Theory of Dark Matter Direct Detection*, *JCAP* **02** (2013) 004, [[1203.3542](#)].

[78] N. Anand, A. L. Fitzpatrick and W. C. Haxton, *Weakly interacting massive particle-nucleus elastic scattering response*, *Phys. Rev. C* **89** (2014) 065501, [[1308.6288](#)].

[79] L. Vietze, P. Klos, J. Menéndez, W. C. Haxton and A. Schwenk, *Nuclear structure aspects of spin-independent WIMP scattering off xenon*, *Phys. Rev. D* **91** (2015) 043520, [[1412.6091](#)].

[80] E. E. Jenkins, A. V. Manohar and P. Stoffer, *Low-Energy Effective Field Theory below the Electroweak Scale: Anomalous Dimensions*, *JHEP* **01** (2018) 084, [[1711.05270](#)].

[81] L. Naterop and P. Stoffer, *Low-energy effective field theory below the electroweak scale: one-loop renormalization in the 't Hooft-Veltman scheme*, *JHEP* **02** (2024) 068, [[2310.13051](#)].

[82] S. R. Coleman, J. Wess and B. Zumino, *Structure of phenomenological Lagrangians. 1.*, *Phys. Rev.* **177** (1969) 2239–2247.

[83] C. G. Callan, Jr., S. R. Coleman, J. Wess and B. Zumino, *Structure of phenomenological Lagrangians. 2.*, *Phys. Rev.* **177** (1969) 2247–2250.

[84] H.-L. Li, Z. Ren, M.-L. Xiao, J.-H. Yu and Y.-H. Zheng, *Complete set of dimension-nine operators in the standard model effective field theory*, *Phys. Rev. D* **104** (2021) 015025, [[2007.07899](#)].

[85] H.-L. Li, Z. Ren, M.-L. Xiao, J.-H. Yu and Y.-H. Zheng, *Operators for generic effective field theory at any dimension: on-shell amplitude basis construction*, *JHEP* **04** (2022) 140, [[2201.04639](#)].

[86] S.-Z. Jiang, Q. Wang and Y. Zhang, *Computation of the p^6 order low-energy constants with tensor sources*, *Phys. Rev. D* **87** (2013) 094014, [[1203.0712](#)].

[87] J. F. Donoghue, J. Gasser and H. Leutwyler, *The Decay of a Light Higgs Boson*, *Nucl. Phys. B* **343** (1990) 341–368.

[88] A. Krause, *Baryon Matrix Elements of the Vector Current in Chiral Perturbation Theory*, *Helv. Phys. Acta* **63** (1990) 3–70.

[89] E. E. Jenkins and A. V. Manohar, *Baryon chiral perturbation theory using a heavy fermion Lagrangian*, *Phys. Lett. B* **255** (1991) 558–562.

[90] G. Ecker and M. Mojzis, *Low-energy expansion of the pion - nucleon Lagrangian*, *Phys. Lett. B* **365** (1996) 312–318, [[hep-ph/9508204](#)].

[91] N. Fettes, U.-G. Meissner, M. Mojzis and S. Steininger, *The Chiral effective pion nucleon Lagrangian of order p^{**4}* , *Annals Phys.* **283** (2000) 273–302, [[hep-ph/0001308](#)].

[92] S. Weinberg, *Nuclear forces from chiral Lagrangians*, *Phys. Lett. B* **251** (1990) 288–292.

[93] S. Weinberg, *Effective chiral Lagrangians for nucleon - pion interactions and nuclear forces*, *Nucl. Phys. B* **363** (1991) 3–18.

[94] S. Weinberg, *Three body interactions among nucleons and pions*, *Phys. Lett. B* **295** (1992) 114–121, [[hep-ph/9209257](#)].

[95] V. Cirigliano, M. L. Graesser and G. Ovanesyan, *WIMP-nucleus scattering in chiral effective theory*, *JHEP* **10** (2012) 025, [[1205.2695](#)].

[96] M. Hoferichter, P. Klos and A. Schwenk, *Chiral power counting of one- and two-body currents in direct detection of dark matter*, *Phys. Lett. B* **746** (2015) 410–416, [[1503.04811](#)].

[97] P. Klos, *Few-neutron systems and WIMP-nucleus interactions from chiral effective field theory*. PhD thesis, Darmstadt, Tech. Hochsch., 2018.

[98] B. D. Serot, *Semileptonic Weak and Electromagnetic Interactions with Nuclei: Nuclear Current Operators Through Order $(v/c)^{**2}$ (Nucleon)*, *Nucl. Phys. A* **308** (1978) 457–499.

[99] W. Haxton and C. Lunardini, *A Mathematica script for harmonic oscillator nuclear matrix elements arising in semileptonic electroweak interactions*, *Comput. Phys. Commun.* **179** (2008) 345–358, [[0706.2210](#)].

[100] xQCD collaboration, Y.-B. Yang, A. Alexandru, T. Draper, J. Liang and K.-F. Liu, πN and strangeness sigma terms at the physical point with chiral fermions, *Phys. Rev. D* **94** (2016) 054503, [[1511.09089](#)].

[101] R. Gupta, S. Park, M. Hoferichter, E. Mereghetti, B. Yoon and T. Bhattacharya, *Pion–Nucleon Sigma Term from Lattice QCD*, *Phys. Rev. Lett.* **127** (2021) 242002, [[2105.12095](#)].

[102] M. Hoferichter, J. R. de Elvira, B. Kubis and U.-G. Meißner, *On the role of isospin violation in the pion–nucleon σ -term*, *Phys. Lett. B* **843** (2023) 138001, [[2305.07045](#)].

[103] W. Haxton, K. McElvain, T. Menzo, E. Rule and J. Zupan, *Effective theory tower for $\mu \rightarrow e$ conversion*, [2406.13818](#).

[104] J. S. O’ Connell, T. W. Donnelly and J. D. Walecka, *Semileptonic weak interactions with C^{12}* , *Phys. Rev. C* **6** (1972) 719–733.

[105] E. Del Nobile, *The Theory of Direct Dark Matter Detection: A Guide to Computations*, [2104.12785](#).

[106] P. Coloma, P. B. Denton, M. C. Gonzalez-Garcia, M. Maltoni and T. Schwetz, *Curtailing the Dark Side in Non-Standard Neutrino Interactions*, *JHEP* **04** (2017) 116, [[1701.04828](#)].

[107] G. L. Fogli, E. Lisi, A. Marrone, D. Montanino and A. Palazzo, *Getting the most from the statistical analysis of solar neutrino oscillations*, *Phys. Rev. D* **66** (2002) 053010, [[hep-ph/0206162](#)].

[108] M. Cadeddu, F. Dordei, C. Giunti, Y. F. Li, E. Picciau and Y. Y. Zhang, *Physics results from the first COHERENT observation of coherent elastic neutrino-nucleus scattering in argon and their combination with cesium-iodide data*, *Phys. Rev. D* **102** (2020) 015030, [[2005.01645](#)].

[109] O. G. Miranda, D. K. Papoulias, G. Sanchez Garcia, O. Sanders, M. Tórtola and J. W. F. Valle, *Implications of the first detection of coherent elastic neutrino-nucleus scattering (CEvNS) with Liquid Argon*, *JHEP* **05** (2020) 130, [[2003.12050](#)].

[110] E. Vitagliano, I. Tamborra and G. Raffelt, *Grand Unified Neutrino Spectrum at Earth: Sources and Spectral Components*, *Rev. Mod. Phys.* **92** (2020) 45006, [[1910.11878](#)].

[111] T. A. Mueller et al., *Improved Predictions of Reactor Antineutrino Spectra*, *Phys. Rev. C* **83** (2011) 054615, [[1101.2663](#)].

[112] V. I. Kopeikin, *Flux and spectrum of reactor antineutrinos*, *Phys. Atom. Nucl.* **75** (2012) 143–152.

[113] V. De Romeri, D. K. Papoulias and G. Sanchez Garcia, *Implications of the first CONUS+ measurement of coherent elastic neutrino-nucleus scattering*, *Phys. Rev. D* **111** (2025) 075025, [[2501.17843](#)].

[114] L. Wolfenstein, *Neutrino Oscillations in Matter*, *Phys. Rev. D* **17** (1978) 2369–2374.

[115] K. Scholberg, *Prospects for measuring coherent neutrino-nucleus elastic scattering at a stopped-pion neutrino source*, *Phys. Rev. D* **73** (2006) 033005, [[hep-ex/0511042](#)].

[116] S. Davidson, C. Pena-Garay, N. Rius and A. Santamaria, *Present and future bounds on nonstandard neutrino interactions*, *JHEP* **03** (2003) 011, [[hep-ph/0302093](#)].

[117] M. Alpízar-Venegas, L. J. Flores, E. Peinado and E. Vázquez-Jáuregui, *Exploring the standard model and beyond from the evidence of CEvNS with reactor antineutrinos in CONUS+*, *Phys. Rev. D* **111** (2025) 053001, [[2501.10355](#)].

[118] E. E. Jenkins, A. V. Manohar and M. Trott, *Renormalization Group Evolution of the Standard Model Dimension Six Operators I: Formalism and lambda Dependence*, *JHEP* **10** (2013) 087, [[1308.2627](#)].

[119] E. E. Jenkins, A. V. Manohar and M. Trott, *Renormalization Group Evolution of the Standard Model Dimension Six Operators II: Yukawa Dependence*, *JHEP* **01** (2014) 035, [[1310.4838](#)].

[120] R. Alonso, E. E. Jenkins, A. V. Manohar and M. Trott, *Renormalization Group Evolution of the Standard Model Dimension Six Operators III: Gauge Coupling Dependence and Phenomenology*, *JHEP* **04** (2014) 159, [[1312.2014](#)].

[121] S. D. Bakshi, M. Chala, Á. Díaz-Carmona, Z. Ren and F. Vilches, *Renormalization of the SMEFT to dimension eight: Fermionic interactions I*, *JHEP* **12** (2025) 214, [[2409.15408](#)].

[122] R. Boughezal, Y. Huang and F. Petriello, *Renormalization-group running of dimension-8 four-fermion operators in the SMEFT*, *Phys. Rev. D* **110** (2024) 116015, [[2408.15378](#)].

[123] X.-X. Li, Z. Ren and J.-H. Yub, *Complete tree-level dictionary between simplified BSM models and SMEFT $d \leq 7$ operators*, *Phys. Rev. D* **109** (2024) 095041, [[2307.10380](#)].

[124] H.-L. Li, Y.-H. Ni, M.-L. Xiao and J.-H. Yu, *Complete UV resonances of the dimension-8 SMEFT operators*, *JHEP* **05** (2024) 238, [[2309.15933](#)].

- [125] W. Rarita and J. Schwinger, *On a theory of particles with half integral spin*, *Phys. Rev.* **60** (1941) 61.
- [126] M. Fierz and W. Pauli, *On relativistic wave equations for particles of arbitrary spin in an electromagnetic field*, *Proc. Roy. Soc. Lond. A* **173** (1939) 211–232.
- [127] G. Panico and A. Wulzer, *The Composite Nambu-Goldstone Higgs*, vol. 913. Springer, 2016, [10.1007/978-3-319-22617-0](https://doi.org/10.1007/978-3-319-22617-0).
- [128] G. Buchalla, O. Catá and C. Krause, *On the Power Counting in Effective Field Theories*, *Phys. Lett. B* **731** (2014) 80–86, [[1312.5624](https://arxiv.org/abs/1312.5624)].
- [129] PARTICLE DATA GROUP collaboration, R. L. Workman et al., *Review of Particle Physics*, *PTEP* **2022** (2022) 083C01.
- [130] J. Liang, Y.-B. Yang, T. Draper, M. Gong and K.-F. Liu, *Quark spins and Anomalous Ward Identity*, *Phys. Rev. D* **98** (2018) 074505, [[1806.08366](https://arxiv.org/abs/1806.08366)].
- [131] H.-W. Lin, R. Gupta, B. Yoon, Y.-C. Jang and T. Bhattacharya, *Quark contribution to the proton spin from 2+1+1-flavor lattice QCD*, *Phys. Rev. D* **98** (2018) 094512, [[1806.10604](https://arxiv.org/abs/1806.10604)].
- [132] R. Gupta, B. Yoon, T. Bhattacharya, V. Cirigliano, Y.-C. Jang and H.-W. Lin, *Flavor diagonal tensor charges of the nucleon from (2+1+1)-flavor lattice QCD*, *Phys. Rev. D* **98** (2018) 091501, [[1808.07597](https://arxiv.org/abs/1808.07597)].
- [133] N. Fettes and U.-G. Meissner, *Pion nucleon scattering in chiral perturbation theory. 2.: Fourth order calculation*, *Nucl. Phys. A* **676** (2000) 311, [[hep-ph/0002162](https://arxiv.org/abs/hep-ph/0002162)].
- [134] S. Hamoudou, J. Kumar and D. London, *Dimension-8 SMEFT matching conditions for the low-energy effective field theory*, *JHEP* **03** (2023) 157, [[2207.08856](https://arxiv.org/abs/2207.08856)].